

University of Kentucky

UKnowledge

Theses and Dissertations--Radiation Medicine

Radiation Medicine


2023

DOSIMETRIC AND CLINICAL INVESTIGATION INTO DOSE VARIATIONS OF THE TARGET AND ORGANS AT RISK IN HIGH DOSE RATE GYNECOLOGICAL BRACHYTHERAPY

Brien Washington

University of Kentucky, washington.brien@gmail.com

Author ORCID Identifier:

 <https://orcid.org/0009-0005-0279-5016>

Digital Object Identifier: <https://doi.org/10.13023/etd.2023.266>

[Right click to open a feedback form in a new tab to let us know how this document benefits you.](#)

Recommended Citation

Washington, Brien, "DOSIMETRIC AND CLINICAL INVESTIGATION INTO DOSE VARIATIONS OF THE TARGET AND ORGANS AT RISK IN HIGH DOSE RATE GYNECOLOGICAL BRACHYTHERAPY" (2023).

Theses and Dissertations--Radiation Medicine. 6.

https://uknowledge.uky.edu/radmed_etds/6

This Doctoral Dissertation is brought to you for free and open access by the Radiation Medicine at UKnowledge. It has been accepted for inclusion in Theses and Dissertations--Radiation Medicine by an authorized administrator of UKnowledge. For more information, please contact UKnowledge@lsv.uky.edu.

STUDENT AGREEMENT:

I represent that my thesis or dissertation and abstract are my original work. Proper attribution has been given to all outside sources. I understand that I am solely responsible for obtaining any needed copyright permissions. I have obtained needed written permission statement(s) from the owner(s) of each third-party copyrighted matter to be included in my work, allowing electronic distribution (if such use is not permitted by the fair use doctrine) which will be submitted to UKnowledge as Additional File.

I hereby grant to The University of Kentucky and its agents the irrevocable, non-exclusive, and royalty-free license to archive and make accessible my work in whole or in part in all forms of media, now or hereafter known. I agree that the document mentioned above may be made available immediately for worldwide access unless an embargo applies.

I retain all other ownership rights to the copyright of my work. I also retain the right to use in future works (such as articles or books) all or part of my work. I understand that I am free to register the copyright to my work.

REVIEW, APPROVAL AND ACCEPTANCE

The document mentioned above has been reviewed and accepted by the student's advisor, on behalf of the advisory committee, and by the Director of Graduate Studies (DGS), on behalf of the program; we verify that this is the final, approved version of the student's thesis including all changes required by the advisory committee. The undersigned agree to abide by the statements above.

Brien Washington, Student

Dr. Wei Luo, Major Professor

Dr. Lee Johnson, Director of Graduate Studies

DOSIMETRIC AND CLINICAL INVESTIGATION INTO DOSE VARIATIONS OF
THE TARGET AND ORGANS AT RISK IN HIGH DOSE RATE GYNECOLOGICAL
BRACHYTHERAPY

DISSERTATION

A dissertation submitted in partial fulfillment of the
requirements for the degree of Doctor of Philosophy in the
College of Medicine
at the University of Kentucky

By
Brien Timothy Washington
Lexington, Kentucky
Director: Dr. Wei Luo, Associate Professor of Radiation Oncology
Lexington, Kentucky
2023

Copyright © Brien Timothy Washington 2023

ABSTRACT OF DISSERTATION

DOSIMETRIC AND CLINICAL INVESTIGATION INTO DOSE VARIATIONS OF THE TARGET AND ORGANS AT RISK IN HIGH DOSE RATE GYNECOLOGICAL BRACHYTHERAPY

The technological advancements in brachytherapy have allowed for increased precision and better-quality treatments. This is apparent in treating GYN cancers of the uterine cervix. Lengthy low dose rate (LDR) treatments, implant systems, and two-dimensional (2D) image-guided treatments have been replaced by quicker high dose rate (HDR) treatments and adaptive treatment planning with three-dimensional (3D) imaging modalities. However, this increased precision can result in reduced dosimetric accuracy. Implant systems were designed to conform to the prescribed dose, and 2D plans were only concerned with dose to two organs at risk (OAR) parameters. Now, planners must consider added OAR position data and multiple OAR dosimetric parameters when planning adaptive 3D HDR cervical cancer brachytherapy treatment plans. This results in interfraction dose variations, and dose variations (DV) from the prescribed dose.

The purpose of this dissertation is the investigation of the dosimetric and clinical effects of DVs from the prescribed dose. DVs are uncertainties in the context of brachytherapy. The reduction of uncertainties for patient treatments is the goal of any physicist. And the first step to reducing uncertainties is to identify and quantify them. DV uncertainty was quantified using statistical models to identify trends in the DV data and to determine the effect on OARs. This DV uncertainty quantification established the DV portion of the cervical cancer brachytherapy uncertainty budget. The known DV uncertainty from the statistical models was used to hypothesize the clinical effect of DV uncertainty on clinical outcomes via Monte Carlo simulations of patient treatments. Lastly, the actual clinical outcomes were evaluated under the influence of DV uncertainty to determine the clinical effect of DV uncertainty.

In this dissertation, we have found that DV uncertainty results in tumor coverage loss and affects clinical outcomes. There is a 32.5% probability of under-dosing the high-risk clinical target volume (HRCTV), 1% of local control is loss for every -5% DV uncertainty, and 1% of pelvic control is loss for every -1.4% DV uncertainty. This effect is more profound for larger tumors. DV uncertainty reduces the local control probability by as much as 2.68% for large HRCTVs, DV uncertainty increases the treatment failure rate by as much as 1.7% (24σ) for large HRCTVs, and 1% of local control is loss for every 7.23 cm^3 increase in HRCTV size. From the results of this dissertation, DV uncertainty has a profound effect on HDR brachytherapy for cervical cancer. DV uncertainty must be mitigated in clinic to improve treatment quality and clinical outcomes.

KEYWORDS: Dose variation, dose uncertainty, outcome modeling, high dose-rate brachytherapy, intracavity brachytherapy.

Brien Washington

04/26/2023

Date

ACKNOWLEDGMENTS

It has been a journey for me of trials and tribulations to get to this point, but I would not have had it any other way. I came to the University of Kentucky as a timid and grateful master's student, because I did not think that I was cut out for graduate school. However, I am leaving as a confident Medical Physicist with a PhD. I would like to acknowledge the entire Radiation Medicine department for being there for me and believing in me at the times I didn't believe in myself. I would especially like to acknowledge my advisor, Dr. Wei Luo, for being there for me every step of the way, giving me words of encouragement to get the job done, and helping me develop into the clinical physicist and researcher that I am today.

Next, I would like to acknowledge Dr. Dennis Cheek and Dr. Damodar Pokhrel for their mentorship throughout my time here at the University of Kentucky. I remember sitting in their respective offices after a disappointing qualifying exam score, and they both encouraged me to stay on the course to complete this degree. I would also like to acknowledge Dr. Mahesh Kudrimoti for going above and beyond for me throughout my time here, and Dr. Chi Wang for providing invaluable guidance on the advanced statistical models used in this dissertation. Lastly, I would like to acknowledge my outside examiner, Dr. Akinbode Adedeji, for taking the time to sit on my dissertation defense committee.

I would like to acknowledge Dr. Lee Johnson, Dr. Janelle Molloy, Dr. Marcus Randall, Dr. Denise Fabian, and Dr. Mark Bernard for their teaching, clinical training, research training, and mentorship along the way. Also, I would like to acknowledge Dr. James Wanliss for mentoring me as an undergraduate researcher at Presbyterian College.

This journey started with your guidance and relentless encouragement of my abilities early on.

Finally, I would like to acknowledge my family and friends who have helped me out and encouraged me throughout this journey. I honestly would not have made it to this point if it were not for you all. I am, because you all are.

TABLE OF CONTENTS

ACKNOWLEDGMENTS.....	iii
LIST OF TABLES.....	viii
LIST OF EQUATIONS.....	xi
CHAPTER 1. Introduction	1
1.1 <i>An Overview of Cervical Cancer</i>	1
1.2 <i>Advancements in Cervical Cancer Radiation Therapy</i>	2
1.3 <i>Uncertainties in Brachytherapy</i>	3
1.4 <i>Purpose of Dissertation and Dissertation Outline</i>	6
CHAPTER 2. Statistical Analysis of High Risk Clinical Target Volume (HRCTV) and Organs at Risk (OAR) Dose Variations ²⁹	9
2.1 <i>Abstract</i>	9
2.2 <i>Introduction</i>	10
2.3 <i>Materials and Methods</i>	12
2.3.1 <i>Dose Variation</i>	12
2.3.2 <i>Basic Statistics</i>	14
2.3.3 <i>Correlations</i>	14
2.3.4 <i>Distribution Fitting</i>	14
2.3.5 <i>Probability of Clinically Significant Dose Variation</i>	16
2.4 <i>Results</i>	16
2.4.1 <i>Basic Statistics</i>	16
2.4.2 <i>Correlations</i>	18
2.4.3 <i>Fitted Distributions</i>	19
2.5 <i>Discussion</i>	22
2.6 <i>Conclusion</i>	26
CHAPTER 3. Defining Clinical Outcomes in Radiation Therapy	27
3.1 <i>Locational Disease Control, Recurrence, and Failure</i>	27
3.2 <i>Dose Response Curves</i>	28
3.3 <i>Reference TCP and NTCP Curves Used in this Dissertation</i>	29
CHAPTER 4. The Hypothesized Effects of HRCTV and OAR Dose Variations on Clinical Outcomes in HDR Brachytherapy for Cervical Cancer.....	32
4.1 <i>Abstract</i>	32
4.2 <i>Introduction</i>	33
4.3 <i>Materials and Methods</i>	35
4.3.1 <i>Determination of DV Uncertainty Distributions</i>	35

4.3.2	Reference Dose Response Curves	36
4.3.3	Monte Carlo (MC) Simulation and Convolution.....	36
4.3.3.1	MC Simulation of Patient Treatments and Convolution Process	36
4.3.3.2	Determination of Treatment Success and Treatment Failure	37
4.3.4	Model Generated R' Shaping Parameter Estimation	37
4.3.5	Utility Concept	38
4.3.6	Statistical Analysis	38
4.3.7	Model Accuracy Testing	39
4.4	<i>Results</i>	39
4.4.1	HRCTV and OAR Dose Variations.....	39
4.4.2	Model Generated R' Shaping Parameters	41
4.4.3	Effects of Dose Variation Uncertainty on TCP and NTCP	42
4.4.4	Treatment Failure Rates.....	44
4.4.5	Utility Analysis.....	47
4.5	<i>Discussion</i>	48
4.6	<i>Conclusion</i>	51
CHAPTER 5. The Clinical Effect of Dose Variation Uncertainty for Cervical Cancer High Dose-Rate (HDR) Brachytherapy		52
5.1	<i>Abstract</i>	52
5.2	<i>Introduction</i>	53
5.3	<i>Materials and Methods</i>	54
5.3.1	Patient Selection	54
5.3.2	Dosimetric Parameters.....	54
5.3.3	Clinical Outcomes	55
5.3.4	Utility	56
5.3.5	Statistical Analysis	56
5.4	<i>Results</i>	56
5.4.1	TCP Curves	57
5.4.2	DV, CI, COIN, and HRCTV Logistic Regression.....	59
5.4.3	Utility Analysis.....	60
5.4.4	Control versus Recurrence Parameter t-tests	61
5.5	<i>Discussion</i>	62
5.6	<i>Conclusion</i>	68
CHAPTER 6. Dissertation Summary		70
6.1	<i>Clinical Impact</i>	70
6.2	<i>Study Limitations</i>	73
6.3	<i>Future Research Directions</i>	74
APPENDICES.....		76
[APPENDIX 1. GLOSSARY]		77
[APPENDIX 2. DETAILED RESULTS FROM CHAPTER 4].....		80
[APPENDIX 3. DETAILED RESULTS FROM CHAPTER 5].....		81

REFERENCES.....	86
VITA.....	94

LIST OF TABLES

Table 2.1. The mean and standard deviation for HRCTV D90, and OAR D0.1 cc and D2 cc.	17
Table 2.2. Pearson correlation statistics.....	19
Table 2.3. Probabilities and statistics from distributions. The probabilities were calculated using the Generalized extreme-value and normal CDF determined from their RSS scores.	21
Table 2.4. 95% Confidence intervals for HRCTV IDVs from prescription.	22
Table 3.1. Summary of published dose response curves and their shaping parameters used in this study. Both Logistic and Probit sigmoid equations were used. TCP1 was derived from the retroEMBRACE study of locally advance cervical cancer (LACC) radiotherapy, TCP2A was derived from patients diagnosed with stage IB-IVA cervical cancer, TCP2B represented large HRCTV size patients, and TCP2C represented a poor response to EBRT pre-brachytherapy. The NTCP was derived from the D2 cc of the bladder and rectum..	31
Table 4.1. Distribution statistics for the target dose variation (DV) uncertainty distributions used in this study. The Double Weibull, Beta, and GEV distributions represented the rectum, bladder, and sigmoid, respectively.	40
Table 4.2. Local control differences of R' from the reference curves for Beta and Normal distribution DV uncertainty sampling.....	42
Table 4.3. Statistical analysis and differences in complication probability between R' and R for the OARs.	44
Table 4.4. Statistical analysis of predicted treatment failure rates.	45
Table 4.5. Comparison of optimal doses (EQD ₂) and corresponding utilities (U) calculated with DV and without DV (reference).	47
Table 5.1. Statistics of all dependent and independent variables.	57
Table 5.2. The shaping parameters of the dose response curves derived from the LF, LC, and pelvic recurrence data sets. The curves derived by LF data provide the non-LF probability dose response curves, the curves derived from LR data provided the LC probability dose response curves, and the curves derived from pelvic data provided the pelvic control probability dose response curves.	59
Table 5.3. HRCTV size, DV, COIN, CI, and c2 logistic regression statistics for all patients.	60

LIST OF FIGURES

Figure 1.1. Work-flow of uncertainties at every step of brachytherapy from TG 138¹¹. TG 138 focused on uncertainties out of the scope of clinicians and left clinical uncertainties for clinicians to investigate. 4

Figure 1.2. Coronal (A) and sagittal (B) views of high dose-rate (HDR) tandem and ovoid (T&O) brachytherapy for cervical cancer. The green insertions are the tandem and two ovoid applicators, the high-risk clinical target volume (HRCTV)/uterine cervix is delineated in blue, the bladder is delineated in yellow, the rectum is delineated in brown, the sigmoid colon is delineated in fuchsia, and the bowel is delineated in salmon-pink. .. 6

Figure 2.1. HRCTV course DVs correlated with HRCTV EQD2 DVs. A $\pm 5\%$ HRCTV course DV correlates to a -6.1% and 6.8% HRCTV EQD2 DV..... 13

Figure 2.2 The HRCTV PPV as an empirical distribution plotted with the theoretical normal distribution's PDF. The HRCTV dose variations from prescription is on the x-axis and the probability density of the variations is on the y-axis. 50 calculation points were used for both datasets to determine the best fit distribution. 15

Figure 2.3. Histograms of all evaluated structures (bin width = 5%). Plot A is the HRCTV IDVs, plots B and C are the rectum D2cc and D0.1cc, plots D and E the bladder D2cc and D0.1cc, plots F and G the sigmoid D2cc and D0.1cc, and plots H and I the bowel D2cc and D0.1cc. 18

Figure 2.4. Scatter plot of bladder D2cc vs. HRCTV D90. The HRCTV D90 IDVs are on the x-axes and the corresponding bladder D2cc IDVs are on the y-axes. 19

Figure 2.5. Best fitted distributions and a fitted normal distribution for HRCTV D90 (A & C) determined from the distribution fitting. The HRCTV IDVs are on the x-axis and the corresponding probability density is on the y-axis. Q-Q plots and Anderson Darling (AD) test results are also tabulated (B & D) to statistically validate the fitted distributions. The respective fitted distribution quantiles are on the x-axis and the HRCTV IDVs are on the y-axis. AD p-values > 0.05 mean the distribution statistically fits the data. AD p-values < 0.05 mean the distributions do not statistically fit the data. From the AD test and Q-Q plots, HRCTV IDVs are not normally distributed..... 20

Figure 2.6. Visualized probabilities of under and overdosing the HRCTV Generalized-extreme value and normal distribution CDF. HRCTV IDVs are on the x-axis, and the IDV probabilities are on the y-axis. Under-dosing the HRCTV was defined as HRCTV IDVs less than -5% , overdosing the HRCTV was defined as HRCTV IDVs greater than 5% . .. 22

Figure 3.1. Anatomy of the female pelvis displaying the true (lesser) and false (greater) pelvis. The image is from "The Pelvic Girdle." *TeachMeAnatomy*, <https://teachmeanatomy.ingo/pelvis/bones/pelvic-girdle/>. 28

Figure 3.2. An example TCP and NTCP curve displaying the therapeutic window. 29

Figure 4.1. The five DV uncertainty distributions used in this study for DV sampling. The Beta (A) was the best fitted DV distribution for the HRCTV. The HRCTV Normal distribution (B) represented an 11% random uncertainty. The Double Weibull (C), Beta (D), and Generalized-Extreme Value (GEV) (E) distributions represented the rectum, bladder, and sigmoid DV uncertainty, respectively..... 41

Figure 4.2. Comparison between the reference, Beta-sampled, and Normal sampled TCP curves. A. TCP1; B. TCP2A; C. TCB2B; D. TCP2C..... 43

Figure 4.3. Comparison of NTCP curves between R' and R (rectum, bladder, sigmoid, and composite of the three organs). A 10 Gy HRCTV dose escalation from 85-95 Gy was observed. 44

Figure 4.4. Treatment failure rate predictions and analysis..... 46

Figure 4.5. Utility curves for R' and R. A. TCP1; B. TCP2A; C. TCP2B; D. TCP2C. 48

Figure 5.1. Dose response curves derived from LF, LR, and pelvic recurrence data. The curves derived by LF data provide the non-LF probability dose response curves, the curves derived from LR data provided the LC probability dose response curves, and the curves derived from pelvic data provided the pelvic control probability dose response curves. A is from all cervical cancer patients, B is from LACC patients. 58

Figure 5.2. Logistic regression for DV (A), COIN (B), c2 (C), and HRCTV (D) using the local and pelvic recurrence datasets..... 60

Figure 5.3. Utility calculations for the three-year LACC TCP derived from LR data, TCP1, and TCP2A. Our risk-free local control (RFLC) probability decreased to 72.8%, but the optimal dose prediction increased to 83.6 Gy..... 61

Figure 5.4. Figure 1 from Gonzalez et al.⁵⁹ displaying increased dose conformity with T&R + IS applicator. 64

Figure 5.5. Dose Variation (DV) and Conformity index (CI) (A) and c2 (B). DV is directly proportional to CI and c2. DV has a strong correlation to CI and moderate correlation to c2..... 66

Figure 5.6. The three-year locally advanced cervical cancer (LACC) TCP curve derived from computed tomography (CT) based brachytherapy patients compared to reference TCP curves derived magnetic resonance imaging (MRI) based brachytherapy patients..... 68

LIST OF EQUATIONS

Equation 2.1	12
Equation 2.2	13
Equation 2.3	15
Equation 2.4	16
Equation 2.5	16
Equation 3.1	30
Equation 3.2	30
Equation 4.1	36
Equation 4.2	38
Equation 5.1	54
Equation 5.2	55
Equation 5.3	55

CHAPTER 1. INTRODUCTION

1.1 An Overview of Cervical Cancer

According to the American Cancer Society (ACS), Gynecological (GYN) cancers will account for 12.1% and 11.1% of cancer incidences and deaths in women in 2023¹, respectively. Cervical cancers are one of the most common GYN cancer and will account for 1.47% of cancers incidences in women, and 1.50% of women cancer deaths. The standard for cancer prognosis and treatment evaluation is the 5-year survival rate. The 5-year survival rate for cervical cancer is 81% for all Federation Internationale de Gynecologie et d'Obstetrique (Federation of Gynecology and Obstetrics, FIGO) stages. Cervical cancer treatment consists of a combination of surgery, chemotherapy, radiation therapy (RT), and immunotherapy. Treatment combinations vary depending on the stage. However, RT is a standard of care for cervical cancer, regardless of stage.

Cervical cancer RT consists of two types of treatments: external beam radiation therapy (EBRT) and brachytherapy. EBRT externally delivers radiation dose to the tumor via medical linear accelerators (LINACs), while brachytherapy (the prefix “brachy” means short distance) internally delivers radiant dose close to or within the tumor. Brachytherapy delivers the dose via intracavity or interstitial applicators. The intracavity applicators are tandems, ovoids, and rings, and are inserted into the vaginal cavity to access the cervix. Interstitial applicators like needles and ribbons are inserted directly into the cervix or uterus and other tissues that include the disease. EBRT is the primary portion of RT with prescription doses ranging from 45 to 50 Gy (1 Gy = 1 J/Kg) over 25 treatments known as

fractions, and brachytherapy is the boost portion of RT with prescriptions ranging from 5 to 7 Gy for 4 to 6 fractions².

1.2 Advancements in Cervical Cancer Radiation Therapy

Cervical cancer RT has evolved since RT's inception over a century ago. Many of these advancements have occurred within the last two-to-three decades due to modernizations in and around the field. Three-dimensional (3D) medical imaging modalities such as magnetic resonance imaging (MRI), computed tomography (CT), and positron emission tomography (PET) are now used for RT treatment planning. Using 3D imaging for treatment planning is an upgrade from 2D treatment planning for both EBRT and brachytherapy. EBRT has experienced the most advancements from 3D imaging in recent years, but brachytherapy has experienced a fair amount of advancement as well.

For most of the 20th century, brachytherapy was conducted using low dose rate (LDR, 0.40 to 2.00 Gy/h) treatments via 2D treatment planning and, or implantation system techniques. Implantation system techniques were fine for delivering doses to the tumor, but they provided limited information for organs at risk (OAR) dose, and there were limitations on treatment standardization. The International Commission on Radiation Units report 38 (ICRU 38) mitigated this by standardizing 2D brachytherapy dosimetry using point doses for the tumor (Point A) and OARs (rectal and bladder points), and reference volume descriptions³. This allowed the cervical cancer brachytherapy process to be uniform for tumor and OAR dose reporting. ICRU 38's recommendations were suited for 2D LDR and high dose-rate (HDR, > 12 Gy/h) brachytherapy, but there were limitations for its use in 3D brachytherapy.

HDR and 3D brachytherapy were popularized at the turn of the century and became the standard of care shortly after⁴⁻⁶. HDR provides shorter treatment times and improved local control (LC) of the gross disease in the cervix, uterus, and vagina when compared to LDR. The limitation of HDR versus LDR is that treatments are fractionated due to radiobiological concerns, and acute OAR toxicity is more likely. When compared to 2D brachytherapy, 3D brachytherapy provides more anatomical information with volumetric dose parameters. Point doses were still relevant in 3D brachytherapy⁷, but volumetric dose coverage improved the quality of treatments⁶. The volumes of interest are now the gross tumor volume (GTV), high-risk clinical target volume (HTCTV), rectum, bladder, and sigmoid per the updated ICRU 89 recommendations⁸. Now, planners must consider additional variables in their treatment planning. The increased precision and advancements of HDR and 3D treatment planning is beneficial to brachytherapy, but it also brings about a variety of uncertainties.

1.3 Uncertainties in Brachytherapy

Brachytherapy procedures are subject to varying levels of uncertainties at each step of the brachytherapy process. From source construction and calibration to delivery of clinical plans, uncertainties will exist⁹⁻¹¹. The American Association of Physicists in Medicine's (AAPM) task group report number 138 (TG 138) recognized the effect of brachytherapy uncertainties in the clinical setting and offers guidance to clinicians to navigate these uncertainties¹¹. Their definition of uncertainty comes from the recommendations provided by the National Institute of Standards and Technology (NIST) Technical Note 1297¹². Uncertainties were defined as either type A or type B uncertainties. Type A (random) uncertainties are evaluated using statistical methods and type B

(systematic) uncertainties are evaluated by other methods. Both type A and B uncertainties are to be added in quadrature for uncertainty analysis in brachytherapy. TG 138's primary focus was to investigate uncertainties out of the scope of clinicians, such as Monte Carlo simulations of sources and further elaborations on uncertainties of AAPM task group 43 (TG 43) dosimetric parameters (Figure 1.1). The study of clinical uncertainties was not a focus of TG 138, but some guidance was provided for studying them. This guidance included as a theoretical maximum allowed dosimetric uncertainty of 20%¹¹. In short, clinical uncertainties are uncertainties that clinicians have some sense of control over.

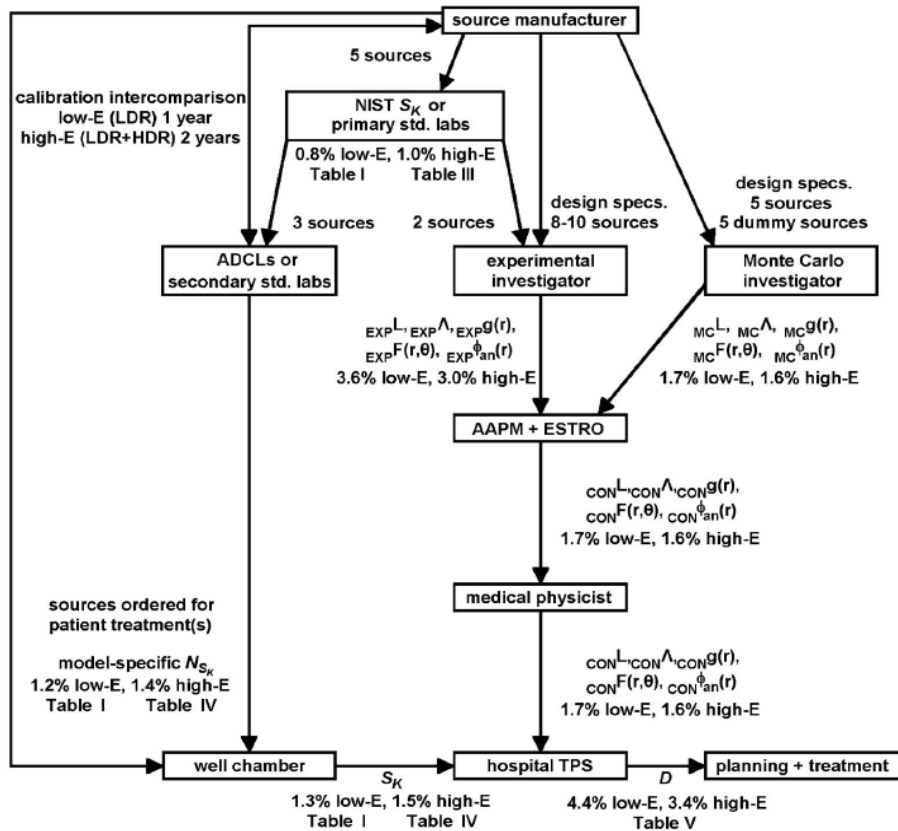


Figure 1.1. Work-flow of uncertainties at every step of brachytherapy from TG 138¹¹. TG 138 focused on uncertainties out of the scope of clinicians and left clinical uncertainties for clinicians to investigate.

Some clinical brachytherapy uncertainties are similar from one brachytherapy technique or procedure to another brachytherapy technique or procedure. These uncertainties include structure delineation and structure motion¹³⁻²³. However, this is not the case for all clinical uncertainties. Low energy brachytherapy sources are more subject to tissue heterogeneities than high energy sources, HDR brachytherapy does not suffer from inter-source attenuation like interstitial LDR brachytherapy, and tandem and ovoid (T&O, Figure 1.2) procedures will have different uncertainties than tandem and ring (T&R) procedures or vaginal cylinder procedures^{13,24}. It is accepted that delineation of the HRCTV and OAR motion are the most essential components of the cervical cancer brachytherapy uncertainty budget²⁵. HDR T&O brachytherapy treatments are online adaptive procedures at our institution: every fraction has a new plan on a new set of images. It is the goal to deliver the prescribed dose to the HRCTV every fraction, but dose variations (DV) from the prescription are inevitable due to the nature of adaptive procedures. DVs are not considered an uncertainty in statistical terms, but DVs are a form of error or uncertainty in the context of brachytherapy²⁶. DVs from the prescribed dose may not be the dominating factor for HDR T&O ICBT uncertainties, but it is an important component of the HDR T&O ICBT uncertainty budget due to the nature of adaptive procedures. Despite the importance of DVs, it has not been studied with the same rigor as the mentioned uncertainties. The American Brachytherapy society recommends no more than a 0.25 Gy DV per fraction²⁷. This equates to a 3.57 to 5.00% per-fraction DV tolerance for 5 to 7 Gy fractions. However, this recommendation was based on physician intuition for point doses. Sharma et al. used this tolerance to study the dosimetric effect of DV on point doses²⁸. They found that the average Point A DV from the prescribed dose was $1.55\% \pm 1.07\%$ and

recommended narrowing the DV constraint of $\pm 5\%$. Despite their conclusions, their work did not account for the modernized volumetric parameters used today, nor did they assess the effect DV uncertainty has on clinical outcomes.

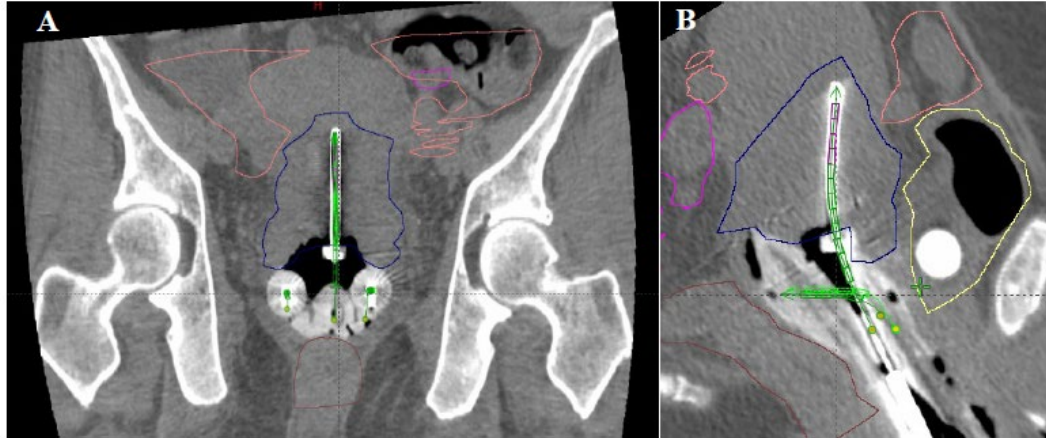


Figure 1.2. Coronal (A) and sagittal (B) views of high dose-rate (HDR) tandem and ovoid (T&O) brachytherapy for cervical cancer. The green insertions are the tandem and two ovoid applicators, the high-risk clinical target volume (HRCTV)/uterine cervix is delineated in blue, the bladder is delineated in yellow, the rectum is delineated in brown, the sigmoid colon is delineated in fuchsia, and the bowel is delineated in salmon-pink.

1.4 Purpose of Dissertation and Dissertation Outline

The purpose of this dissertation is to investigate the dosimetric and clinical effect of DV uncertainty from the prescribed dose in 3D, HDR brachytherapy for cervical cancer. Increased precision from the advancements in cervical cancer brachytherapy can reduce accuracy, but to what extent that reduced accuracy effects dosimetry and clinical outcomes is not known. The findings of this dissertation will increase plan quality, improve clinical outcomes, and provide insight to DV uncertainty and other relative dosimetry parameters in cervical cancer brachytherapy.

Chapter 2 is a statistical analysis of dosimetry in HDR cervical cancer dosimetry. Fifty patients were used for the analysis. We determined the best statistical model to

describe DV uncertainty and determined the dosimetric effect DV uncertainty has on OARs. Chapter 2 is a modified version of the following published manuscript:

²⁹Washington B, Randall M, Fabian D, Cheek D, Wang C, Luo W. Statistical Analysis of Interfraction Dose Variations of High-Risk Clinical Target Volume and Organs at Risk for Cervical Cancer High-Dose-Rate Brachytherapy. *Adv Radiat Oncol.* 2022;7(6):101019. doi:10.1016/j.adro.2022.101019

Chapter 3 is an introduction to assessing clinical outcomes in RT to clarify the findings and conclusions of Chapters 4 through 6.

In **Chapter 4** we used the dosimetric findings from Chapter 2 to hypothesize the clinical effect of DV uncertainty. The clinical outcomes were generated using Monte Carlo simulation sampling from known DV uncertainty distributions and published reference dose response curves. The DV uncertainty distributions were calculated from 100 patients to further validate the findings in Chapter 2. The utility model was also introduced for cervical cancer brachytherapy. Chapter 4 is a version of the following manuscript submitted to *Medical Physics* edited for this thesis:

Washington, B., Kudrimoti, M., Fabian, D., Cheek, D., Wang C., Pokhrel D., Luo W. Effects of interfraction dose variations of target and organs at risk on clinical outcomes in high dose rate brachytherapy for cervical cancer. Submitted to *Medical Physics* on December 31st 2022.

Chapter 5 is the observed clinical effects of DV uncertainty. Clinical outcomes were evaluated as a function of DV uncertainty, dose, relative dosimetry, and HRCTV size. This chapter evaluated 117 cervical cancer patients treated with HDR T&O brachytherapy.

Chapter 6 is the summary, conclusion, limitations, and future research directions of this dissertation. We assessed the clinical impact of our findings and make recommendations based on the presented data.

CHAPTER 2. STATISTICAL ANALYSIS OF HIGH RISK CLINICAL TARGET VOLUME (HRCTV) AND ORGANS AT RISK (OAR) DOSE VARIATIONS²⁹

2.1 Abstract

Purpose: High dose rate (HDR) brachytherapy for cervical cancer treatment includes significant uncertainties. This study's purpose was to quantify the interfraction dosimetric variation (IDV) of the high-risk clinical target volume (HRCTV) from the prescribed dose and the corresponding effect on organ at risk (OAR) dose based on a comprehensive statistical analysis.

Methods and Materials: Fifty cervical cancer patients treated with HDR tandem and ovoid (T&O) brachytherapy from October 2019 to December 2020 were retrospectively analyzed. The OARs of interest were the rectum, bladder, sigmoid, and bowel. The dosimetric parameters evaluated for all patients was the dose absorbed by 90% of the HRCTV (D_{90}) and the dose absorbed by 0.1 ($D_{0.1cc}$) and 2 cm³ (D_{2cc}) of each respective OAR. The doses were converted to their equivalent dose in 2 Gy fractions (EQD_2) to standardize the analysis. The HRCTV variations were from the prescribed dose and the OAR variations were from their expected EQD_2 . Linear regression was conducted for HRCTV EQD_2 IDVs and their raw course IDV to interpolate the results. Distribution fitting of the HRCTV variations was determined to quantify the IDV. Comparative statistics of the HRCTV variations with the OAR variations were conducted to determine correlations.

Results: The mean HRCTV EQD_2 variation from the prescribed dose was $-3.54\% \pm 11.9\%$. The HRCTV variations and OAR variations showed moderate to weak linear correlations despite the variations being relative to each other. The rectum D_{2cc} had the strongest correlation ($R^2 = 0.136$, $p = 0.009$). There was a 32.5% (2.62% 95% confidence interval)

probability of under-dosing the HRCTV (-5% raw dose variation from prescription) and a 22.5% (2.62% 95% confidence interval) probability of overdosing the HRCTV (+5% raw dose variation from prescription). This tendency to under-dose the HRCTV was a consequence of HRCTV IDV not being normally distributed.

Conclusions: HRCTV dose variations and OAR dose variations were moderately to weakly correlated with the rectum D_{2cc} having the strongest correlation. HRCTV IDV were best described as a left skewed distribution that indicates a tendency of under-dosing the HRCTV. The clinical significance of such dose variations is expected and will be further investigated in this thesis.

2.2 Introduction

Brachytherapy procedures are subject to varying levels of uncertainties, from source construction and calibration to delivery of clinical plans⁹⁻¹¹. These uncertainties can result from technology or clinical procedures. Uncertainties associated with clinical procedures that clinicians have control over are called clinical uncertainties. Clinical uncertainties include the uncertainties of structure delineation and organ motion¹³⁻²³.

It is accepted that HRCTV delineation and OAR motion are the most significant components of the brachytherapy treatment uncertainty budget²⁵. At our institution, HDR intracavity (ICBT) brachytherapy treatments are online adaptive procedures: every fraction has a new CT scan and plan which results in interfraction dose variations (IDV) of the HRCTV, especially, IDVs from the prescribed dose. Although dose variations (DV) may not be considered an uncertainty in statistical terms, they are considered a form of uncertainty in brachytherapy²⁶. IDVs from the prescribed dose may not be dominant among

HDR T&O ICBT uncertainties, but they are important as they may have a significant impact on clinical outcomes. However, this type of uncertainty has not been studied with the same rigor as the aforementioned uncertainties.

There have been studies of IDVs of OARs and the target volume or point^{21,23,30}. These studies acknowledge that IDVs are forms of uncertainties in brachytherapy, but mostly focus on deformable image registration (DIR) dosimetric parameters and their variation from dose-volume histogram (DVH) dosimetric parameters, not the variation of dose from the given prescription. Chakraborty et al.³¹ and Jamema et al.³² studied the effect of interfraction applicator position on OAR dose in cervical cancer brachytherapy in addition to the spatial change of the dosimetric parameters. However, neither focused on the IDV of the HRCTV nor its corresponding effect on OAR dose. Sharma et al studied Point A dose variations from the given prescription in fractionated brachytherapy²⁸. Despite the importance of continuing to use point doses in modern day cervical cancer brachytherapy, volumetric parameters such as the HRCTV have taken priority to Point A and other point dose parameters⁷.

To our knowledge, HRCTV dose variations from the given prescription and the corresponding effect on OAR dose in HDR T&O ICBT have not been studied. Therefore, in this study we evaluate the IDV of the HRCTV from the prescribed dose and the corresponding effects on OAR dose in HDR T&O ICBT. Furthermore, we studied the distribution of IDVs from the prescribed dose to quantify the corresponding uncertainty.

2.3 Materials and Methods

2.3.1 Dose Variation

The DVs were calculated from 50 patients diagnosed with stage I-IVB cancers of the uterine cervix and treated with HDR T&O brachytherapy at our institutions from 2019 to 2021. The HRCTV, rectum, bladder, sigmoid, and bowel were the structures evaluated in this study. The delineation of structures followed the International Commission on Radiation Units report 89 (ICRU 89) and was conducted on CT images⁸. The HRCTV was delineated as the entire cervix, uterus, parametrium, and vagina. The HDR dose prescriptions ranged from 5-7 Gy for 3-5 fractions, yielding an equivalent dose in 2 Gy fractions (EQD_2) range of 18.8-40 Gy ($\alpha/\beta = 10$ Gy). Treatment planning for each fraction was conducted in the Varian Eclipse brachytherapy treatment planning system (TPS).

The HRCTV IDVs were calculated from the prescribed brachytherapy course dose and the prescribed brachytherapy EQD_2 . The published version of this manuscript calculated HRCTV IDVs from the prescribed course dose²⁹, but HRCTV DVs from the prescribed EQD_2 are more relevant clinically and for this thesis. Furthermore, HRCTV Course DVs and EQD_2 DVs are correlated one-to-one (Figure 2.1, $R^2 = 0.997$, $p < 0.001$). OARs do not have a dose prescribed to them, so OAR IDVs were from their expected EQD_2 ($\alpha/\beta = 3$ Gy). Using EQD_2 is also analogous to IDVs because EQD_2 is used for the entire brachytherapy course dose. The calculation of IDVs was done using the percent difference equation:

Equation 2.1.

$$\% \text{ difference} = \frac{\text{Dose delivered} - \text{Prescription or expected dose}}{\text{Prescription or tolerance dose}} \cdot 100$$

Where the dose delivered is D_{90} for the HRCTV, and dose in 0.1 cc ($D_{0.1cc}$) and 2 cc (D_{2cc}) for the OARs. The American Brachytherapy Society (ABS) estimated a tolerance HDR dose variation of ± 0.25 Gy per fraction from a given prescription²⁷. This equates to a $\pm 5\%$ variation for 5 Gy per fraction and a $\pm 3.57\%$ variation for 7 Gy per fraction. This is consistent with a clinically significant dose tolerance of $\pm 5\%$ for radiation therapy. Where -5% variations are under-dosed conditions and $+5\%$ variations are overdosed conditions. A $\pm 5\%$ DV equates to a -6.1% and 6.8% HRCTV EQD_2 under and overdose condition (Figure 2.1, Equation 2-).

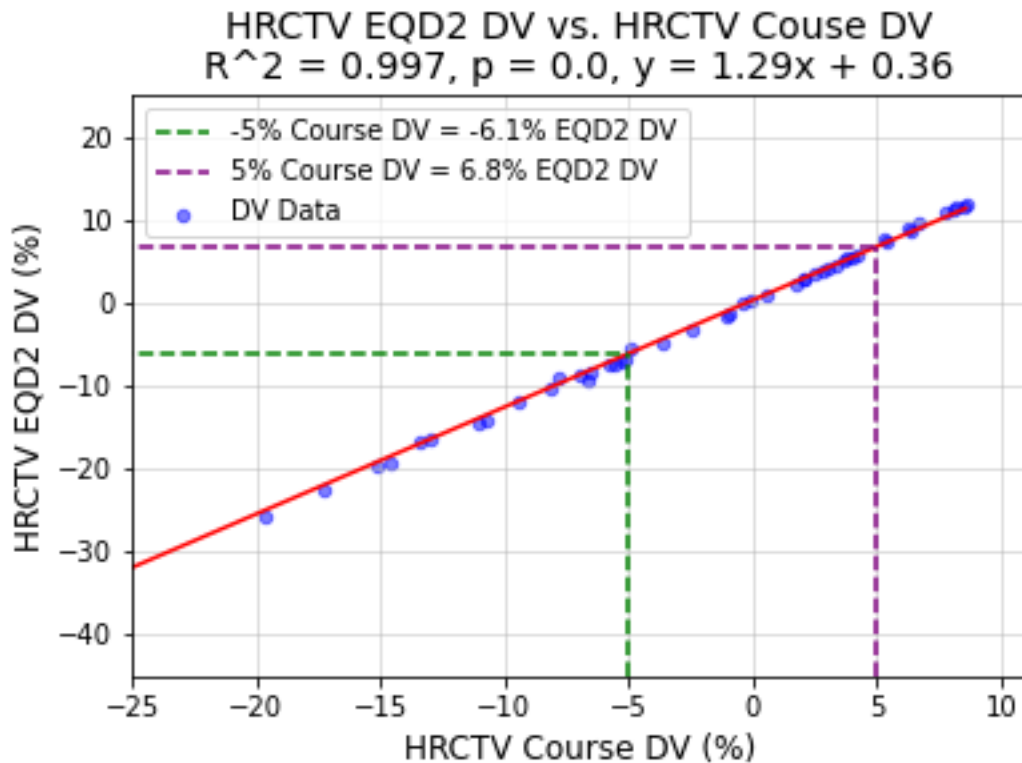


Figure 2.1. HRCTV course DVs correlated with HRCTV EQD2 DVs. A $\pm 5\%$ HRCTV course DV correlates to a -6.1% and 6.8% HRCTV EQD2 DV.

Equation 2.2

$$EQD2_{DV}(\%) = 1.29 \cdot RawCourse_{DV}(\%) + 0.36\%$$

2.3.2 Basic Statistics

Data analysis was performed in Python 3.7 via the use of the SciPy and DistFit packages. The mean, standard deviation, and median were calculated for each structure's dosimetric dataset. The 95% confidence interval was calculated for all relevant parameters.

2.3.3 Correlations

Simple linear regression using the Pearson correlation coefficients (R and R^2) was calculated for each OAR dosimetric parameter IDV against HRCTV IDV. Using Pearson coefficients quantified the effect HRCTV IDV uncertainty had on OAR IDV uncertainty. The R coefficient determined the direction of the correlation (range = ± 1), and the R^2 coefficient quantified to strength of the correlation (range = 0,1). Statistical significance for the analysis was determined as p-values < 0.05 .

2.3.4 Distribution Fitting

The HRCTV distribution was fitted to 89 different distributions using the DistFit function in Python 3.7 to find the best fit distribution. The histogram bin width can affect the fitted distribution. Therefore, distribution fitting was performed with limited dependence on histogram bin width to obtain an accurate fit³³. To accurately fit a distribution to the HRCTV, the IDV data was plotted as an empirical distribution, analogous to a line histogram (Figure 2.2). Each respective probability density function (PDF) was plotted along with the empirical distribution of the IDVs. Distribution fits were ranked according to their residual sum of squares (RSS) score: the lower the score the better the fit. The RSS is the sum of squared distances from a given point on the empirical

distribution curve to the corresponding point on the PDF curve. The RSS equation is shown in Equation (2.3):

Equation 2.3

$$RSS = \sum_i^n (y_i - f(x_i))^2$$

Where n is the maximum data point, y_i is the i^{th} point of the empirical distribution, and $f(x_i)$ is the i^{th} point of the PDF. There were 50 evaluation points to fit and score the distributions.

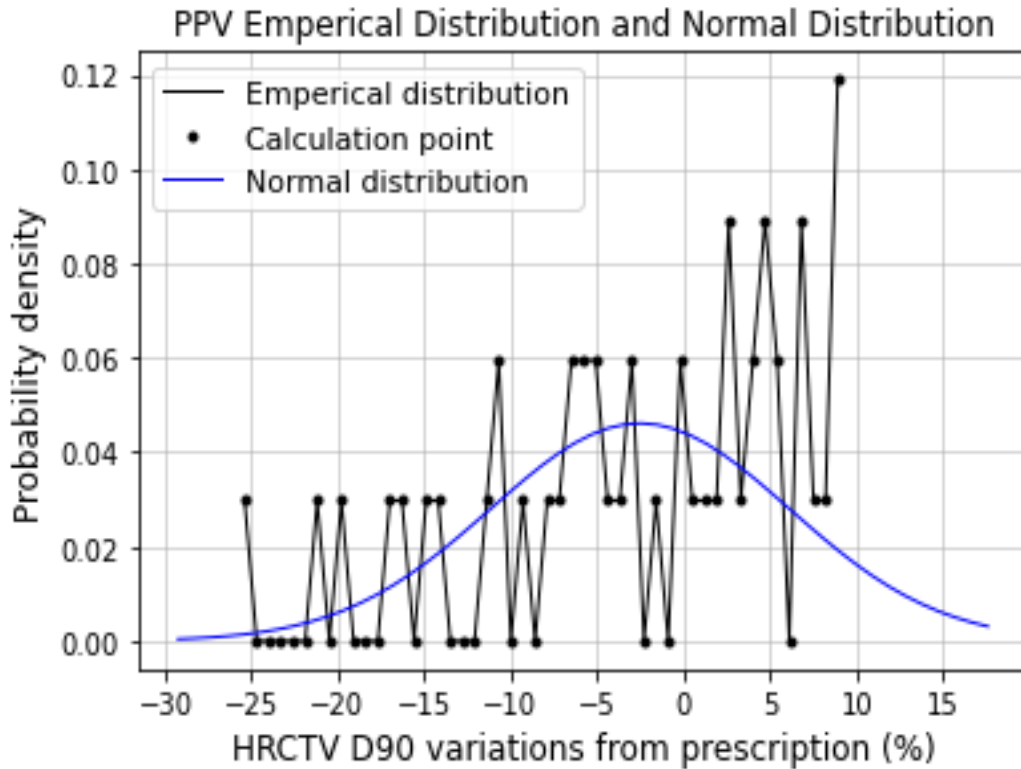


Figure 2.2 The HRCTV PPV as an empirical distribution plotted with the theoretical normal distribution’s PDF. The HRCTV dose variations from prescription is on the x-axis and the probability density of the variations is on the y-axis. 50 calculation points were used for both datasets to determine the best fit distribution.

The RSS is only a relative measurement parameter and does not determine the statistical significance of a fitted distribution. Therefore, an Anderson-Darling (AD) test

was performed to determine whether the fits determined by the RSS were statistically significant³⁴. The AD test uses a distribution specific term to calculate the test statistic and served mostly as a test of normality. AD test p-values < 0.05 indicate that the data does not fit the distribution. Additionally, quantile-quantile (Q-Q) plots of the datasets were tabulated for visual interpretations of the AD test results.

2.3.5 Probability of Clinically Significant Dose Variation

Each fitted distribution has a corresponding cumulative distribution function (CDF(x)) and survival function (SF(x) = 1-CDF(x)) as a function of dose variation of “x”. Evaluating CDFs at some desired value gives the probability of the variable obtaining a value less than or equal to “x”. The same can be said for calculating probabilities greater than or equal to some desired value using a distribution’s survival function, which is one minus a distribution’s CDF. The probability of a patient’s treatment course resulting in an under or overdose of the HRCTV was calculated using the best fitted distribution’s CDF and survival function as shown in Equations (2.4) and (2.5):

Equation 2.4

$$\text{Under dose probability (\%)} = CDF(-5\%) \times 100$$

Equation 2.5

$$\text{Overdose probability (\%)} = (1 - CDF(5\%)) \times 100$$

2.4 Results

2.4.1 Basic Statistics

Fifty patients were analyzed for HRCTV IDVs from the prescribed dose and OAR IDVs from their expected dose. The mean HRCTV EQD_2 DV was $-3.54\% \pm 11.9\%$,

ranging from -37.6% to 11.9%. Nineteen of the 50 patients had their HDR T&O ICBT course result in an average under-dosing of the HRCTV with a mean variation of -11.6%. Ten of the 50 patients had their HDR T&O ICBT course result in an average overdosing of the HRCTV with a mean variation of 7.45%. The Bladder D_{2cc} had the largest IDV range (-51.3% to 61.9%) as indicated in Figure 2.1. By inspection, the OAR distributions appear to take different shapes than the HRCTV distributions despite the variations being relative to each other. The mean and standard deviations for all structures are tabulated in Table 2.1.

Table 2.1. The mean and standard deviation for HRCTV D_{90} , and OAR $D_{0.1cc}$ and D_{2cc} .

Structure and parameter	Mean \pm σ variation (%)
HRCTV D90	-3.54 \pm 11.9
Rectum D2cc	-35.9 \pm 16.8
Rectum D01.cc	0.04 \pm 27.3
Bladder D2cc	-7.27 \pm 19.2
Bladder D0.1cc	54.3 \pm 39.1
Sigmoid D2cc	-38.1 \pm 19.8
Sigmoid D0.1cc	2.18 \pm 35.0

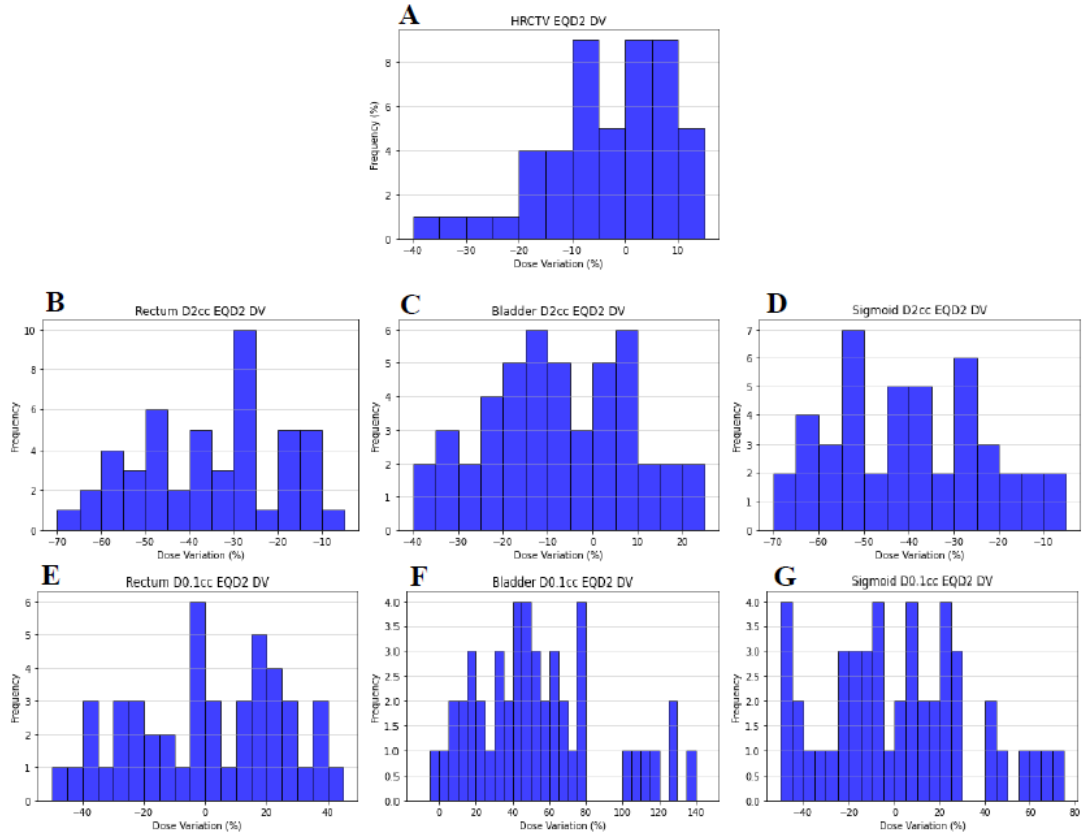


Figure 2.3. Histograms of all evaluated structures (bin width = 5%). Plot A is the HRCTV IDVs, plots B and C are the rectum D_{2cc} and $D_{0.1cc}$, plots D and E the bladder D_{2cc} and $D_{0.1cc}$, plots F and G the sigmoid D_{2cc} and $D_{0.1cc}$, and plots H and I the bowel D_{2cc} and $D_{0.1cc}$.

2.4.2 Correlations

The HRCTV DV and OAR DV had moderate to weak linear correlations with a descending slope. The rectum D_{2cc} and $D_{0.1cc}$ DVs showed statistically significant linear correlations to HRCTV DVs ($p = 0.009$ and 0.035). There were no other statistically significant linear correlations of OAR IDVs to HRCTV IDVs. The rectum D_{2cc} IDV had the strongest R and R^2 values of -0.369 and 0.136 , respectively. Table 2 summarizes the OAR IDVs correlated to HRCTV IDVs.

Table 2.2. Pearson correlation statistics.

Structure and Parameter	<i>R</i>	<i>R</i> ²	<i>p</i>
Bladder D2cc	-0.241	0.058	0.095
Bladder D0.1cc	-0.169	0.028	0.247
Rectum D2cc	-0.369	0.136	0.009
Rectum D0.1cc	-0.302	0.091	0.035
Sigmoid D2cc	-0.144	0.021	0.323
Sigmoid D0.1cc	-0.090	0.008	0.537

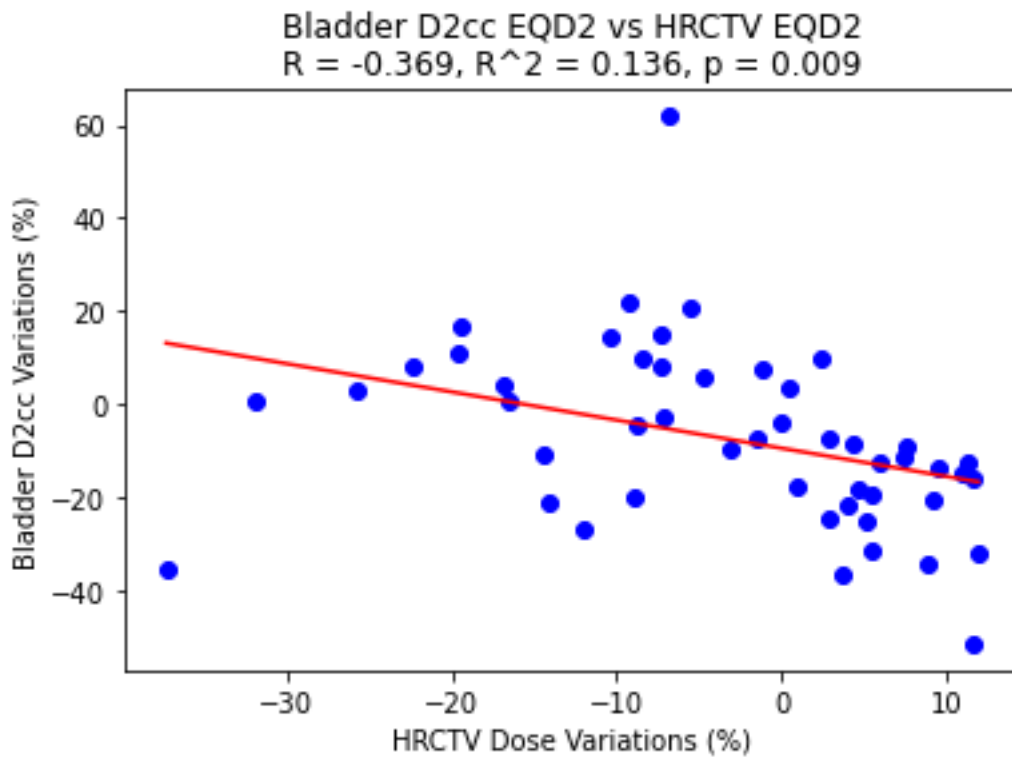


Figure 2.4. Scatter plot of bladder D_{2cc} vs. HRCTV D_{90} . The HRCTV D_{90} IDVs are on the x-axis and the corresponding bladder D_{2cc} IDVs are on the y-axis.

2.4.3 Fitted Distributions

HRCTV DVs are not normally distributed (AD p-value = 0.031). Figure 2.5 displays the best fit distributions for the HRCTV IDVs determined from the distribution fitting, and the corresponding normal distributions if the IDVs were normally distributed.

The best fit distribution for HRCTV IDVs is the left-skewed Generalized-extreme value (GEV, AD p-value = 0.354).

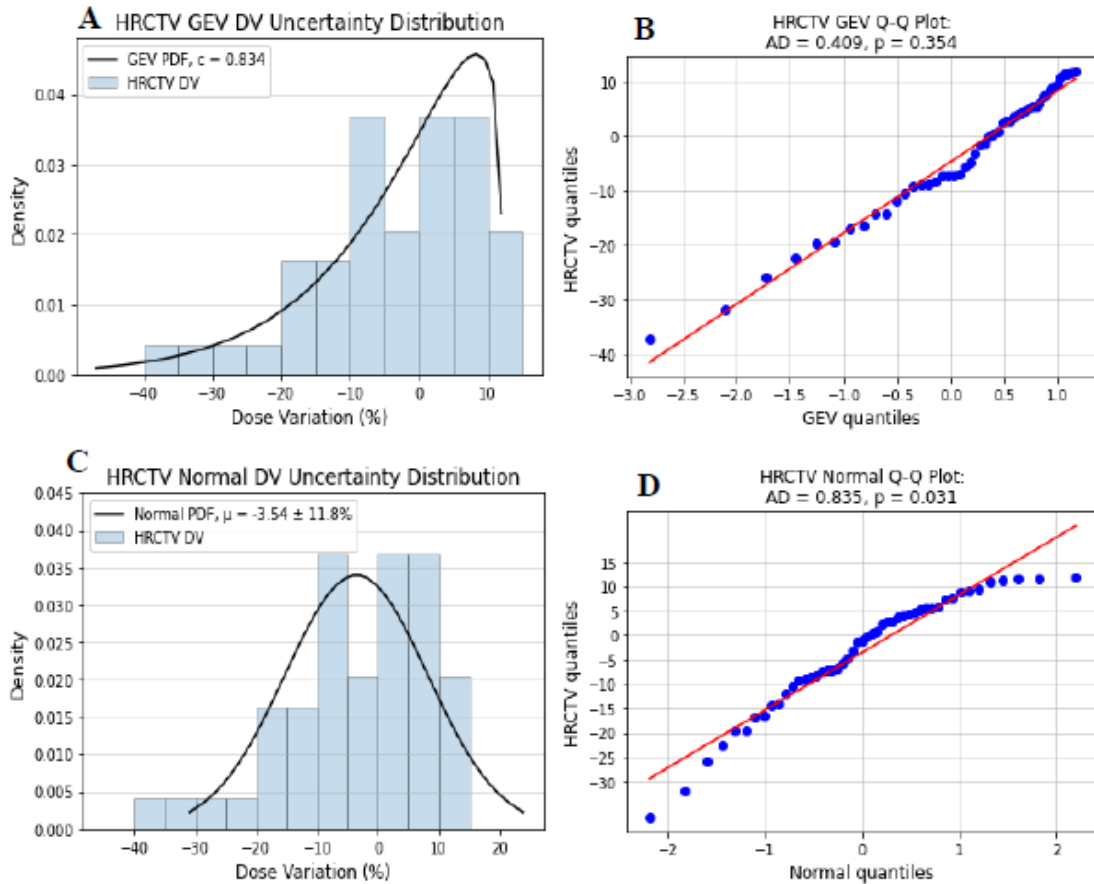


Figure 2.5. Best fitted distributions and a fitted normal distribution for HRCTV D_{90} (A & C) determined from the distribution fitting. The HRCTV IDVs are on the x-axis and the corresponding probability density is on the y-axis. Q-Q plots and Anderson Darling (AD) test results are also tabulated (B & D) to statistically validate the fitted distributions. The respective fitted distribution quantiles are on the x-axis and the HRCTV IDVs are on the y-axis. AD p-values > 0.05 mean the distribution statistically fits the data. AD p-values < 0.05 mean the distributions do not statistically fit the data. From the AD test and Q-Q plots, HRCTV IDVs are not normally distributed.

The calculated probabilities from the GEV and normal distributions' CDF and SF of under (-5% DV) and overdosing (+5% DV) the HRCTV, respectively, are tabulated in

Table 2.3. Recall that the displayed IDVs are calculated from the EQD_2 calculations, thus, the $\pm 5\%$ DV equates to -6.1% and 6.8% (Equation 2.2) in these calculations. The respective distributions' corresponding mean, median, and standard deviations are also tabulated in Table 2.3. The GEV distribution had a higher probability of under-dosing the HRCTV (32.5%), when compared to overdosing the HRCTV (22.5%). Figure 2.6 provides a visual of the HRCTV under and overdosing probabilities calculated from the GEV's CDF.

Table 2.3. Probabilities and statistics from distributions. The probabilities were calculated using the Generalized extreme-value and normal CDF determined from their RSS scores.

	Under-dose probability (%)	Overdose Probability (%)	Significant variation probability (%)	Mean \pm Std (%)	Median (%)
Generalized-extreme Value	32.5	22.5	55.0	-3.44 \pm 13.0	-0.08
Normal	41.4	18.9	60.4	-3.54 \pm 11.8	-3.54

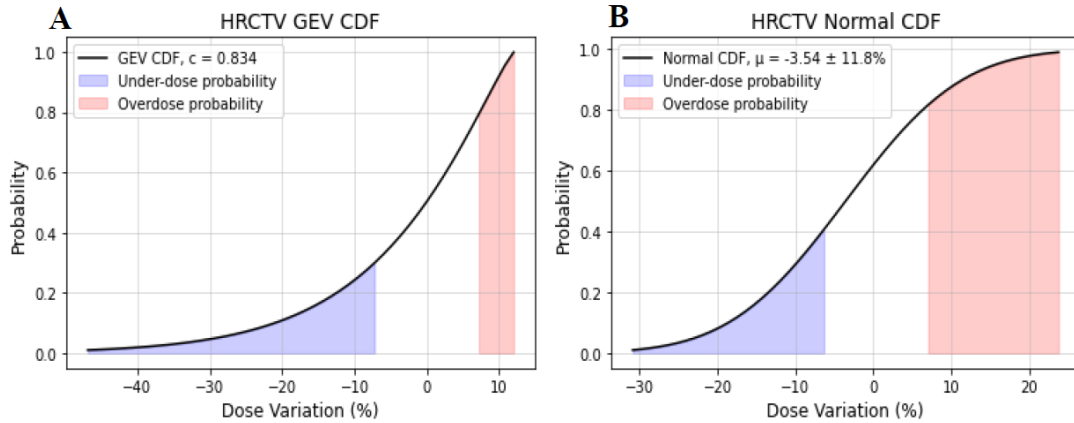


Figure 2.6. Visualized probabilities of under and overdosing the HRCTV Generalized-extreme value and normal distribution CDF. HRCTV IDVs are on the x-axis, and the IDV probabilities are on the y-axis. Under-dosing the HRCTV was defined as HRCTV IDVs less than -5%, overdosing the HRCTV was defined as HRCTV IDVs greater than 5%.

The 95% confidence interval for the mean HRCTV IDV, GEV-calculated under-dose probability, and GEV-calculated overdose probability are tabulated in Table 2.4. The clinically significant IDV probability is implied from the under-dose and overdose probabilities.

Table 2.4. 95% Confidence intervals for HRCTV IDVs from prescription.

Dataset	Variation from prescription
HRCTV D_{90} mean variation	$-3.54\% \pm 2.42\%$
Under-dose probability	$32.5\% \pm 2.62\%$
Overdose probability	$22.5\% \pm 2.62\%$

2.5 Discussion

In this study, HRCTV interfraction dose variations (IDVs) from the prescription and the corresponding effect on OAR dose have been successfully evaluated. We have found large HRCTV and OAR IDVs, the dosimetric effect HRCTV IDVs has on OAR

dose, investigated the non-normality of HRCTV IDV distributions, and identified HRCTV IDV uncertainty as a left-skewed distribution. The dosimetric effect of IDVs has been studied in previous literature. Sharma et al studied IDVs of the target from the prescribed dose at Point A and the IDV of OAR dose for point dose parameters²⁸. They found that the average IDV of Point A doses from prescription was $1.55\% \pm 1.07\%$ and recommended narrowing the $\pm 5\%$ dose variation (DV) constraint. Our results showed larger DVs ($-3.54\% \pm 11.9\%$, range = -37.6% to 11.9%) for volumetric treatment planning, thus, we do not recommend narrowing the $\pm 5\%$ DV constraint due to planner feasibility considerations.

The variation of HRCTV dose is an important issue as it may affect clinical outcomes, however, the clinical effect of it has not been well addressed in the literature. The clinical effects of IDVs are beyond the scope of this chapter, but the clinical significance of the results in this chapter was anticipated and can be estimated based on certain models. Estimated using the dose response curves proposed by Tanderup, et al.²⁵, up to -9.1% change in local control (LC) and 12.4% change in morbidity could be caused by the DVs in this study. This estimate may not be accurate but indicates that IDVs may have significant effects on clinical outcomes. More thorough and systematic analysis will be performed based on biological modeling and clinical data later in this thesis.

Moderate to weak linear correlations between OAR IDVs and HRCTV IDVs were found in this study. A strong linear correlation would indicate that a simple relationship between the respective variations is evident. That is, the cause of the OAR IDVs can simply be explained from HRCTV IDVs. This is not the case. Only the rectum had statistically significant correlations to the HRCTV IDVs, implying that rectal dose is impacted the most by HRCTV IDVs. Also, the R^2 values of 0.091 and 0.136 for the rectum $D_{0.1cc}$ and D_{2cc}

implies that HRCTV DVs roughly accounts for 9.10%-13.6% of the rectal dose uncertainty budget. The lack of statistically significant correlations for the bladder and sigmoid IDVs tells us there is more to the cause of their varying dose than just the HRCTV IDVs, despite the two being relative to each other.

Uncertainties in brachytherapy are assumed to be random and, thus, normally distributed^{26,35}. Nesvacil et al studied the simulated effect of systemic and random uncertainties on tumor control probability (TCP) and normal tissue complication probability (NTCP) models²⁶. Systematic uncertainties were defined as consistent errors that are out of the control of clinicians, and random uncertainties were defined as DVs. They found that that TCP and NTCP models were generally robust to varying degrees of random uncertainties, but systematic uncertainties can affect the models. We have found that HDR T&O brachytherapy IDVs are not normally distributed, and, thus, cannot be assumed as a random uncertainty. The distribution of HRCTV IDVs is left-skewed, meaning there is a higher probability of under-dosing the HRCTV than overdosing it. Assuming a normal distribution would result in either equal probabilities of under and overdosing the HRCTV or overestimate the under-dose probability and underestimate the overdose probability as we have seen from the fitted normal distribution (Table 2.3). The fitted GEV distribution determined from the RSS-score ($32.5\% \pm 2.62\%$, 95% confidence interval) supports the claim that there is a tendency to under-dose the HRCTV throughout a patient's course of treatment, thus meaning the IDV distribution is left-skewed and non-normal. The observed non-random effect of dosimetric variations on TCP and NTCP models and clinical outcomes will be investigated further in this thesis.

The large IDVs found in this study indicated that delivering the prescribed dose to the target while sparing OARs is not always obtainable. Any techniques that can improve target coverage and OAR sparing should be encouraged to apply in clinical practice. Recently, clinical trials of hyaluronate gel injection spacers between the vagina and rectum have shown promising results in reducing rectum dose without sacrificing tumor coverage in GYN brachytherapy^{36,37}. The effect of differing dose per fraction on OAR EQD₂ is recognized in reduced in this chapter. The published version of this chapter used the conservative 80% tolerance to provide a standard and uniform analysis^{27,38,39}. The OAR results of this chapter are in line with the published version: moderate to weak linear correlations. The clinical implications of differing dose prescription on OAR dose uncertainty is recommended for future research.

Interfraction contour variability and OAR motion may also affect IDVs. However, interfraction contour variability and OAR motion were different uncertainties and not the focus of this study. In this study, we accepted the provided contours as the true anatomy and ignored possible OAR motion.

In this study we only evaluated the correlations of HRCTV IDVs on the $D_{0.1cc}$ and D_{2cc} of OARs. However, for larger volume organs such as the sigmoid and the bowel, the D_{5cc} and D_{10cc} via dose surface histograms (DSH) are of clinical interest and are recommended for study purposes by ICRU 89⁸. Volume coverage parameters such as the volume that receives 75% of the dose (V_{75}) for OARs and the volume that receives 100% of the dose (V_{100}) for HRCTV could also be used for evaluating HRCTV IDVs from the prescribed dose⁸. Observations of the radiobiological and clinical effect of HRCTV IDVs will be examined later in this thesis. A proper uncertainty analysis (adding uncertainties in

quadrature) of the observed variations was not conducted in this study and is recommended in future studies^{10,24}.

2.6 Conclusion

Dose variations of the HRCTV from prescription and the corresponding effect on OAR dosimetric parameters were evaluated in this study. Moderate to weak linear correlations existed with HRCTV D_{90} variations from the prescribed dose and OAR dosimetric parameters. HRCTV D_{90} variations from the given prescription were well within the tolerance thresholds of $\pm 5\%$ in mean, but they formed a left skewed distribution best described by the left-skewed Generalized-extreme value distribution that indicated an increased probability to exceed this tolerance with an increased tendency to under-dose the HRCTV. The clinical significance of such dose variations is expected and will be thoroughly and systematically investigated later in this thesis.

CHAPTER 3. DEFINING CLINICAL OUTCOMES IN RADIATION THERAPY

3.1 Locational Disease Control, Recurrence, and Failure

Cancer treatment outcomes are evaluated using the 5-year survival rate¹: the percentage of patients in a study alive five years after diagnosis. The 5-year survival rate is good for evaluating comprehensive cancer treatment but is not ideal for evaluating radiation therapy (RT) clinical outcomes. RT clinical outcomes are evaluated using locational disease metrics such as local control (LC), local recurrence (LR), local failure (LF), regional control (RC), and regional recurrence (RR). LC, LR, and LF are predominantly used in RT due to their locations being in, or closely around the radiation field. RC and RR is defined as disease control or recurrence in the lymph nodes and, or tissue near the primary tumor. RC and RR are not used as often as LC, LR, and LF in RT, but they are still important for evaluating clinical outcomes. Using these locational disease metrics allows for evaluation of only the RT portion of treatment, and not the comprehensive cancer treatment.

Cervical cancer RT outcomes are mostly evaluated using one-to-three-year LC, LR, and LF rates⁴⁰⁻⁴⁹. LC is defined as curing or stabilizing the disease within the true (lesser) pelvis. The true pelvis contains the urinary bladder, colon, and reproductive organs (Figure 3.1). LR is the return of the disease within the true pelvis. LF is the return of the disease within the true pelvis, or residual disease within the true pelvis after completion of RT. RC is defined as stabilizing the disease with in the false (greater) pelvis or pelvic lymph nodes, and RR is the return of the disease within the false pelvis or pelvic lymph nodes⁴³. In this thesis, RC and RR will be defined as pelvic control and recurrence, respectively. Figure 3.1 displays the anatomy of the female true and false pelvis.

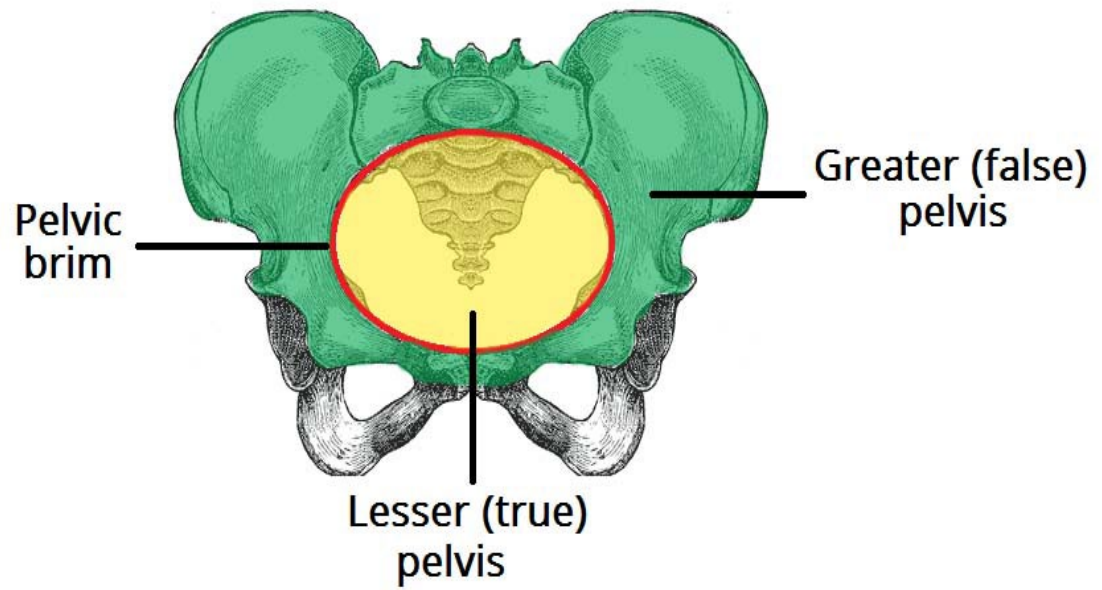


Figure 3.1. Anatomy of the female pelvis displaying the true (lesser) and false (greater) pelvis. The image is from “The Pelvic Girdle.” *TeachMeAnatomy*, <https://teachmeanatomy.com/pelvis/bones/pelvic-girdle/>.

RT has side effects that can result in OAR morbidity. Common cervical RT side effects are rectal bleeding, vaginal bleeding, vasomotor symptoms, urinary incontinence, constipation, diarrhea, and various forms of fistulae. These side effects are graded on a 1-4 scale with increasing severity.

3.2 Dose Response Curves

RT clinical outcome data is discrete, thus logistic and Probit regression techniques are used to derive sigmoid curves as a function of dose. These sigmoid curves are probability curves known as dose response curves. Tumor dose response curves are called tumor control probability (TCP) curves, and OAR dose response curves are called normal tissue complication probability (NTCP) curves. TCP and NTCP curves are standards for predicting and evaluating clinical outcomes in RT.

The therapeutic window can be derived from TCP and NTCP curves. The therapeutic window is a quantitative end point used to evaluate the therapeutic gain and OAR morbidity risk of a particular RT dose. The therapeutic window is the range of RT doses that provide approximately 80-90% LC probability and 10-20% OAR morbidity probability. Figure 3.2 displays an example therapeutic window derived from TCP and NTCP curves.

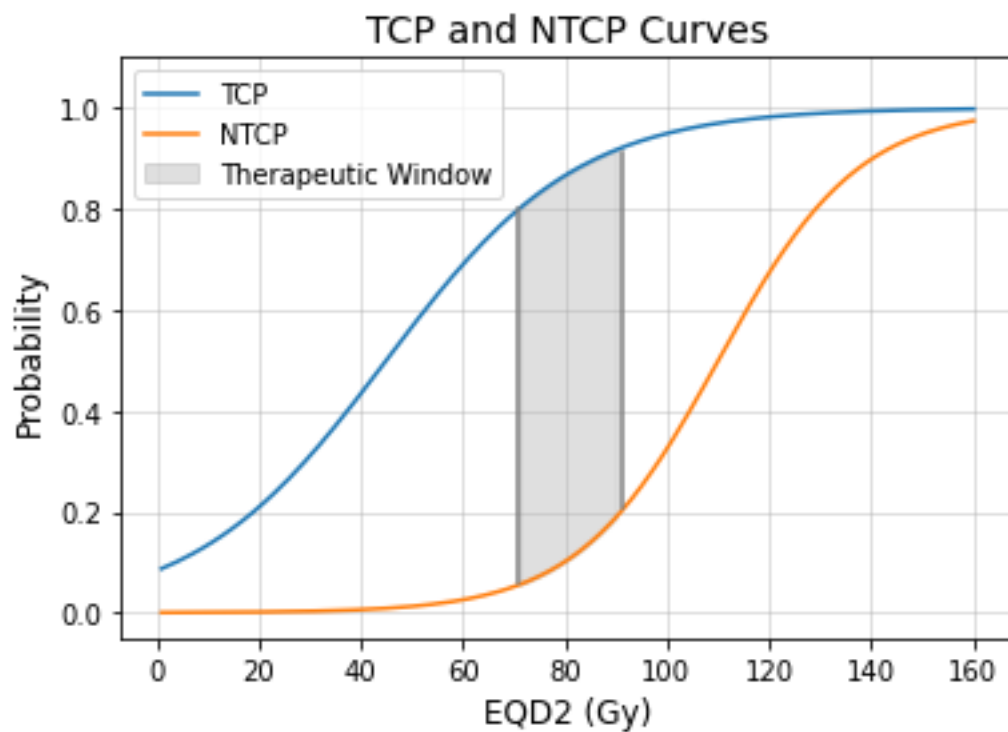


Figure 3.2. An example TCP and NTCP curve displaying the therapeutic window.

3.3 Reference TCP and NTCP Curves Used in this Dissertation

Published cervical cancer RT TCP and NTCP curves were used as a reference in this study. The reference TCP and NTCP curves used Logistic and Probit Regression to derive their dose response curves. Logistic (Equation 3.1) and Probit (Equation 3.2)

Regression have equations to plot their dose response curves using shaping parameters derived from the regression:

Equation 3.1

$$R = \frac{1}{1 + e^{4 \cdot \gamma \cdot (1 - \frac{D}{D_{50}})}} ,$$

Equation 3.2

$$R = 0.5 + 0.5 \operatorname{erf}\left(\frac{t}{\sqrt{2}}\right), \quad t = \frac{D - D_{50}}{(\gamma \cdot \sqrt{2\pi})^{-1} \cdot D_{50}} ,$$

where R is the dose response probability, γ is the steepness parameter representing 1% of disease control change per increase of dependent variable, and D_{50} is the dose of 50% response⁵⁰.

Four TCP curves derived from three-year LC rates of the HRCTV D_{90} dose were used: the TCP curve derived by Tanderup et al.⁴² from the retroEMBRACE data (TCP1, $N = 488$), and the three-tumor size specific TCP curves derived by Dimopoulos et al.⁴¹ (TCP2A-C). The three TCP2 groups were: gross tumor volume (GTV) diameters > 2 cm (TCP2A, $N = 141$) at diagnosis, GTV diameters > 5 cm (TCP2B, $N = 77$) at diagnosis, and HRCTV diameters > 5 cm post-EBRT and pre-brachytherapy (TCP2C). In this thesis, TCP1 and TCP2A served as an aggregate for cervical cancer RT, TCP2B represented large tumors, and TCP2C represented large tumors having a poor EBRT response prior to brachytherapy. All of the reference TCP curves in this thesis were derived from patients treated with MRI-based brachytherapy. The reference NTCP curve was derived by Georg et al.⁵¹ ($N = 141$ patients) from late effects of the rectum and bladder D_{2cc} . Table 1 summarizes the reference TCP and NTCP curves used in this thesis.

Table 3.1. Summary of published dose response curves and their shaping parameters used in this study. Both Logistic and Probit sigmoid equations were used. TCP1 was derived from the retroEMBRACE study of locally advanced cervical cancer (LACC) radiotherapy, TCP2A was derived from patients diagnosed with stage IB-IVA cervical cancer, TCP2B represented large HRCTV size patients, and TCP2C represented a poor response to EBRT pre-brachytherapy. The NTCP was derived from the D_{2cc} of the bladder and rectum.

Study	Model Type	Dose Response Curve	D_{50} (Gy)	γ
Tanderup et al. ⁴² (TCP1)	Logistic	TCP	36.0	0.47
Dimopoulos et al. ⁴¹ (TCP2a)	Probit	TCP (2 cm < GTV)	45.0	0.60
Dimopoulos et al. ⁴¹ (TCP2b)	Probit	TCP (5 cm < GTV)	61.0	1.10
Dimopoulos et al. ⁴¹ (TCP2c)	Probit	TCP (5 cm < HRCTV)	68.0	2.00
Georg et al. ⁵¹ (NTCP)	Probit	NTCP	110	2.00

CHAPTER 4. THE HYPOTHESIZED EFFECTS OF HRCTV AND OAR DOSE VARIATIONS ON CLINICAL OUTCOMES IN HDR BRACHYTHERAPY FOR CERVICAL CANCER

Nomenclature update. Throughout the rest of this thesis, the term “interfractional dose variation (IDV)” is substituted for “dose variation (DV)”. Both terms convey the same thing, the term DV is just more relevant for the rest of this thesis due to the patient data collected.

4.1 Abstract

Purpose. Dose usually varies from the prescribed dose to the target and expected dose for organs at risk (OAR) in adaptive brachytherapy. This study was to investigate the effect of such dose variation (DV) uncertainties on clinical outcomes in high dose rate (HDR), tandem and ovoid (T&O) brachytherapy for cervical cancer.

Materials and Methods. DV uncertainty distributions were calculated from 100 patients diagnosed with FIGO stage IB-IVA cervical cancer and treated with HDR T&O brachytherapy at our institutions from 2018 to 2020. The HDR EQD_2 prescriptions ranged from 6.25-40 Gy ($\alpha/\beta = 10$ Gy). The best fit DV distribution was used for high-risk clinical target volume (HRCTV) DV uncertainty and a normal distribution used as a reference. The best fit DV distribution was used for OARs ($\alpha/\beta = 3$ Gy). An in-house developed Monte Carlo (MC) clinical outcome simulation model was used. MC simulation was used to simulate dose delivery, DV-affected dose response curves, and predict treatment failure rates. The optimal dose and probability of risk-free local control (RFLC) was also calculated using the utility concept. Dose response curves derived from published data served as a reference for all model generated data. Statistical Analysis was done using Student’s t-test and Kolmogorov-Smirnov Two Sample test.

Results. The HRCTV DV distribution was non-normal and left-skewed. Statistically significant differences were observed for treatment failure rates between normal and left-skewed DV distributions. DV uncertainty increased the treatment failure rate by 1.70% (24.1σ), reduced the local control probability by 2.68%, and affected large tumors the most. OAR DV uncertainty reduced the OAR complication probability by 2.64% and 8.88% at 75 Gy and 90 Gy EQD_2 , and theoretically allows for a 10 Gy EQD_2 dose escalation to the HRCTV. Utility with respect to DV uncertainty increased the RFLC probability by 6.70% and predicted an optimal dose range of 83 Gy-91 Gy EQD_2 .

Conclusion. The left-skewed HRCTV DV distribution can increase the treatment failure rate, and reduce the local control probability. Consideration of OAR DV uncertainty can reduce the OAR morbidity and allow HRCTV dose escalation. Utility with respect to DV uncertainty predicts an optimal dose range of 83-91 Gy EQD_2 , consistent with previous studies that used clinical data.

4.2 Introduction

Brachytherapy procedures are subject to varying levels of uncertainties at every step of the brachytherapy process⁹⁻¹¹. Guidance on handling specific uncertainties was provided by the American Association of Physicist in Medicine Task Group 138 (AAPM TG-138), but clinical uncertainties was left for clinicians to investigate. Clinical uncertainties are uncertainties that clinicians have some control over. They include, but are not limited to, structure contouring and motion¹³⁻²³. It is generally accepted that structure contouring and motion are the dominant forms of clinical uncertainties in high dose rate (HDR)

brachytherapy for cervical cancer²⁵. However, other forms of clinical uncertainties exist that can affect dosimetry and clinical outcomes.

Dose to a target or dose to an organ at risk (OAR) can vary from the prescribed dose for the target or the expected dose for the OAR. Such dose variations (DV) are considered a form of uncertainty in adaptive brachytherapy procedures like HDR. HDR brachytherapy is prone to have DVs. Both Hellebust et al.¹⁵ and Nesvacil et al.⁵² successfully quantified a 10% DV uncertainty for the dose delivered to 90% (D_{90}) of the high-risk clinical target volume (HRCTV) as a function of interobserver contour variability and structure motion, respectively, in HDR brachytherapy for cervical cancer. DVs do not dominate the brachytherapy uncertainty budget, but they can still influence dosimetry and clinical outcomes.

The clinical effect of uncertainties can be investigated using biological modeling^{26,53}. Biological modeling simplifies clinical outcome data to a quantitative endpoint. The most common biological models in radiotherapy are tumor control probability (TCP) and normal tissue complication probability (NTCP). Nesvacil et al.²⁶ developed a TCP Monte Carlo (MC) simulation model to hypothesize the clinical effect a 10% DV with a normal distribution has on local control (LC). They found that DVs have a negligible effect on LC at clinically relevant doses, if one assumes DVs are a random uncertainty and normally distributed. In our previous study (Chapter 2) on HDR brachytherapy dosimetry, we found evidence suggesting DVs may not be considered a random uncertainty²⁹. The distribution of actual DVs in HDR brachytherapy for cervical cancer was non-normal and left-skewed. In this chapter, we aim to quantify the clinical

effect of DV uncertainties in HDR brachytherapy for cervical cancer using the DV distributions derived from actual patient data and biological modeling.

4.3 Materials and Methods

4.3.1 Determination of DV Uncertainty Distributions

DVs were calculated from 100 patients diagnosed with FIGO stage IB-IVA cervical cancer and treated with HDR T&O brachytherapy at our institutions from 2018 to 2020. The HRCTV, rectum, bladder, and sigmoid were the structures evaluated in this study. The HDR dose prescriptions ranged from 5-7 Gy for 1-5 fractions, yielding an equivalent dose in 2 Gy fractions (EQD_2) range of 6.25-40 Gy ($\alpha/\beta = 10$ Gy). The HRCTV DVs were calculated from the prescribed brachytherapy EQD_2 , and the OAR DVs from their expected D_{2cc} EQD_2 ($\alpha/\beta = 3$ Gy). The OARs of interest were the bladder, rectum and sigmoid.

Determining best fit DV distributions was described in Chapter 2 and our previous study²⁹. In brief, Python 3.7's DistFit package was used to fit the DV distributions to 89 different probability density functions (PDF). The fits were ranked using residual sum of square (RSS) scores. The DistFit analysis provided the RSS score, shaping parameters, plotting location, and the scale of the PDF.

Five DV distributions were used in this study. The best fit distribution and a normal distribution was used for the HRCTV. The best fit distribution represented the DV from clinical data, and the normal distribution represented DVs as a reference. Only the best fit distribution was used for OARs.

4.3.2 Reference Dose Response Curves

The previously mentioned (Table 3.1) published cervical cancer RT TCP and NTCP curves were used as a reference in this study. TCP1 and TCP2A served as an aggregate for cervical cancer radiotherapy, TCP2B and TCP2C are tumor volume dependent dose response curves, and the one NTCP curve derived by George et al^{41,42,51}.

4.3.3 Monte Carlo (MC) Simulation and Convolution

4.3.3.1 MC Simulation of Patient Treatments and Convolution Process

The effect of DV on dose response was estimated using a convolution method as described in Equation 4.1:

Equation 4.1

$$R'(D) = R(D) \otimes DV(D).$$

Where $R'(D)$ is the convolved dose response curve, $R(D)$ is the reference dose response curve, \otimes is the convolution operator, and $DV(D)$ is the DV uncertainty distribution. Convolution is a “blurring” technique, and is accepted as a method of uncertainty evaluation in RT⁵⁴. An in-housed-developed Monte Carlo (MC) Convolution model was developed using Python 3.7 to evaluate the effect on dose response. MC can increase the statistical power and identify likely trends in the data.

Ten-thousand treatments were simulated at each dose in the range of clinical interest (RoCI) by sampling DVs from DV uncertainty distributions and applying them to said dose. The RoCI corresponded to the total dose of cervical cancer radiotherapy (70 Gy-100 Gy EQD2), implying HDR brachytherapy prescriptions ranging from 25-55 Gy EQD_2

plus 45 Gy of EBRT in 1.8 Gy fractions without any uncertainty applied. This dose with HDR DVs was used to calculate the convolved dose response curve R' .

4.3.3.2 Determination of Treatment Success and Treatment Failure

Treatment failures are generally defined as local recurrences or local failures in cervical cancer radiotherapy clinical outcome studies⁴¹⁻⁴⁹. Treatment responses for all simulated treatments were determined via probabilities from the reference dose response curves and an event simulator. The probabilities obtained from the reference dose response curves only provided the likelihood of a treatment response, they did not simulate a treatment response. An event simulator was used to simulate treatment responses with respect to the likelihood of observing that response. The event simulator dichotomized the data: 1 for treatment response, and 0 for no treatment response.

The treatment failure rate was calculated from the dichotomized data. The percentage of non-treatment responses served as the treatment failure rate for the HRCTV. The treatment failure rate was also calculated without DV uncertainty to serve as a control variable. The model was iterated 30 times to satisfy the central limit theorem for a valid t-test, and to account for the lack of a desired value and cost function use. Without a desired value, a cost function could not minimize the solution space and chose one output. Thus, mean treatment failure rates predicted by the model determined the likely output.

4.3.4 Model Generated R' Shaping Parameter Estimation

The shaping parameters for the Logistic and Probit sigmoid equations are D_{50} and γ (Equations 3.1 and 3.2). These parameters can be estimated from likelihood estimations or analytically^{55,56}. The parameters were estimated analytically in this study. The D_{50}

estimation was determined from inspection of the dose of 50% response on the plotted model generated R' curves. From the known R' and D_{50} , the γ parameter was calculated by solving for γ in Equations 3.1 and 3.2.

4.3.5 Utility Concept

The probability of risk-free local control (RFLC) can be computed from a TCP and NTCP curve. This is known as the utility of a treatment, and was proposed by Schultheiss et al.⁵⁷ and used by Boyer et al.⁵³. Analytically, utility is defined as:

Equation 4.2

$$U(D) = TCP(D) \cdot (1 - NTCP(D)).$$

Where $U(D)$ is the utility function, and $TCP(D)$ and $NTCP(D)$ are the dose response curves. Subtracting the NTCP by one gives the probability of not having a complication. Thus, multiplying this probability by the TCP gives the probability of RFLC. The dose of maximum RFLC probability is the predicted optimal dose. Utility can be thought of as a probability or likelihood quantification of the therapeutic ratio or window. The utility of the simulated dose response curves, R' , was calculated for every R' in this study, and was evaluated against the utility of the reference dose response curves.

4.3.6 Statistical Analysis

Statistical analysis was done using Python 3.7's SciPy Statistics package. Student t-test and Kolmogorov-Smirnov Two Sample (KS2) test were used to compare the model generated R' curves to the reference dose response curves. The Student's t-test compared the means of the curves in the RoCI, and the KS2 test compared the distribution of

probabilities within the curves. The Student's t-test was also used for the treatment failure rate and utility curve analyses.

Dose response probability differences in the RoCI were also evaluated. The clinically relevant doses in this study were 75 Gy, 80 Gy, 85 Gy, 90 Gy, and 95 Gy EQD_2 . The 65 Gy and 70 Gy EQD_2 were added for OAR NTCP evaluation. Dose response probabilities greater than 1% at these doses were of interest in this study⁵⁸. The 85 Gy probability differences was deemed most important due to prescription recommendations from literature^{2,41,42}.

4.3.7 Model Accuracy Testing

The model was tested by running a simulation on the reference dose response curves without any DV uncertainty applied. The expected dose response curve and failure rate is known from the reference dose response curves. As mentioned in section 4.3.3.2, this served as the control variable for the treatment failure rate analyses, too. Deviations from the reference curve was the model's statistical uncertainty.

4.4 Results

4.4.1 HRCTV and OAR Dose Variations

The DV uncertainty distributions used by the two simulation models are summarized in Table 1. The best fit DV uncertainty distribution for the HRCTV was the Beta distribution. This Beta distribution is non-normal, left skewed, and consistent with the generalized extreme value (GEV) distribution from Chapter 2²⁹. This Beta distribution had a mean DV = $-1.53\% \pm 11.0\%$. The normal distribution with a 0.00% mean DV and

standard deviation consistent with the Beta distribution was created for comparison. A Beta distribution was also the best fit for the bladder ($-5.97\% \pm 21.2\%$). The Double Weibull distribution was the best fit for the rectum ($-41.8\% \pm 18.1\%$), and the GEV was the best fit for the sigmoid ($-38.3 \pm 19.3\%$). Figure 4.1 displays the DV uncertainty distributions used in this study.

Table 4.1. Distribution statistics for the target dose variation (DV) uncertainty distributions used in this study. The Double Weibull, Beta, and GEV distributions represented the rectum, bladder, and sigmoid, respectively.

Data	Distribution	Location	Scale	Shaping parameter(s)	Mean DV (%)	Std (%)
HRCTV Beta	Beta	-0.90	1.06	9.79, 1.94	-1.53	11.0
HRCTV Normal	Normal	0.00	0.11	n/a	0.00	11.0
Rectum	Double Weibull	-0.42	0.17	1.58	-41.8	18.1
Bladder	Beta	-0.87	2.47	9.52, 19.5	-5.97	21.2
Sigmoid	GEV	-0.46	0.18	0.17	-38.3	19.3

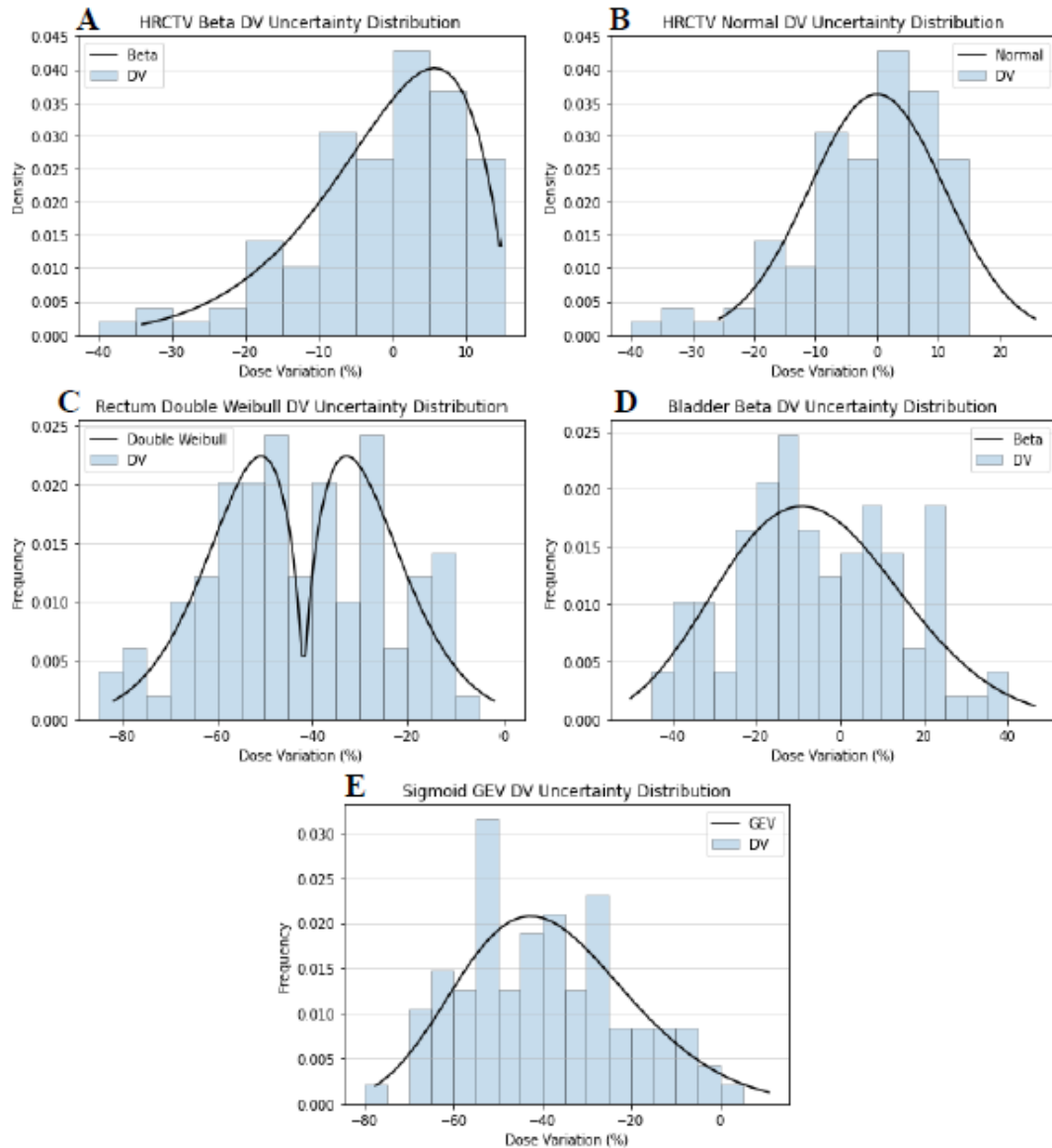


Figure 4.1. The five DV uncertainty distributions used in this study for DV sampling. The Beta (A) was the best fitted DV distribution for the HRCTV. The HRCTV Normal distribution (B) represented an 11% random uncertainty. The Double Weibull (C), Beta (D), and Generalized-Extreme Value (GEV) (E) distributions represented the rectum, bladder, and sigmoid DV uncertainty, respectively.

4.4.2 Model Generated R' Shaping Parameters

Differences in shaping parameters were observed for the model generated R' curves vs the four reference TCP curves. A 4.5 and 4.7 Gy D_{50} difference was observed for the

Beta and Normal-sampled R' curves vs TCP2A. Negligible shaping parameter differences were observed for the model generated R' curves vs the other reference TCP curves.

Differences in shaping parameters were also observed for OARs. A 23, -2, 15, and 8 Gy D_{50} difference was observed for the bladder (133 Gy), rectum (108 Gy), sigmoid (125 Gy), and composite OAR (118 Gy) R' curves. A 0.36, 0.43, 0.38, and 0.41 γ difference was observed for the bladder (2.36), rectum (2.43), sigmoid (2.38), and composite OAR (2.41) R' curves.

4.4.3 Effects of Dose Variation Uncertainty on TCP and NTCP

The model-generated R' curves had up to -3.88% LC probability differences from the reference TCP curves. Up to -1.31% differences in TCP were found between the Beta and Normal DV affected responses. At 85 Gy EQD_2 , the optimal dose prescription, TCP2B showed sensitivity to the Beta DV uncertainty distribution (-1.59%), and TCP2C showed sensitivity to both DV uncertainty distributions (-2.68% and -1.51% for the Beta and Normal-sampled R' curves, respectively). The TCP1 and TCP2A were robust to DV uncertainty. Table 4.2 summarizes, and Figure 4.2 displays the LC differences from the reference TCP curves.

Table 4.2. Local control differences of R' from the reference curves for Beta and Normal distribution DV uncertainty sampling.

Reference TCP	TCP1		TCP2A		TCP2B		TCP2C	
	Beta	Normal	Beta	Normal	Beta	Normal	Beta	Normal
75 Gy	-0.78	-0.50	-1.21	-0.80	-2.17	-1.44	-3.88	-2.78
80 Gy	-0.73	-0.46	-0.96	-0.54	-1.76	-0.99	-3.11	-1.80
85 Gy	-0.67	-0.41	-0.86	-0.46	-1.59	-0.86	-2.68	-1.51
90 Gy	-0.60	-0.36	-0.84	-0.48	-1.56	-0.91	-2.35	-1.46
95 Gy	-0.52	-0.31	-0.85	-0.53	-1.56	-1.01	-1.93	-1.31

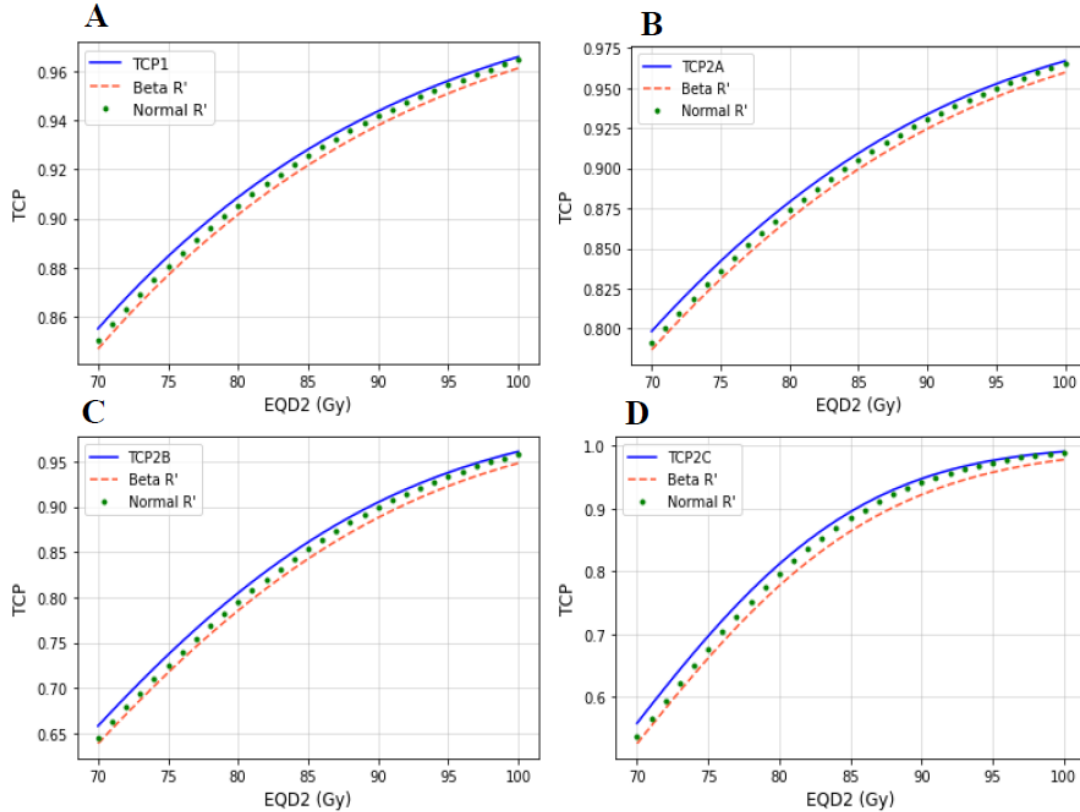


Figure 4.2. Comparison between the reference, Beta-sampled, and Normal sampled TCP curves. A. TCP1; B. TCP2A; C. TCP2B; D. TCP2C.

Statistically significant differences from the reference NTCP curve was observed for OARs. The rectum and sigmoid R' curves were statistically different for the t-test. The rectum, sigmoid, and composite R' curves were statistically different for the KS2 test. The recommended EQD_2 dose limit for the rectum and sigmoid of 75 Gy had a -3.90% and -3.35%, respectively, CP difference from the reference NTCP curve. The recommended dose limit for the bladder had a complication probability difference of -1.47% at 90 Gy. The composite OAR R' curve had a -1.47% and -8.88% CP difference at 75 and 90 Gy, respectively. The results are summarized in Table 4.3. Figure 4.3 displays NTCP curves for the three organs at risk. It shows all four curves experienced a reduction in complication

probability in the RoCI. A 10 Gy HRCTV dose escalation was also observed from the CP differences in Figure 3.

Table 4.3. Statistical analysis and differences in complication probability between R' and R for the OARs.

	Statistics		Complication Probability (CP) Difference (%)						
	t-test	KS2	65 Gy	70 Gy	75 Gy	80 Gy	85 Gy	90 Gy	95 Gy
Rectum	< 0.001	0.001	-1.21	-2.27	-3.90	-6.26	-9.46	-13.5	-18.3
Bladder	0.699	0.068	0.04	-0.24	-0.63	-1.09	-1.45	-1.47	-0.86
Sigmoid	< 0.001	0.016	-0.98	-1.91	-3.35	-5.42	-8.17	-11.6	-15.4
Composite	< 0.001	0.068	-0.71	-1.47	-2.64	-4.28	-6.40	-8.88	-11.5

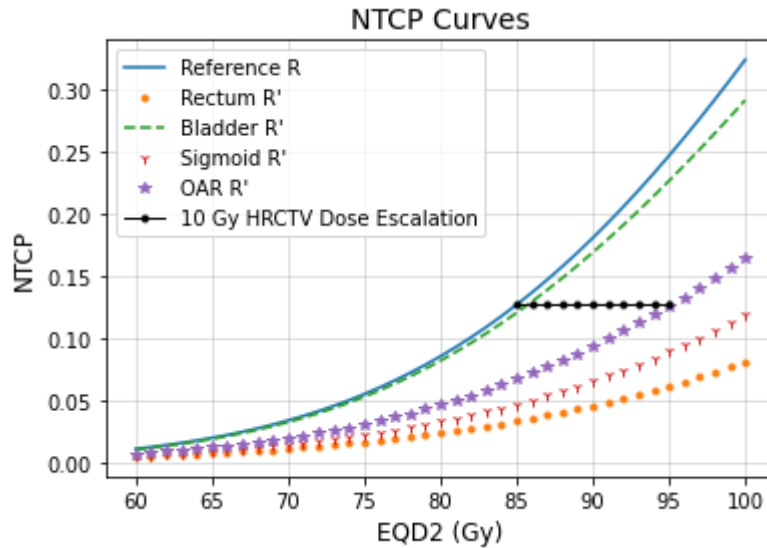


Figure 4.3. Comparison of NTCP curves between R' and R (rectum, bladder, sigmoid, and composite of the three organs). A 10 Gy HRCTV dose escalation from 85-95 Gy was observed.

4.4.4 Treatment Failure Rates

Statistically significant differences were observed for the Beta-sampled and Normal-sampled treatment failure rates against the control treatment failure rates (Table 4.4). Figure 4.4A,C,E,G visualizes the difference in magnitude that Beta-sampled and Normal-sampled DV uncertainty had on failure rates. The Beta-sampled failure rates were 7.00σ (TCP1), 18.3σ (TCP2A), 14.3σ (TCP2B), and 24.1σ (TCP2C) away from the control

failure rates. The Normal-sampled failure rates were 2.20σ (TCP1), 6.67σ (TCP2A), 6.00σ (TCP2B), and 12.1σ (TCP2C) away from the control failure rates. The Beta-sampled failure rates were statistically different from the control failure rate at every prescription dose in the RoCI for all four reference TCP curves (Figure 4B,D,F,H). The Normal-sampled failure rates had variable p-values for lower prescription EQD_{2s} , but was statistically different at higher prescription EQD_{2s} (Figure 4B,D,F,H).

Table 4.4. Statistical analysis of predicted treatment failure rates.

Reference Curve	Control Failure Rate (%)	Beta-sampled Failure Rate (%)	t-test p-value	Normal-sampled Failure Rate (%)	t-test p-value
TCP1	8.11 ± 0.05	8.46 ± 0.05	< 0.001	8.22 ± 0.05	< 0.001
TCP2A	10.5 ± 0.03	11.0 ± 0.07	< 0.001	10.7 ± 0.05	< 0.001
TCP2B	16.6 ± 0.07	17.6 ± 0.07	< 0.001	17.0 ± 0.07	< 0.001
TCP2C	16.1 ± 0.07	17.8 ± 0.09	< 0.001	17.0 ± 0.07	< 0.001

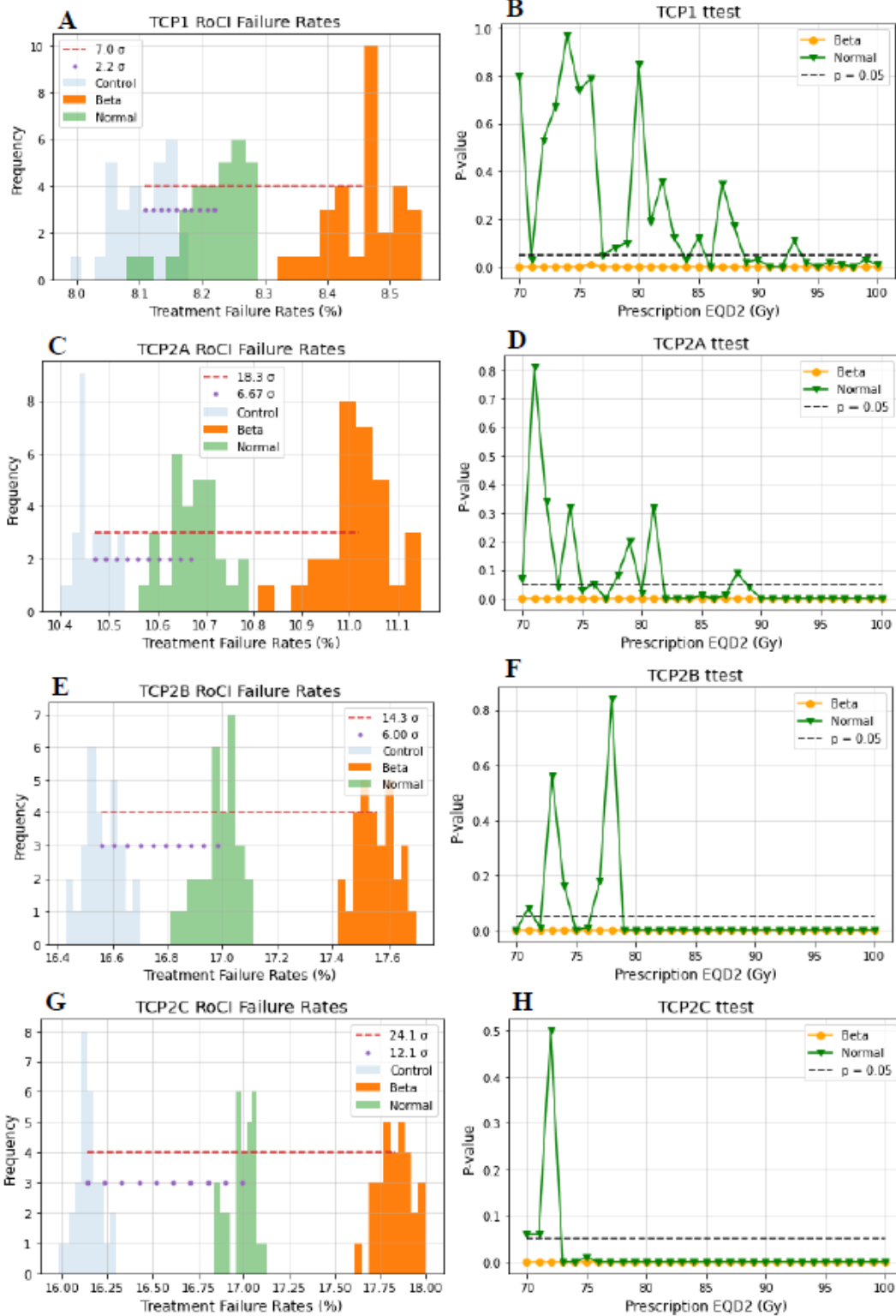


Figure 4.4. Treatment failure rate predictions and analysis.

4.4.5 Utility Analysis

The utility curves were derived from the DV uncertainty dose response (R') and reference dose response (R) as shown in Figure 4.5. Differences in RFLC probability and optimal dose were observed for R' and R . The peak-to-peak comparison shows that the maximum RFLC probability increase was 13.2% for TCP2C utility, this was observed from the HRCTV-rectum utility calculation. This yielded an optimal dose increase of 14 Gy. The HRCTV-composite OAR curve (average of the rectum, bladder and sigmoid curves) utility yielded an optimal dose range of 83-91 Gy EQD_2 . Table 4.5 summarizes these results.

Table 4.5. Comparison of optimal doses (EQD_2) and corresponding utilities (U) calculated with DV and without DV (reference).

Utility Curve	TCP1		TCP2A		TCP2B		TCP2C	
	EQD_2 (Gy)	U (%)	EQD_2 (Gy)	U (%)	EQD_2 (Gy)	U (%)	EQD_2 (Gy)	U (%)
Reference	76	82.1	80	79.0	86	74.1	87	77.4
HRCTV & Rectum DV Uncertainty	90	89.5	93	88.4	97	86.4	96	89.6
HRCTV & Bladder DV Uncertainty	78	83.6	81	80.5	86	75.1	87	77.6
HRCTV & Sigmoid DV Uncertainty	86	88.0	89	86.5	94	83.7	93	87.0
HRCTV & Composite OAR DV Uncertainty	83	86.4	86	84.4	91	80.8	91	84.0

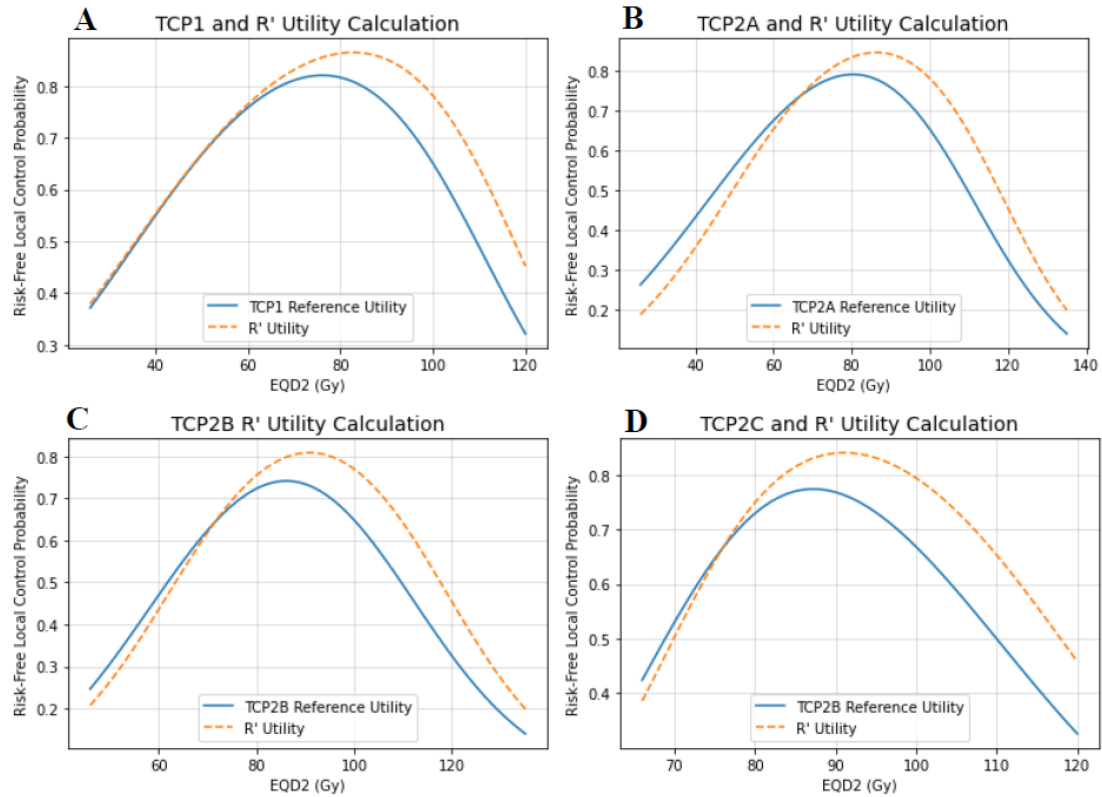


Figure 4.5. Utility curves for R' and R. A. TCP1; B. TCP2A; C. TCP2B; D. TCP2C.

4.5 Discussion

Multiple clinical outcome simulations under the influence of dose variations (DV) from the prescribed or expected dose was successfully conducted. We have doubled our sample size and found that DV uncertainty is still non-normal and left skewed. This supports our hypothesis that DV uncertainty is not random and is indicative of underdosing the HRCTV in HDR brachytherapy for cervical cancer. It has been shown that DV uncertainty can result in higher treatment failure rates, reduced local control (LC) probabilities, and reduced morbidity probabilities. It has also been shown that consideration of HRCTV and OAR DV uncertainty yields an optimal dose consistent with recommended cervical cancer radiotherapy prescriptions.

DV uncertainty in adaptive procedures is usually not the most significant portion of the brachytherapy uncertainty budget. However, it has been shown that DVs are relevant for clinical investigation. As mentioned prior, literature suggests a 10.0% DV uncertainty^{15,52}. Nesvacil et al. used these findings to simulate the clinical effect of DV uncertainty²⁶. DVs were assumed to be normally distributed and a random uncertainty. They concluded that DVs have a minor effect on dose response curves when viewed as a random uncertainty, but systematic uncertainties can cause LC probability differences by as much as 5% at 85 Gy EQD_2 . Our results both agreed and disagreed with their findings. Our results agreed that DV uncertainty has a minor effect on dose response curves in the range of clinical interest (RoCI, 70 Gy-100 Gy EQD_2) for aggregate TCP curves (TCP1 and TCP2A). However, our results also showed that DV uncertainty affects larger tumors in the RoCI. Recall that reference curves TCP2B and TCP2C represented GTV diameters > 5 cm at diagnosis, and HRCTV diameters > 5 cm at the time of brachytherapy, respectively⁴¹. Our model predicted the largest differences in LC probability (-2.17% and -3.88%, Table 4.3 and Figure 4.2) and treatment failure rate (1.0% and 1.7%, Table 4.4 and Figure 4.4) for TCP2B and TCP2C, respectively. This suggests an increased sensitivity to DV uncertainty for patients with larger tumors.

Of note, the predicted treatment failure rate was significantly elevated for DV sampling from the Beta distribution. The Beta-sampled failure rates were 2-3 σ further from the reference failure rates than the Normal-sampled failure rate, and all Beta-sampled failure rates in the RoCI were statistically different from the reference failure rates (Figure 4.4). Thus, treatment failure is not just sensitive to DV uncertainty, but it is also sensitive to the type of DV uncertainty. The Beta distribution in this study was derived from clinical

DVs, and is indicative of HRCTV coverage loss. There are ways to mitigate DV uncertainty and lack of coverage. For instance, one can add packing or spacers to increase the distance between the target and OARs in HDR intracavity brachytherapy. Also, interstitial brachytherapy can increase dose coverage and reduce the effects of DV uncertainty^{2,36,37,59-61}, but procedures are recommended to have only one or two implantations to reduce morbidity and thus patients need to stay in hospital with the implants for a couple of days²⁸. This makes HDR brachytherapy an inpatient procedure, reducing a major advantage of it. Those methods can be tested in future studies.

Limiting OAR dose is often the secondary objective in RT. OAR DV uncertainty leads to a drastic shift in the convolved NTCP curve. This broadens the therapeutic window and can allow for a 10 Gy EQD_2 dose escalation to the HRCTV (Figure 4.4). A 10 Gy EQD_2 HRCTV dose escalation is similar to an additional 7 Gy HDR fraction. This result is consistent to what has been found in other simulation and clinical studies^{26,36,37,59}. Dose escalation was also observed for the utility calculations under the influence of HRCTV and OAR DV uncertainty. The utility of a treatment is the probability of risk-free local control (RFLC), and is analogous to the therapeutic ratio or window. The DV uncertainty utility calculations resulted in optimal doses ranging from 83-91 Gy. Not only was this a shift to higher doses from the reference utility calculations, but the predicted optimal doses are consistent with conclusions from clinical outcome studies. It is accepted that at least 85 Gy EQD_2 is the optimal dose in cervical cancer radiotherapy^{2,41,42}, and that 90 Gy-95 Gy EQD_2 is advantageous for larger tumors. The DV uncertainty utility predictions agreeing with these studies are encouraging for its clinical use.

Our results show DV uncertainty has a noticeable clinical effect, but limited consideration of patient tumor volume for the DV uncertainty distribution calculation is a limitation of this study, for that could affect the dosimetry and the simulated clinical outcomes. It has been shown that Logistic and Probit dose response curves have inherent uncertainties⁵⁵. Thus, these inherent uncertainties and inaccuracies are also considered a limitation in this study. There is an emphasis in the literature to use additional parameters to evaluate dosimetry and predict clinical outcomes^{21,23,30,41,42,59,62,63}. The inclusion of multiple parameters such as volume, tumor size, tumor asymmetry, and dose location will all be of interest for future research. Interfraction contour variability and CT delineation uncertainty were not considered in this study but will be discussed in future research, too.

4.6 Conclusion

Dose variations (DV) in HDR brachytherapy for cervical cancer have significant effects on clinical outcomes. This study shows that HRCTV DV uncertainty is not a random uncertainty due to its left-skewed distribution. HRCTV DV uncertainty increases the treatment failure rate and reduces local control probability, especially for large tumors. The reduction in OAR complication probability theoretically allows for a 10 Gy EQD_2 dose escalation to the HRCTV. The utility of a cervical radiotherapy treatment scheme was also introduced in this study. Evaluation of utility under the influence of HRCTV and OAR DV uncertainty predicts the optimal dose of risk-free local control to be in the range of 83-91 Gy EQD_2 .

CHAPTER 5. THE CLINICAL EFFECT OF DOSE VARIATION UNCERTAINTY FOR CERVICAL CANCER HIGH DOSE-RATE (HDR) BRACHYTHERAPY

5.1 Abstract

Purpose. To determine the effect that dose variation (DV) uncertainty and relative dosimetry has on clinical outcomes.

Materials and Methods. Local control (LC), local recurrence (LR), local failure (LF), pelvic control, and pelvic recurrence were evaluated for 117 cervical cancer patients. Eighty-four of the 117 patients were locally advanced cervical cancer (LACC) patients. Logistic regression was used for Dose, DV, the conformal index (COIN), conformity index (CI), the COIN isodose gradient parameter (c_2), and high-risk clinical target volume (HRCTV) to determine their clinical outcome dependencies. A threshold prescription dose of 75 Gy for high and low dose prescription treatments, and a threshold HRCTV of 35 cm^3 for large and small HRCTVs was also used for analyses. McFadden's Pseudo R^2 p-values were used for logistic regression fits, and Student's t-test for comparing treatment success versus treatment failure parameters.

Results. Dose ($p < 0.001$ and $p = 0.033$), DV ($p = 0.045$ and 0.027), COIN ($p = 0.044$ and 0.031), and c_2 ($p = 0.032$ and 0.012) all had statistically significant logistic regression fits with LC and pelvic control. HRCTV had a statistically significant logistic regression fit with LC ($p = 0.044$).

Conclusion. DV uncertainty, relative dosimetry, and HRCTV size all effect clinical outcomes. Approximately 5% and 1.4% DVs can affect 1% of LC and pelvic control,

respectively. Lower COIN and c_2 values improve LC probabilities. Approximately 1% of LC is lost for every 7.23 cm^3 increase in HRCTV.

5.2 Introduction

The dosimetric and hypothesized clinical effect of dose variation (DV) uncertainty has been thoroughly investigated in this thesis. As we have seen in Chapters 2 and 4, DV uncertainty is a left skewed distribution that is indicative of high-risk clinical target volume (HRCTV) dose coverage loss. We know from our statistical models in Chapter 2 we know there is approximately a 32.5% probability (Table 2.3, Figure 2.6A) that a patient's high dose-rate (HDR) tandem and ovoid (T&O) brachytherapy treatment will result in a clinical under-dosing event per American Brachytherapy Society (ABS) guidelines ($\pm 5\%$ DV)²⁷. Also, we know that known DV uncertainties can hypothetically reduce local control (LC) probabilities by as much as 2.68% and increase the local recurrence (LR) or local failure (LF) rates by as much as 1.70% (24.1σ , $p < 0.001$) from our findings in Chapter 4. From the observed effects of DV uncertainty we have shown, we must investigate DV uncertainty's true clinical effects.

DV can be related to dose conformity. Dose conformity indices are plan quality metrics used to evaluate treatment plans. They are often used to evaluate external beam radiation therapy (EBRT) treatment plans, but they can also be used to evaluate brachytherapy treatment plans. Dose conformity is of interest in brachytherapy due to the prevalent use of volumetric treatment planning. The clinical effect of tumor size is known in brachytherapy: Tanderup et al. found that an additional 5 Gy EQD_2 is required for every additional 10 cc of HRCTV⁴². Despite dose conformity being related to volumetric

parameters, the clinical effects of dose conformality are still unknown. Only the dosimetry of dose conformality in brachytherapy has been investigated in the literature⁶⁴⁻⁶⁷.

Due to the known effects of DV uncertainty uncovered in this thesis, and the lack of brachytherapy dose conformality clinical outcome research, we aim to quantify the clinical effects of DV uncertainty and dose conformality.

5.3 Materials and Methods

5.3.1 Patient Selection

One-hundred and seventeen cervical cancer patients were selected for this chapter. The patient characteristics are comparable to what was chosen for Chapters 2 and 4. The 117 patients were staged I-IVB and were treated at our institution from January 2017 to January of 2021. Patients received 3-month follow ups for the first year, and 6-month follow ups from then on out.

5.3.2 Dosimetric Parameters

The HRCTV dose of interest was D_{90} and the OAR dose of interest was D_{2cc} . HRCTV and OAR DV uncertainty was calculated as defined in Equation 2.1. Two conformity indices were used in this study to quantify volumetric dose coverage. The first was a standard RT conformity index (CI), and the second was conformal index (COIN) for HDR brachytherapy⁶⁷. The COIN is also known as the Paddick CI⁶⁸ in stereotactic radiosurgery and is comprised of two components.

Equation 5.1

$$c_1 = \frac{HRCTV_{Rx}}{HRCTV},$$

where $HRCTV_{Rx}$ is the volume of the HRCTV receiving the prescription dose, and $HRCTV$ is the target volume. This also standard radiation therapy, CI (CI (%) = $c_1 \cdot 100$).

Equation 5.2

$$c_2 = \frac{HRCTV_{Rx}}{Vol_{Rx}},$$

where Vol_{Rx} is the prescription isodose volume. By definition, DV is directly proportional to c_2 . Thus, COIN is defined as:

Equation 5.3

$$COIN = c_1 \cdot c_2,$$

COIN accounts for HRCTV coverage with c_1 and the irradiation of normal structures just outside of the HRCTV with c_2 . Also, c_2 serves as an isodose gradient parameter.

5.3.3 Clinical Outcomes

One, two, and three-year LC, LR, LF, pelvic control, and pelvic recurrence rates were calculated for all 117 cervical cancer patients. Recall from Chapter 3 that LC, LR, and LF refers to the true (lesser) pelvis, and pelvic control and recurrence refers to the false (greater) pelvis and pelvic lymph nodes. One, two, and three-year dose response curves were derived from the LF, LR, and pelvic data using logistic regression. The dose response curves derived from the LF data provided the probability of non-LF as a function of dose. The dose response curves derived from LR data provided the probability of achieving LC as a function of dose. The dose response curves derived from pelvic data provided the probability of achieving pelvic control as a function of dose. Logistic regression was also used for the LF, LR, and pelvic recurrence datasets as a function of DV, COIN, CI, c_2 and tumor volume. Shaping parameter estimation was conducted as described in section 4.3.4.

A threshold dose and volume were used for the HRCTV. The threshold dose was 75 Gy EQD2⁴⁰ and the threshold volume was 35 cc⁵⁹. High and low dose treatments were above and below 75 Gy, large and small HRCTVs were above and below 35 cc.

5.3.4 Utility

The utility was calculated as described in Section 4.3.5, Equation 4.2. The utility was only calculated for the three-year locally advanced cervical cancer (LACC) LR-TCP curve to compare to the reference TCP1 and TCP2A curves derived from LACC patient data. The reference normal tissue complication probability (NTCP) curve was used for all three utility calculations.

5.3.5 Statistical Analysis

Logistic regression fits were evaluated using MLE and McFadden's Pseudo R^2 for p-values. Two tailed t-tests were used to evaluate LF versus no LF, LC versus LR, and pelvic control versus pelvic recurrence for DV, COIN, CI, and c_2 . A right tailed t-test was used for dose, and a left tailed t-test was used for HRCTV size.

5.4 Results

Table 5.1 summarizes the variables in this study. The median follow-up time was 26.1 months, and the median age was 47.6 years old. One-hundred and seventeen patients were evaluated for the three-year data, 109 for the two-year data, and 94 for the one-year data. The mean dose delivered, HRCTV size, DV, COIN, CI, and c_2 was 75.8 ± 9.42 Gy, 45.7 ± 20.2 cc, $-0.19 \pm 10.9\%$, 0.42 ± 0.08 , $88.9 \pm 5.01\%$, and $46.9 \pm 9.40\%$ for all cervical cancer patients. Eighty-four locally advanced cervical cancer (LACC) patients were

evaluated in this study. The LACC patient’s mean delivered dose, HRCTV size, DV, COIN, CI, and c_2 was 77.3 ± 9.48 Gy, 46.9 ± 20.3 cc, $-1.13 \pm 11.1\%$, 0.42 ± 0.08 , $88.5 \pm 5.20\%$, and $47.9 \pm 9.30\%$ (Table A3.4). DV, COIN, CI, and c_2 had minor changes between all patients, high dose treatments (Table A3.1), low dose treatments (Table A3.2), large HRCTV size (Table A3.9), and small HRCTV size (Table A3.10). The mean dose delivered for high dose treatments was 81.7 ± 6.16 Gy (Table A3.1) and the mean dose for low dose treatments was 66.7 ± 5.68 Gy (Table A3.2). The mean HRCTV size was 57.2 ± 19.0 cm^3 for large HRCTVs (Table A3.9) and 30.2 ± 7.17 cm^3 (Table A3.10) for small HRCTVs.

The 3-year LC, LF, and pelvic control rates were 86.2%, 28.4%, and 69.8% for all patients, and 77.4%, 28.6%, and 65.5% for LACC patients. Stage I and II had CIs above 90% and had the highest LC rates at 93.5% and 77.8% for all patients, respectively. Stage II had the highest LF rate at 33.3% and stage III had the lowest LF rate at 28.9%.

Table 5.1. Statistics of all dependent and independent variables.

	N	HRCTV (cc)	EQD2 (Gy)	DV %	COIN	CI	C2	LC (%)	LR (%)	LF (%)	RC (%)	RR (%)
1-Year	94	45.7 ± 20.5	75.8 ± 9.07	0.18 ± 10.5	0.42 ± 0.08	89.1 ± 4.69	47.1 ± 9.5	86.2	14.9	23.4	74.5	26.6
2-Year	109	46.7 ± 20.4	75.8 ± 9.49	-0.50 ± 10.9	0.42 ± 0.08	88.8 ± 5.03	47.3 ± 9.4	81.7	19.3	27.5	69.7	31.2
3-Year	116	45.7 ± 20.2	75.8 ± 9.42	-0.19 ± 10.9	0.42 ± 0.08	88.9 ± 5.01	46.9 ± 9.4	81.0	19.8	28.4	69.8	31.0
3-Year LACC	84	46.9 ± 20.3	77.3 ± 9.48	-1.13 ± 11.1	0.42 ± 0.08	88.5 ± 5.20	47.9 ± 9.3	77.4	23.8	28.6	65.5	35.7
Stage I	31	42.6 ± 24.7	71.8 ± 8.40	2.91 ± 10.9	0.39 ± 0.07	90.2 ± 5.12	43.5 ± 8.6	93.5	9.70	32.3	83.9	19.4
Stage II	27	43.4 ± 13.6	75.4 ± 8.98	2.10 ± 9.20	0.41 ± 0.08	90.4 ± 4.07	45.8 ± 8.7	77.8	25.9	33.3	70.4	33.3
Stage III	45	47.3 ± 22.7	79.9 ± 9.58	-2.11 ± 11.4	0.42 ± 0.08	87.7 ± 5.25	48.1 ± 10.4	75.6	26.7	28.9	60.0	42.2
Stage IV	12	46.7 ± 11.6	74.9 ± 6.38	-2.70 ± 11.9	0.45 ± 0.07	88.1 ± 5.27	51.3 ± 7.00	75.0	33.3	33.3	66.7	41.7

5.4.1 TCP Curves

All but the Stage II dose response curve had a statistically significant fit to the clinical outcome data. The one, two, and three-year dose response curves had similar shaping parameters. The stage III dose response curve derived from LF data had the highest D_{50} at 71.1 Gy while the stage II dose response curve derived from LF data had the lowest

D_{50} at 61.7 Gy. The stage IV dose response curve derived from LF data had the steepest slope with $\gamma = 7.35$ and the stage II dose response curve derived from LF data had the shallowest slope at $\gamma = 0.96$. In general, the dose response curves derived from LF data had higher D_{50} values and steeper slopes than the dose response curves derived from LR data. Figure 5.1 displays and Table 5.2 summarizes the shaping parameters and dose response curve fit p-values.

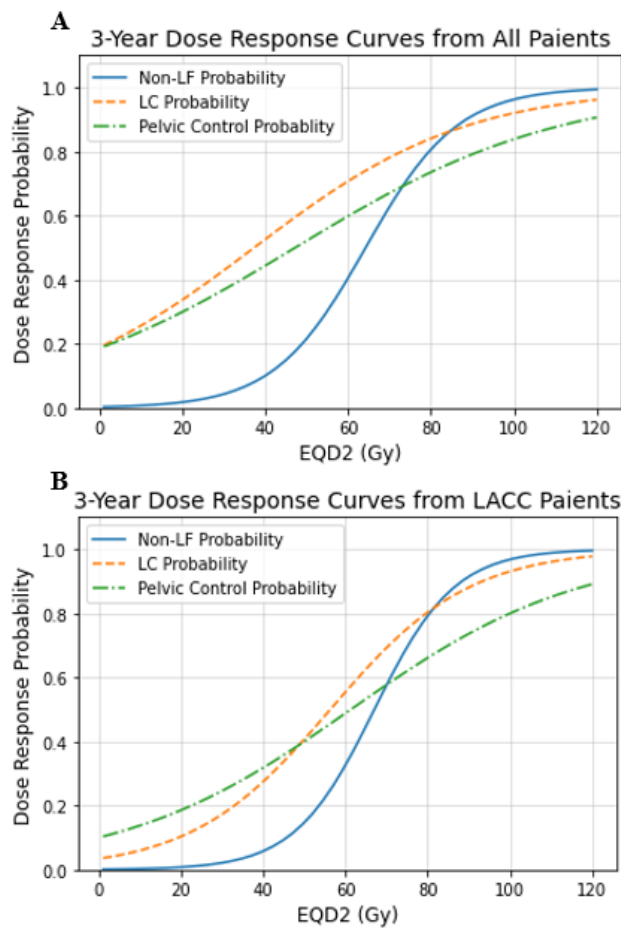


Figure 5.1. Dose response curves derived from LF, LR, and pelvic recurrence data. The curves derived by LF data provide the non-LF probability dose response curves, the curves derived from LR data provided the LC probability dose response curves, and the curves derived from pelvic data provided the pelvic control probability dose response curves. A is from all cervical cancer patients, B is from LACC patients.

Table 5.2. The shaping parameters of the dose response curves derived from the LF, LC, and pelvic recurrence data sets. The curves derived by LF data provide the non-LF probability dose response curves, the curves derived from LR data provided the LC probability dose response curves, and the curves derived from pelvic data provided the pelvic control probability dose response curves.

All Treatments									
	Non-LF Probability Dose Response Curves			LC Probability Dose Response Curves			Pelvic Control Probability Dose Response Curves		
Dataset	D_{50}	γ	p-value	D_{50}	γ	p-value	D_{50}	γ	p-value
1-Year	59	1.252	0.001	2.74	0.019	0.043	13.4	0.066	0.101
2-Year	62.4	1.312	< 0.001	31.5	0.283	0.028	26.2	0.101	0.051
3-Year	64.2	1.453	< 0.001	37.3	0.363	0.016	47.2	0.368	0.033
3-Year LACC	67	1.728	< 0.001	56.3	0.836	0.004	61.3	0.548	0.019
Stage I	63.5	1.969	0.005	164	1.211	0.016	39.6	0.532	0.034
Stage II	61.7	0.958	0.027	24.6	0.154	0.056	34.1	0.200	0.083
Stage III	71.1	2.601	< 0.001	67.4	1.764	0.001	74.4	1.396	0.006
Stage IV	69.7	7.349	0.002	69.7	7.349	0.002	71.6	7.349	0.001

5.4.2 DV, CI, COIN, and HRCTV Logistic Regression

COIN and the c_2 isodose gradient parameter were statistically significant for all patient LF, LR, and pelvic recurrence logistic regression fits. DV was statistically significant for LR and pelvic recurrence fits, and HRCTV size was only statistically significant for LR fits. Only DV and c_2 were statistically significant for LACC LF and pelvic recurrence fits (Table A3.4, DV $p = 0.034$ for both, c_2 $p = 0.046$). Table 5.3 summarizes the shaping parameters and regression statistics of the fits and Figure 5.2 displays the resultant sigmoid curves.

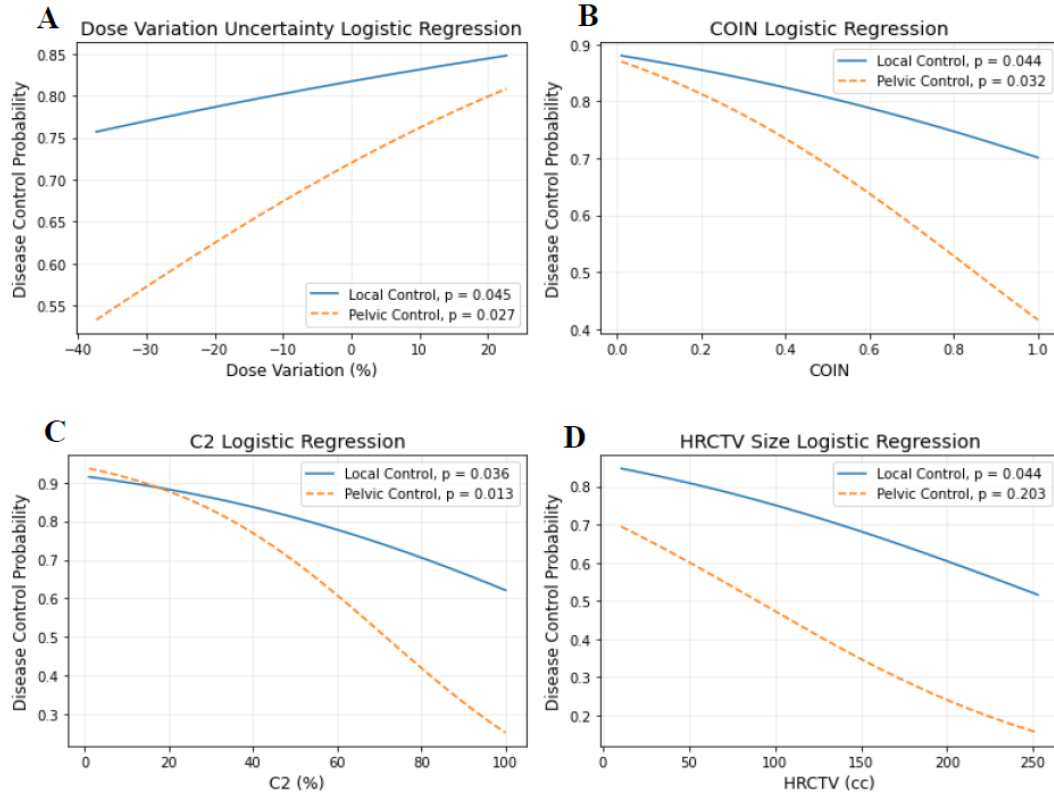


Figure 5.2. Logistic regression for DV (A), COIN (B), c_2 (C), and HRCTV (D) using the local and pelvic recurrence datasets.

Table 5.3. HRCTV size, DV, COIN, CI, and c_2 logistic regression statistics for all patients.

Variable	LF Logistic Regression			LR Logistic Regression			Pelvic Recurrence Logistic Regression		
	50% Response	γ	p	50% Response	γ	p	50% Response	γ	p
HRCTV (cc)	131	-0.536	0.491	262	-0.446	0.044	89.4	-0.233	0.203
DV (%)	-137	-0.248	0.064	-155	-0.374	0.045	-43.0	-0.236	0.027
COIN	1.10	-0.422	0.048	1.74	-0.501	0.044	0.85	-0.480	0.031
CI (%)	-407	-0.199	0.070	-802	-0.328	0.052	-156	-0.136	0.069
C2 (%)	88.0	-0.549	0.032	126	-0.598	0.036	71.5	-0.682	0.012

5.4.3 Utility Analysis

As stated in Table 4.5, the optimal dose and probability of risk-free local control (RFLC) was 76 Gy and 82.1% for TCP1 and 80 Gy and 79% for TCP2A. The RFLC

probability for our three-year LACC LR-TCP curve was reduced to 72.8%, but the optimal dose prediction increased to 83.6 Gy (Figure 5.3).

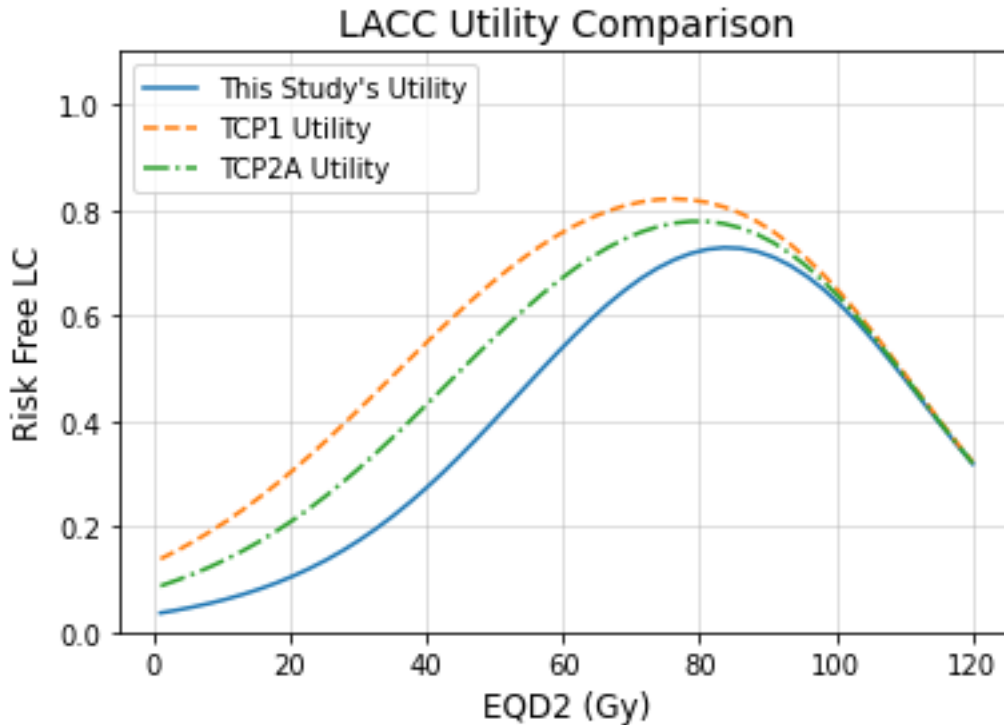


Figure 5.3. Utility calculations for the three-year LACC TCP derived from LR data, TCP1, and TCP2A. Our risk-free local control (RFLC) probability decreased to 72.8%, but the optimal dose prediction increased to 83.6 Gy.

5.4.4 Control versus Recurrence Parameter t-tests

Only dose was statistically different for LF versus no LF patients, and LR versus LC patients. Dose was also statistically different for high dose stage I, III, and IV patients. HRCTV size, DV, COIN, CI and c_2 were not statistically different for LF versus no LF patients and LR versus LC patients. Only stage III and IV LC and LR dose was statistically different for all and high dose patients ($p = 0.005$ and 0.016 for all and high dose patients).

HRCTV size, DV, and CI were statistically significant for all patients two and three-year pelvic control versus pelvic recurrence high dose treatments (Table A3.8, $p =$

0.023, 0.021, 0.019 for 3-year). COIN was statistically significant for one-year pelvic rates and Stage I pelvic rates (Table A3.7, $p = 0.009$ and 0.025). Dose and DV were statistically significant for Stage III pelvic rates (Table A3.7, $p = 0.018$ and 0.043). The c_2 parameter was statistically significant for one-year rates ($p = 0.006$).

5.5 Discussion

The clinical effect of dose, dose variation (DV) uncertainty, dose coverage, and tumor volume were successfully investigated in this chapter. Local control (LC), local recurrence (LR), local failure (LF), pelvic control, and pelvic recurrence were the clinical outcome endpoints. A prescription dose threshold of 75 Gy^{40} was used to evaluate clinical outcome dependencies for high dose prescription treatments, low dose prescription treatments, and all dose prescription treatments. A HRCTV size threshold of 35 cc^{59} was also used to evaluate clinical outcome dependencies for large and small sized HRCTVs. It has been shown that in addition to dose, dose variation (DV) uncertainty, the conformal index (COIN), the standard conformity index (CI), the conformal isodose gradient index (c_2), and HRCTV size can be used to predict clinical outcomes in cervical cancer HDR brachytherapy. Also, a novel method to correct TCP curves for DV uncertainty has been introduced.

As we have shown throughout this dissertation, research of DV uncertainty in cervical cancer HDR brachytherapy is limited. Although the dosimetry of DV uncertainty has been studied by this research group and moderately in the literature, there has not been a DV uncertainty clinical outcome study to our knowledge. Our results show that LC is affected by approximately 1% for every 6.63% of DV uncertainty (linear approximation of

Figure 5.2A). Recall that this DV is from EQD2 DV uncertainty, not from the raw planned DV uncertainty. Using the Equation 2.2, we see that 6.63% EQD2 DV equates to a true 4.86% DV uncertainty. Therefore, approximately 5% of DV uncertainty affects LC by 1%, and our models predict that a $\pm 5\%$ DV uncertainty occurs in 55.0% of treatments, with 32.5% (Table 2.3, Figure 2.6A) of those treatments resulting in under-dose conditions. Our models show that this effect is more profound disease control within the greater pelvis. Approximately 1% of pelvic control is affected for every 2.17% of DV uncertainty, meaning 1.40% for the true DV uncertainty (linear approximation of Figure 5.2A and Equation 2.2). This is a narrow tolerance for planners. DV uncertainty is inevitable in HDR T&O brachytherapy: our DV standard deviation was 10.9% (8.17% true DV), consistent with other DV uncertainty studies^{15,26,52}. Combating DV uncertainty with improved applicator placement or improved packing to lower OAR dose will help, but we believe that there are other methods to combat DV uncertainty.

It is known that T&O plans deliver lower doses than T&R plans^{59,69}, and the corresponding DV uncertainty associated with T&Os has been well documented in this dissertation. From our results, we recommend that T&R brachytherapy be used when the benefits of T&O brachytherapy are not clear, because the increased dose of T&R brachytherapy can combat DV uncertainty. Also, T&R dosimetry can improve dose CI due to DV uncertainty being directly proportional to dose coverage. Serban et al.⁶⁹ found that T&R treatments delivered 3.3 Gy more to the HRCTV than T&O treatments and was more conformal, and Gonzalez et al.⁵⁹ found that T&R + IS treatments delivered 4.1 Gy more ($p = 0.013$) to large HRCTVs than T&O treatments. Although relative dosimetry was not evaluated, dose coverage does improve by inspection of Figure 1C from Gonzalez et al.

(Figure 5.4 here). For cases when T&O brachytherapy provides more benefits than T&R brachytherapy, we recommend four to six fractions to reduce the impact of DV uncertainty. Nesvacil et al. showed that increased fractionation can reduce the effect random-like errors can have on LC²⁶. Lastly, we recommend the use of recto-vaginal spacers in T&O brachytherapy in addition to vaginal packing. As we have shown hypothetically in Chapter 4 and clinically in the literature^{36,37}, reductions in OAR dose leads to HRCTV dose escalation. Displacing the radiosensitive rectum from the HRCTV will combat DV uncertainty and improve LC rates.

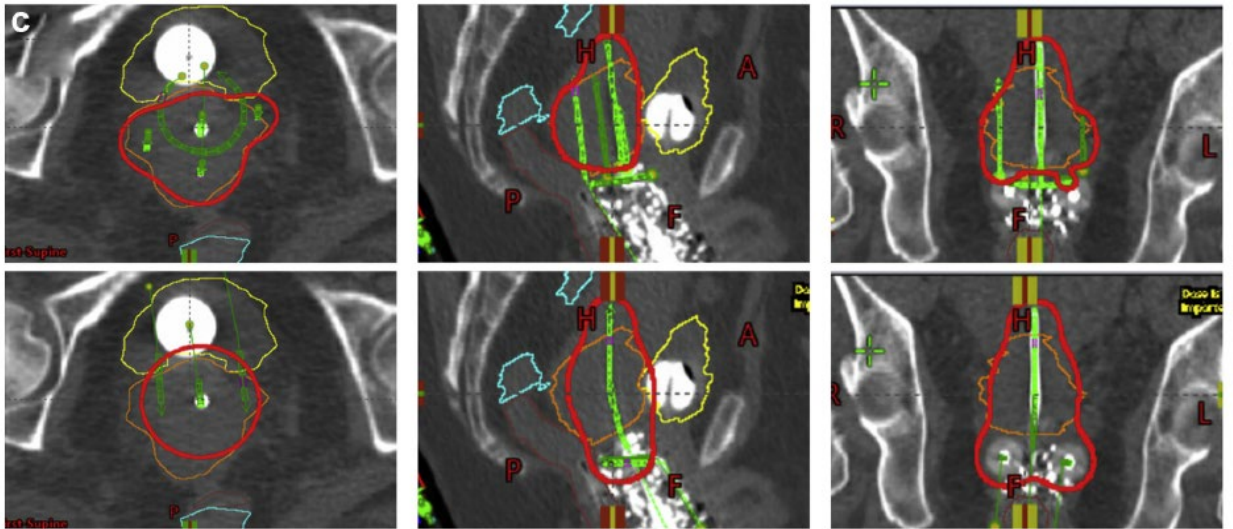


Figure 5.4. Figure 1 from Gonzalez et al.⁵⁹ displaying increased dose conformity with T&R + IS applicator.

We have shown that 1.40% of DV uncertainty can affect 1% of pelvic control probability. Because DV uncertainty is directly proportional to CI (Figure 5.5A), we hypothesize this phenomenon is due to dose being the dominant variable for local control, but dose conformity having importance in preventing disease spread. It is not the primary objective of cervical cancer RT to achieve greater pelvic disease control, but it is a desirable goal to achieve when possible. The ideal COIN value converges to 1.00: the standard CI

value approaches 1.00 (100%) to cover the HRCTV and the c_2 parameter approaches 1.00 (100%) for a lower isodose gradient. This is true for stereotactic treatments using the analogous Paddick Conformal Index⁶⁸, but it is not true for HDR brachytherapy for cervical cancer. Our results show that lower COIN values increase the LC and pelvic control probability (Figure 5.5B), and the ideal COIN value is within the range of 0.40 and 0.45 (Table A3.7 and A3.8). Thus, an ideal 90% HRCTV dose coverage must be paired with a 45 to 50% isodose gradient (c_2) to increase the probability of LC and pelvic control. This isodose gradient means that 50 to 55% of the prescription isodose volume will be outside of the HRCTV. Although this dose gradient may not be ideal for stereotactic plan quality, it can be advantageous for T&O plan quality. Our results show that having a higher isodose gradient to combat lower doses and DV uncertainty is necessary to achieve LC. The same being true for achieving pelvic control implies that higher dose gradients can combat disease spread from microscopic residual disease that just cannot be seen on CT imaging during HRCTV delineation. We hypothesize this is so due to the definition of c_2 : the proportion of the HRCTV receiving the prescription dose with respect to the prescription isodose volume. DV and c_2 are moderately correlated to each other (Figure 5.4B, $R^2 = 0.157$ and $p < 0.001$). Thus, c_2 is a parameter that can be used to describe DV uncertainty in gradient form. It is of interest to test this dependency with a multi-institutional, large patient cohort, using CT and MRI simulations for HRCTV delineation.

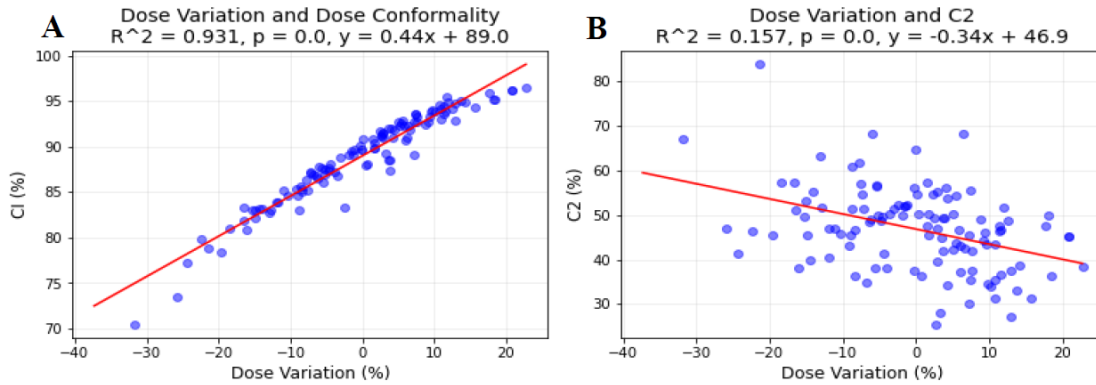


Figure 5.5. Dose Variation (DV) and Conformity index (CI) (A) and c_2 (B). DV is directly proportional to CI and c_2 . DV has a strong correlation to CI and moderate correlation to c_2 .

HRCTV size must also be considered when planning and optimizing HDR cervical cancer plans. We have shown that the LC probability decreases with increasing HRCTV size. Approximately 1% of LC is lost for every 7.23 cm^3 increase in HRCTV size (linear approximation of Figure 5.3D). We have no control over initial tumor size, because shrinking that tumor size is the objective of RT. However, the increased chance of DV uncertainty and reduced CI as a function of HRCTV size is clinically relevant. Currently, DV uncertainty and dose conformity are not treatment planning optimization objects, but side effects of optimizing for dose delivery priorities per clinical protocol. Dose optimization algorithms is beyond the scope of this thesis, but incorporating these parameters with some priority may improve plan quality and improve clinical outcomes. Furthermore, DV uncertainty, dose conformity, and HRCTV size can be of interest to modernized RT modalities such as automatic treatment planning and advanced outcome modeling.

It is imperative to note that the patients evaluated throughout this thesis were treated using computed tomography (CT) based brachytherapy. CT based brachytherapy is a

standard of care, but the inferior soft tissue contrast to magnetic resonance imaging (MRI) based brachytherapy is known to generate systematic contour and under-dosing errors⁷⁰⁻⁷⁴. It is feasible to assume that DV uncertainty is a consequence of CT based brachytherapy due to these systematic errors. The reference TCP curves, TCP1 and TCP2A, were derived from patients exclusively treated with MRI based brachytherapy^{41,42}. Our three-year locally advanced cervical cancer (LACC) TCP curve (LACC LC probability dose response curve in Figure 5.1 B) does show a systematic loss of LC probability that converges to unity at the clinically relevant higher doses (Figure 5.6). We suspect this is due to lower doses delivered (Table 5.1, 77.3 ± 9.48 Gy) versus TCP1 (86 ± 12 Gy)⁴² and TCP2A (86 ± 12 Gy)⁴¹, DV uncertainty, and systematic CT based brachytherapy uncertainties. This makes our clinical findings of COIN and c_2 even more important for they can combat DV uncertainty which maybe a consequence of systematic CT imaging uncertainties. COIN and c_2 considerations in addition to recto-vaginal spacers and high fractionated treatments may mitigate CT based brachytherapy uncertainties altogether. Multi-institutional, retrospective DV uncertainty studies on MRI based brachytherapy and prospective studies on CT and MRI based brachytherapy with considerations of our recommendations are recommended for future studies.

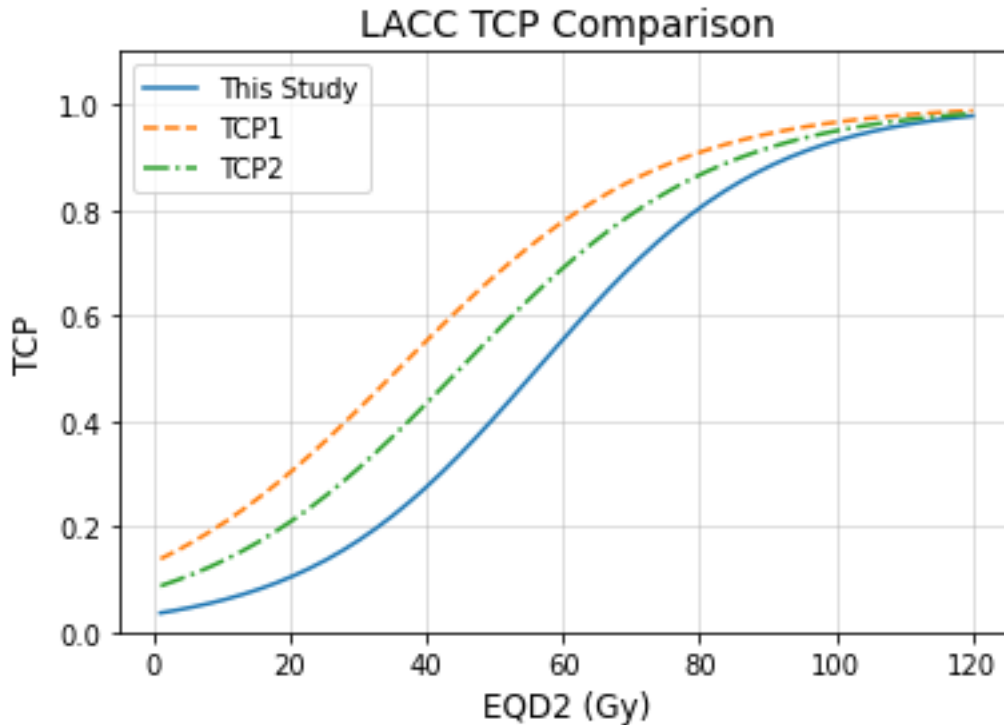


Figure 5.6. The three-year locally advanced cervical cancer (LACC) TCP curve derived from computed tomography (CT) based brachytherapy patients compared to reference TCP curves derived magnetic resonance imaging (MRI) based brachytherapy patients.

The use of this data set can be used to further understand the pathology of cancer spreading post RT. DV, CI, and HRCTV size being statistically different (Appendix A.3.8, $p = 0.023, 0.021, \text{ and } 0.018$) for high dose pelvic recurrence rates are indicative that some areas of the HRCTV do not receive an adequate dose to stabilize the disease within the pelvis. Pelvic control is not the primary goal of cervical cancer RT, but stabilizing the disease within the pelvis is always of interest.

5.6 Conclusion

Dose variation uncertainty has a profound effect on clinical outcomes in HDR brachytherapy for cervical cancer. A 5% and 1.40% dose variation affect 1% of local control and pelvic control, respectively. Other relative dosimetry parameters have strong

correlations in predicting clinical outcomes. The plan quality conformal index, COIN, has shown it is useful in predicting clinical outcomes. According to the COIN data, 90% dose coverage paired with a high isodose gradient (low c_2) improves the probability for local and pelvic control. Furthermore, applicator selection, recto-vaginal spacers, and high fractionated treatments (4-6 fractions) can reduce DV uncertainty and improve clinical outcomes.

CHAPTER 6. DISSERTATION SUMMARY

6.1 Clinical Impact

Dose variations (DV) from the prescribed dose are inevitable in high dose-rate (HDR) brachytherapy for cervical cancer. Understanding the dosimetric and clinical effect this common clinical uncertainty yields is imperative for the field of radiation therapy (RT). The brachytherapy workflow can be hectic, so combatting every form of clinical uncertainty may not be feasible for clinicians. However, we have shown that neglecting DV uncertainty has a non-negligible effect on clinical outcomes: common DVs such as -1.40% and -5% will result in a 1% loss of pelvic and local control (LC), respectively. As stated in Chapter 5, improving applicator placement and vaginal packing will combat DV uncertainty, but this does not combat the major problem in brachytherapy that we have highlighted in this dissertation. The major limitation of brachytherapy is that there are some areas of the high-risk clinical target volume (HRCTV) that do not consistently receive the prescribed dose. Improved applicator placement and packing does not solve this problem. However, we hypothesize that applicator selection, recto-vaginal spacers, and high fractionated treatments (4-6 fractions) can combat DV uncertainty.

Tandem and ovoid (T&O) based brachytherapy is optimal for lateral disease involvement in the parametrium and pelvic sidewall. However, T&O based brachytherapy is also known to deliver lower doses than tandem and ring (T&R) based brachytherapy⁶⁹. Furthermore, T&R and hybrid T&R + interstitial (IS) needle applicators can increase dose conformality. The increased dose conformality decreases the observed dosimetric and clinical effects of DV uncertainty in addition to providing dose escalation without

increasing OAR dose. HDR Syed brachytherapy can also combat DV uncertainty by increasing dose conformality due to its use of IS needles. It is known that IS brachytherapy can increase dose conformality and boost dose to the gross disease^{2,36,37,59-61}. Therefore, any form of IS brachytherapy in addition to T&O brachytherapy is further recommended by this research group to increase dose coverage and combat DV uncertainty. Lastly, based on the data presented in this thesis, it is our recommendation to only use T&O based brachytherapy when the advantages of doing so are obvious over other applicators that provide more conformal dose.

Recto-vaginal spacers can combat DV uncertainty by physically displacing the radio-sensitive rectum further from the HRCTV. The rectum would receive considerably less dose due to this displacement due to the high dose gradients in brachytherapy, thus allowing for higher and more conformal doses to the HRCTV. We discussed the use of recto-vaginal hyaluronate gel injection spacers in Chapter 2^{36,37} and recommend the use of these spacers when feasible to combat the effects of DV uncertainty. We continue to recommend recto-vaginal spacers to combat DV uncertainty and improve dose conformality.

The American Brachytherapy Society (ABS) recommends 4-6 fraction HDR brachytherapy prescriptions to deliver an optimal dose to the HRCTV². We side with the ABS's recommendations of 4-6 fractions, but not just for dose delivery. Nesvacil et al. found that random-like uncertainties tend to cancel out and regress back to a mean value with increased fractionation²⁶. Although we have found there is a 32.5% probability (Table 2.3, Figure 2.6A) of under-dosing (-5% DV) the HRCTV, there is also a 22.5% probability of overdosing (+5% DV) the HRCTV and a 45.0% probability of having a treatment within

a clinically acceptable a DV of $\pm 5\%$. Prescribing high fractionated treatment increases the likelihood of optimal dose delivery and some overdose cases. High fractionated treatments also provide additional opportunities to correct for lower DV treatments earlier in the brachytherapy treatment course. The most impactful argument for high fractionated treatments is that this solution allows for the use of T&O based brachytherapy over T&R based brachytherapy without the use of recto-vaginal spacers. It is the most feasible practice of our recommendations in terms of clinical protocol and workflow. However, care must also be taken for OAR doses in this case.

Relative dosimetry has been investigated dosimetrically in HDR brachytherapy for cervical cancer⁶⁴⁻⁶⁷, but there has been limited research on its clinical effects. The conformal index (COIN) has shown promise as a plan quality and clinical outcome metric. Unlike in stereotactic RT, COIN values that approach 1.00 are not ideal for clinical outcomes in cervical cancer brachytherapy. From our results in Chapter 5, the ideal COIN values range from 0.40 to 0.45. Thus, an ideal 90% dose coverage must be paired with a c_2 isodose gradient of 0.45 (45.0%) to 0.50 (50.0%). This implies that 50 to 55% of the prescription isodose volume must be outside of the HRCTV. This irradiation of normal tissues is not ideal, but it does show that COIN and c_2 values can help combat the effects of DV uncertainty. Optimizing plans with considerations of COIN and c_2 can help mitigate the inevitable DV uncertainty, especially with larger sized HRCTVs.

It is important to note that the patients used in this dissertation were treated exclusively with computed tomography (CT) based brachytherapy. CT based brachytherapy is a standard of care, but it is known to systematically affect delineation and deliver lower doses to the HRCTV than MRI based brachytherapy⁷⁰⁻⁷⁴. This makes DV

uncertainty more likely with CT based brachytherapy. Our locally advanced cervical cancer (LACC) TCP curve shows a systematic loss of LC probability when compared to the reference TCP1 and TCP2A curves that were derived from patients treated exclusively with MRI based brachytherapy (Figure 5.5). CT based brachytherapy is still feasible due to the LC probabilities converging at the optimal higher doses, but the findings of this thesis are more relevant due to the known systematic uncertainties that CT based brachytherapy induces.

The utility concept was for cervical cancer RT was also introduced in this thesis. Utility provides the probability of risk-free local control (RFLC) and predicts the optimal dose to achieve so. We have shown both theoretically (Chapter 4, section 4.4.5) and clinically (Chapter 5, section 5.4.3) that utility calculations under the influence of DV uncertainty can predict clinically relevant doses to achieve LC (83 Gy in Chapter 4 and 83.6 Gy in Chapter 5). The complete clinical ramifications of using this model is beyond the scope of this thesis, but it is recommended for future research.

6.2 Study Limitations

Not evaluating other clinically relevant dosimetric parameters is a limitation of this thesis. HRCTV parameters such as the D_{95} , D_{98} , and D_{100} , and OAR parameters such as the $D_{5\ cc}$ and $D_{10\ cc}$ are relevant clinical parameters not studied in this thesis. Not studying the clinically relevant high-risk gross tumor volume (HR-GTV) and intermediate-risk clinical target volumes (IR-CTV) are also considered a limitation of this thesis. The D_{98} and is known to have a similar effect on the HR-GTV as the D_{90} has on the HRCTV and IR-CTV⁴². Thus, DV uncertainty will apply and may have the same effect on those

parameters as observed in this thesis. The International Commission on Radiation Units report 89 (ICRU 89) recommended more clinical outcome evaluation for bowel dose⁸. Therefore, not including the radiosensitive bowel is considered a limitation in this thesis.

This thesis did not do broad parameter evaluation such tumor histology, tumor pathology, types of chemotherapy, types of surgeries, immunotherapy, dose-rate changes, dose location, application changes, protocol changes etc. Our single institution study mainly focused on tumor type, tumor location, dose, DV uncertainty, HRCTV size, and relative dosimetry. Not addressing the other parameters can be considered a limitation of this thesis. Also, not evaluating over-all treatment time is a limitation of this thesis^{42,63,75,76}.

6.3 Future Research Directions

Expanding on our clinical DV uncertainty findings is essential for future research. A multi-institutional, prospective clinical trial with multiple applicators, recto-vaginal spacers, and high fractionated HDR treatments are ideal to investigate our hypotheses. Also, advanced outcome modeling using machine learning and artificial intelligence techniques is of interest for future research. Artificial intelligence outcome modeling has already shown promising results⁶². Incorporating what is known about DV uncertainty with what machine learning and artificial intelligence can do is imperative for future research.

Expanding on the mentioned limitations to make the findings of this thesis more robust is of interest for future research. Evaluating the DV uncertainty of D_{98} for HR-GTVs, DV uncertainty of D_{90} for IR-CTVs, and the effect on bowel and sigmoid D_{5cc} and D_{10cc} is imperative for future studies.

Chapter 4 showed promise for using DV uncertainty as a method of data augmentation for radiation therapy (RT) machine learning and artificial intelligence models^{77,78}. Data augmentation, machine learning, and artificial intelligence was not the focus of this thesis, but generating large amounts of quality patient data was a result of this thesis. Investigating the potential for data augmentation is of interest for future research.

APPENDICES

[APPENDIX 1. GLOSSARY]

2D	Two-dimension imaging or radiation therapy
3D	Three-dimension imaging or radiation therapy
γ	Gamma shaping parameter for logistic regression sigmoid curves
AAPM	American Association of Physicists in Medicine
ABS	American Brachytherapy Society
ACS	American Cancer Society
AD	Anderson Darling test
C2	Isodose gradient parameter
CDF	Cumulative Density Function
CI	Conformity Index
COIN	Conformal Index
CT	Computed Tomography imaging
D0.1C	Dose delivered to most exposed 0.1 cc of volume
D10CC	Dose delivered to most exposed 10 cc of volume
D2CC	Dose delivered to most exposed 2 cc of volume
D50	Dose of 50% response
D5CC	Dose delivered to most exposed 5 cc of volume
D90	Dose delivered to 90% of volume
D95	Dose delivered to 95% of volume
D98	Dose delivered to 98% of volume
DIR	Deformable Image Registration
DSH	Dose Surface Histogram
DV	Dose Variation
DVH	Dose Volume Histogram
EBRT	External Beam Radiation Therapy
EQD2	Equivalent Dose in 2 Gy Fractions
False Pelvis	The greater pelvic area; the pelvis
FIGO	Federation Internationale de Gynecologie et d'Obstetrique (Federation of Gynecology and Obstetrics)

GEV	Generalized Extreme Value distribution
GTV	Gross Tumor Volume
Gy	Gray (J/kg)
GYN	Gynecology
HDR	High dose-rate
HRCTV	High-risk Clinical Target Volume
$HRCTV_{Rx}$	Prescription dose delivered to HRCTV
HR-GTV	High-risk Gross Target Volume
ICBT	Intracavity Brachytherapy
ICRU	International Commission on Radiation Units
IDV	Interfraction Dosimetric Variation
IR-CTV	Intermediate-risk Clinical Target Volume
IS	Interstitial
KS2	Kolmogorov-Smirnov Two Sample test
LACC	Locally Advanced Cervical Cancer
LC	Local Control
LDR	Low Dose Rate
LF	Local Failure
LINAC	Linear Accelerator
LR	Local Recurrence
MC	Monte Carlo
MLE	Maximum Likelihood Estimation
MRI	Magnetic Resonance Imaging
NIST	National Institute of Standards and Technology
NTCP	Normal Tissue Complication Probability
OAR	Organs at Risk
PDF	Probability Density Function
Pelvic Control	Disease control within the greater pelvic area and, or pelvic lymph nodes
Pelvic Recurrence	Disease return within the greater pelvic area and, or pelvic lymph nodes
PET	Positron Emission Tomography imaging

Q-Q	Quantile-quantile plot
R and R^2 from Chapter 2	Pearson's R and R^2 for linear regression
R and R' from Chapter 4	Reference dose response curve and model generated dose response curve
RC	Disease control in the areas/organs adjacent to the primary tumor and lymph nodes
retroEMBRACE	Retrospective studies from the <i>Image guided intensity modulated External beam radio-chemotherapy and MRI based adaptive BRachytherapy in locally advanced Cervical cancer</i> data.
RFLC	Risk Free Local Control
RoCI	Range of Clinical Interest
RR	Disease recurrence in the areas/organs adjacent to the primary tumor and lymph nodes
RSS	Residual Sum of Squares
RT	Radiation Therapy
SF	Survival Function, $1 - \text{CDF}$
T&O	Tandem and Ovoid
T&R	Tandem and Ring
TCP	Tumor Control Probability
TG	Task Group
True Pelvis	The open cavity of the pelvis that contains the urinary bladder, colon, and reproductive organs
Vol_{Rx}	Prescription isodose volume

[APPENDIX 2. DETAILED RESULTS FROM CHAPTER 4]

Table A2. 1. Statistical analysis of complication rates simulated from sampling DV uncertainty distributions vs sampling from no uncertainty distribution.

Rx	TCP1				
	<u>Reference</u> Average TF Rate (%)	<u>Beta</u> Average TF Rate (%)	p-value	<u>Normal</u> Average TF Rate (%)	p-value
5x4	15.0 ± 0.36	15.4 ± 0.34	< 0.001	15.1 ± 0.36	0.009
5x5	11.3 ± 0.32	11.7 ± 0.34	< 0.001	11.4 ± 0.31	0.132
6x4	10.9 ± 0.33	11.3 ± 0.30	< 0.001	11.0 ± 0.34	0.202
6x5	7.40 ± 0.26	7.92 ± 0.29	< 0.001	7.64 ± 0.25	< 0.001
7x3	12.1 ± 0.30	12.5 ± 0.36	< 0.001	12.2 ± 0.35	0.001
7x4	7.57 ± 0.30	7.95 ± 0.26	< 0.001	7.73 ± 0.28	< 0.001
Composite	10.7 ± 0.31	11.1 ± 0.32	0.006	10.8 ± 0.32	> 0.250
Rx	TCP2				
	<u>Reference</u> Average TF Rate (%)	<u>Beta</u> Average TF Rate (%)	p-value	<u>Normal</u> Average TF Rate (%)	p-value
5x4	20.9 ± 0.41	21.5 ± 0.40	< 0.001	21.0 ± 0.48	0.067
5x5	15.4 ± 0.35	16.2 ± 0.35	< 0.001	15.6 ± 0.36	0.006
6x4	14.8 ± 0.39	15.5 ± 0.32	< 0.001	15.1 ± 0.36	< 0.001
6x5	9.43 ± 0.26	10.2 ± 0.26	< 0.001	9.72 ± 0.29	< 0.001
7x3	16.6 ± 0.37	17.3 ± 0.37	< 0.001	16.8 ± 0.35	0.002
7x4	9.63 ± 0.27	10.3 ± 0.31	< 0.001	9.89 ± 0.31	< 0.001
Composite	14.5 ± 0.34	15.1 ± 0.34	0.004	14.7 ± 0.36	> 0.250
Rx	TCP3				
	<u>Reference</u> Average TF Rate (%)	<u>Beta</u> Average TF Rate (%)	p-value	<u>Normal</u> Average TF Rate (%)	p-value
5x4	35.4 ± 0.42	36.3 ± 0.49	< 0.001	35.8 ± 0.47	< 0.001
5x5	25.6 ± 0.44	26.7 ± 0.46	< 0.001	25.9 ± 0.44	< 0.001
6x4	24.6 ± 0.44	25.7 ± 0.43	< 0.001	24.9 ± 0.43	< 0.001
6x5	14.7 ± 0.35	16.0 ± 0.35	< 0.001	15.3 ± 0.35	< 0.001
7x3	27.9 ± 0.51	28.9 ± 0.43	< 0.001	28.2 ± 0.42	< 0.001
7x4	15.0 ± 0.35	16.2 ± 0.32	< 0.001	15.6 ± 0.37	< 0.001
Composite	23.9 ± 0.42	24.9 ± 0.41	0.009	24.3 ± 0.41	> 0.250
Rx	TCP4				
	<u>Reference</u> Average TF Rate (%)	<u>Beta</u> Average TF Rate (%)	p-value	<u>Normal</u> Average TF Rate (%)	p-value
5x4	46.3 ± 0.43	47.7 ± 0.53	< 0.001	46.4 ± 0.50	0.038
5x5	29.0 ± 0.46	31.1 ± 0.50	< 0.001	29.6 ± 0.40	< 0.001
6x4	27.2 ± 0.45	29.3 ± 0.41	< 0.001	27.8 ± 0.46	< 0.001
6x5	11.5 ± 0.31	13.9 ± 0.37	< 0.001	12.8 ± 0.33	< 0.001
7x3	32.9 ± 0.44	34.8 ± 0.50	< 0.001	33.4 ± 0.48	< 0.001
7x4	12.0 ± 0.31	14.4 ± 0.35	< 0.001	13.2 ± 0.31	< 0.001
Composite	26.5 ± 0.40	28.5 ± 0.44	0.003	27.2 ± 0.41	> 0.250

[APPENDIX 3. DETAILED RESULTS FROM CHAPTER 5]

Table A3. 1. High Dose stats.

	N	HRCTV (cc)	EQD2 (Gy)	DV (%)	COIN	CI (%)	C2 (%)	LC (%)	LR (%)	LF (%)	RC (%)	RR (%)
1-Year	57	45.3 ± 21.6	81.6 ± 5.75	0.25 ± 10.1	0.42 ± 0.08	88.9 ± 4.32	47.0 ± 9.9	87.7	14	14	75.4	26.3
2-Year	67	45.8 ± 20.8	81.7 ± 6.29	-0.26 ± 10.2	0.42 ± 0.08	88.8 ± 4.47	47.0 ± 9.5	83.6	17.9	17.9	71.6	29.9
3-Year	71	44.9 ± 20.6	81.7 ± 6.16	0.09 ± 10.3	0.41 ± 0.08	88.9 ± 4.48	46.7 ± 9.4	84.5	16.9	16.9	73.2	28.2
3-Year LACC	59	45.0 ± 19.2	82.0 ± 6.21	0.27 ± 10.3	0.42 ± 0.08	89.0 ± 4.45	46.9 ± 9.6	84.7	16.9	16.9	71.2	30.5
Stage I	31	42.6 ± 24.7	71.8 ± 8.4	2.91 ± 10.9	0.39 ± 0.07	90.2 ± 5.12	43.5 ± 8.6	93.5	9.7	32.3	83.9	19.4
Stage II	27	43.4 ± 13.6	75.4 ± 8.98	2.1 ± 9.2	0.41 ± 0.08	90.4 ± 4.07	45.8 ± 8.7	77.8	25.9	33.3	70.4	33.3
Stage III	45	47.3 ± 22.7	79.9 ± 9.58	-2.11 ± 11.4	0.42 ± 0.08	87.7 ± 5.25	48.1 ± 10.4	75.6	26.7	28.9	60	42.2
Stage IV	12	46.7 ± 11.6	74.9 ± 6.38	-2.7 ± 11.9	0.45 ± 0.07	88.1 ± 5.27	51.3 ± 7.00	75	33.3	33.3	66.7	41.7

Table A3. 2. Low dose stats.

	N	HRCTV (cc)	EQD2 (Gy)	DV (%)	COIN	CI (%)	C2 (%)	LC (%)	LR (%)	LF (%)	RC (%)	RR (%)
1-Year	38	46.2 ± 18.9	66.9 ± 5.04	0.07 ± 11.2	0.42 ± 0.08	89.3 ± 5.25	47.2 ± 9.0	84.2	18.4	39.5	73.7	28.9
2-Year	43	48.0 ± 19.9	66.7 ± 5.68	-0.88 ± 11.9	0.42 ± 0.08	88.8 ± 5.87	47.9 ± 9.4	79.1	23.3	44.2	67.4	34.9
3-Year	46	46.9 ± 19.8	66.7 ± 5.58	-0.63 ± 11.9	0.42 ± 0.08	88.9 ± 5.79	47.3 ± 9.4	76.1	26.1	47.8	65.2	37
3-Year LACC	26	51.3 ± 22.2	66.5 ± 6.3	-4.38 ± 12.4	0.43 ± 0.07	87.2 ± 6.56	50.0 ± 8.3	61.5	42.3	57.7	53.8	50
Stage I	31	42.6 ± 24.7	71.8 ± 8.4	2.91 ± 10.9	0.39 ± 0.07	90.2 ± 5.12	43.5 ± 8.6	93.5	9.7	32.3	83.9	19.4
Stage II	27	43.4 ± 13.6	75.4 ± 8.98	2.1 ± 9.2	0.41 ± 0.08	90.4 ± 4.07	45.8 ± 8.7	77.8	25.9	33.3	70.4	33.3
Stage III	45	47.3 ± 22.7	79.9 ± 9.58	-2.11 ± 11.4	0.42 ± 0.08	87.7 ± 5.25	48.1 ± 10.4	75.6	26.7	28.9	60	42.2
Stage IV	12	46.7 ± 11.6	74.9 ± 6.38	-2.7 ± 11.9	0.45 ± 0.07	88.1 ± 5.27	51.3 ± 7.00	75	33.3	33.3	66.7	41.7

Table A3. 3. High dose and low dose TCP p-values and shaping parameter estimation.

High Dose									
Dataset	LF			LR			RR		
	D50	Gamma	p-value	D50	Gamma	p-value	D50	Gamma	p-value
1-Year	15.7	0.125	0.035	15.7	0.125	0.035	25.4	0.144	0.072
2-Year	57.4	1.035	0.022	57.4	1.035	0.022	67.3	1.151	0.023
3-Year	56.4	0.902	0.020	56.4	0.902	0.020	66.3	1.256	0.023
3-Year LACC	35.7	0.322	0.035	35.7	0.322	0.035	65.8	0.968	0.035
Stage I	63.5	1.969	0.005	164	1.211	0.016	39.6	0.532	0.034
Stage II	61.7	0.958	0.027	24.6	0.154	0.056	null	null	0.075
Stage III	71.1	2.601	< 0.001	67.4	1.764	0.001	74.4	1.396	0.006
Stage IV	69.7	null	0.002	69.7	null	0.002	71.6	null	0.001
Low Dose									
Dataset	LF TCP			LR TCP			RR TCP		
	D50	Gamma	p-value	D50	Gamma	p-value	D50	Gamma	p-value
1-Year	57.8	0.838	0.061	154.2	0.74	0.042	99.7	0.742	0.065
2-Year	62.6	1.083	0.033	null	null	0.057	90.0	0.657	0.073
3-Year	64.9	0.988	0.037	null	null	0.065	91.4	0.57	0.072
3-Year LACC	68.8	1.739	0.028	18.2	0.036	0.086	68.9	0.561	0.080
Stage I	63.5	1.969	0.005	164.2	1.211	0.016	39.6	0.532	0.034
Stage II	61.7	0.958	0.027	24.6	0.154	0.056	null	null	0.075
Stage III	71.1	2.601	< 0.001	67.4	1.764	0.001	74.4	1.396	0.006
Stage IV	69.7	null	0.002	69.7	null	0.002	71.6	null	0.001

Table A3. 4. All treatment LACC logistic regression fits.

All Treatment 3-Year LACC Data									
Variable	LF TCP			LR TCP			RR TCP		
	50% Response	γ	P	50% Response	γ	P	50% Response	γ	P
HRCTV (cc)	223.8	-0.107	null	-20.25	-0.061	0.34	119.2	-0.123	0.247
DV (%)	-0.48	-0.275	0.034	null	null	0.061	-0.33	-0.19	0.034
COIN	1.65	-0.341	0.066	null	null	0.061	1.14	-0.272	0.074
CI (%)	null	null	0.065	null	null	0.062	null	null	0.079
C2 (%)	92.0	-0.521	0.046	null	null	0.061	80.0	-0.419	0.054

Table A3. 5. High dose logistic regression statistics and parameter estimation for the 3-year all patient and 3-year LACC patient data.

High Dose Treatment 3-Year Data									
Variable	LF Logistic Regression			LR Logistic Regression			RR Logistic Regression		
	50% Response	γ	P	50% Response	γ	P	50% Response	γ	P
HRCTV (cc)	174.1	-0.59	0.028	174.1	-0.59	0.028	91.8	-0.884	0.133
DV (%)	null	null	0.042	null	null	0.042	-0.25	-0.329	0.006
COIN	null	null	0.040	null	null	0.040	null	null	0.068
CI (%)	null	null	0.043	null	null	0.043	null	null	0.057
C2 (%)	null	null	0.040	null	null	0.040	0.87	-0.581	0.041

High Dose Treatment 3-Year LACC Data									
Variable	LF Logistic Regression			LR Logistic Regression			RR Logistic Regression		
	50% Response	γ	P	50% Response	γ	P	50% Response	γ	P
HRCTV (cc)	null	null	0.457	null	null	0.457	93.6	-0.476	0.028
DV (%)	null	null	0.042	null	null	0.042	-0.25	-0.296	0.010
COIN	null	null	0.028	null	null	0.028	null	null	0.073
CI (%)	null	null	0.043	null	null	0.043	null	null	0.064
C2 (%)	0.06	-0.063	0.019	0.06	-0.063	0.019	1.44	-0.337	0.070

Table A3. 6. Low dose logistic regression statistics and parameter estimation for the 3-year all patient and 3-year LACC patient data.

Low Dose Treatment 3-Year Data									
Variable	LF Logistic Regression			LR Logistic Regression			RR Logistic Regression		
	50% Response	γ	P	50% Response	γ	P	50% Response	γ	P
HRCTV (cc)	null	null	null	null	null	0.085	34.9	-0.113	0.319
DV (%)	-0.31	-0.042	0.091	null	null	0.058	null	null	0.081
COIN	0.53	-0.494	0.031	0.78	-0.773	0.027	0.64	-0.668	0.024
CI (%)	null	null	0.092	null	null	0.064	null	null	0.083
C2 (%)	0.52	-0.814	0.012	0.69	-1.06	0.015	0.61	-0.831	0.020

Low Dose Treatment 3-Year LACC Data									
Variable	LF Logistic Regression			LR Logistic Regression			RR Logistic Regression		
	50% Response	γ	P	50% Response	γ	P	50% Response	γ	P
HRCTV (cc)	10.4	-0.041	0.088	null	null	0.263	15.8	-0.049	0.097
DV (%)	0.02	-0.011	0.059	0.36	-0.085	0.084	-0.04	-0.028	0.060
COIN	0.46	-0.63	0.031	0.58	-0.788	0.036	0.52	-0.483	0.057
CI (%)	1.45	-0.113	0.089	null	null	0.087	0.92	-0.074	0.089
C2 (%)	0.49	-1.837	0.004	0.56	-0.966	0.032	0.53	-0.438	0.072

Table A3. 7. All patient pelvic control versus pelvic recurrence t-tests.

All Patient RC versus RR Statistics						
Variable	1-Year			Stage I		
	RC	RR	p	RC	RR	p
Dose (Gy)	75.9 ± 9.35	75.4 ± 8.39	0.404	72.3 ± 8.98	69.5 ± 4.51	0.250
DV (%)	0.92 ± 10.7	-1.96 ± 9.78	0.251	2.74 ± 11.6	3.75 ± 7.84	0.855
COIN	0.41 ± 0.07	0.45 ± 0.09	0.009	0.38 ± 0.06	0.45 ± 0.08	0.025
CI (%)	89.4 ± 4.70	88.3 ± 4.50	0.329	90.1 ± 5.30	90.7 ± 4.30	0.831
c ₂ (%)	45.5 ± 8.20	51.6 ± 11.5	0.006	42.1 ± 7.80	50.3 ± 10.0	0.051
HRCTV (cc)	43.3 ± 17.9	52.4 ± 25.9	0.062	40.2 ± 21.6	54.1 ± 37.5	0.259
2-Year			Stage II			
Dose (Gy)	76.4 ± 9.87	74.6 ± 8.58	0.181	75.6 ± 8.20	74.8 ± 11.1	0.415
DV (%)	0.42 ± 11.0	-2.59 ± 10.4	0.187	1.02 ± 9.13	4.53 ± 4.53	0.38
COIN	0.41 ± 0.07	0.44 ± 0.09	0.083	0.42 ± 0.09	0.40 ± 0.07	0.642
CI (%)	89.1 ± 5.10	88.1 ± 4.90	0.308	90.0 ± 4.20	91.3 ± 3.90	0.479
c ₂ (%)	46.2 ± 8.50	49.9 ± 5.80	0.058	46.6 ± 9.50	44.1 ± 6.90	0.517
HRCTV (cc)	44.6 ± 18.4	51.3 ± 24.1	0.117	44.8 ± 15.6	40.2 ± 7.32	0.437
3-Year			Stage III			
Dose (Gy)	76.5 ± 9.74	74.2 ± 8.55	0.110	82.4 ± 9.68	76.3 ± 8.44	0.018
DV (%)	0.78 ± 11.0	-2.41 ± 10.6	0.151	0.77 ± 12.2	-6.27 ± 9.01	0.043
COIN	0.41 ± 0.07	0.43 ± 0.09	0.111	0.42 ± 0.06	0.43 ± 0.10	0.697
CI (%)	89.3 ± 5.00	88.1 ± 4.90	0.236	88.7 ± 5.70	86.3 ± 4.30	0.140
c ₂ (%)	45.9 ± 8.40	49.3 ± 11.0	0.070	47.1 ± 7.90	49.6 ± 13.3	0.453
HRCTV (cc)	43.8 ± 18.2	50.1 ± 23.9	0.122	43.4 ± 18.2	52.8 ± 27.5	0.182

Table A3. 8. All patient high dose pelvic control versus pelvic recurrence t-tests.

High Dose Patients RC versus RR Statistics						
Variable	1-Year			Stage I		
	RC	RR	p	RC	RR	p
Dose (Gy)	81.8 ± 5.95	81.1 ± 5.27	0.351	72.3 ± 8.98	69.5 ± 4.51	0.250
DV (%)	1.63 ± 9.82	-3.91 ± 10.3	0.077	2.74 ± 11.6	3.75 ± 7.84	0.855
COIN	0.41 ± 0.07	0.44 ± 0.10	0.217	0.38 ± 0.06	0.45 ± 0.08	0.025
CI (%)	89.5 ± 4.10	87.1 ± 4.60	0.067	90.1 ± 5.30	90.7 ± 4.30	0.831
c ₂ (%)	45.7 ± 8.00	50.8 ± 13.8	0.096	42.1 ± 7.80	50.3 ± 10.0	0.051
HRCTV (cc)	40.8 ± 14.8	58.8 ± 32.1	0.006	40.2 ± 21.6	54.1 ± 37.6	0.259
Variable	2-Year			Stage II		
	RC	RR	p	RC	RR	p
Dose (Gy)	82.3 ± 6.51	80.0 ± 5.52	0.087	75.6 ± 8.20	74.8 ± 11.1	0.415
DV (%)	1.45 ± 9.41	-4.49 ± 11.2	0.032	1.02 ± 9.13	4.53 ± 9.48	0.380
COIN	0.41 ± 0.07	0.42 ± 0.10	0.808	0.42 ± 0.09	0.40 ± 0.07	0.642
CI (%)	89.5 ± 3.90	86.9 ± 5.20	0.029	90.0 ± 4.20	91.3 ± 3.90	0.479
c ₂ (%)	46.3 ± 7.90	48.5 ± 12.7	0.402	46.6 ± 9.50	44.1 ± 6.90	0.517
HRCTV (cc)	42.4 ± 15.6	54.4 ± 28.9	0.033	44.8 ± 15.6	40.2 ± 7.32	0.437
Variable	3-Year			Stage III		
	RC	RR	p	RC	RR	p
Dose (Gy)	82.3 ± 6.31	80.0 ± 5.52	0.083	82.4 ± 9.68	76.3 ± 8.44	0.018
DV (%)	1.79 ± 9.56	-4.49 ± 11.2	0.023	0.77 ± 12.2	-6.27 ± 9.01	0.043
COIN	0.41 ± 0.07	0.42 ± 0.10	0.711	0.42 ± 0.06	0.43 ± 0.10	0.697
CI (%)	89.7 ± 4.00	86.9 ± 5.20	0.021	88.7 ± 5.70	86.3 ± 4.30	0.140
c ₂ (%)	46.0 ± 7.90	48.5 ± 12.7	0.321	47.1 ± 7.90	49.6 ± 13.3	0.453
HRCTV (cc)	41.4 ± 15.4	54.4 ± 28.9	0.018	43.4 ± 18.2	52.8 ± 27.5	0.182

Table A3. 9. Large HRCTV stats.

	N	HRCTV (cc)	EQD2 (Gy)	DV (%)	COIN	CI	C2	LC (%)	LR (%)	LF (%)	Pelvic Control (%)	Pelvic Recurrence (%)
1-Year	70	52.7 ± 19.0	75.1 ± 9.56	-2.27 ± 10.4	0.44 ± 0.07	88.1 ± 4.74	49.7 ± 7.7	84.3	17.1	27.1	68.6	32.9
2-Year	83	53.4 ± 18.7	75.0 ± 9.89	-2.84 ± 10.8	0.44 ± 0.07	87.8 ± 5.14	49.8 ± 7.9	79.5	21.7	31.3	63.9	37.3
3-Year	85	53.0 ± 18.7	75.0 ± 9.95	-2.66 ± 11.0	0.44 ± 0.07	87.9 ± 5.17	49.6 ± 7.9	78.8	22.4	31.8	63.5	37.6
3-Year LACC	66	52.9 ± 18.7	76.5 ± 9.95	-2.89 ± 11.3	0.43 ± 0.07	87.7 ± 5.4	49.6 ± 8.0	75.8	25.8	31.8	60.6	40.9

Table A3. 10. Small HRCTV stats

	N	HRCTV (cc)	EQD2 (Gy)	DV (%)	COIN	CI	C2	LC (%)	LR (%)	LF (%)	Pelvic Control (%)	Pelvic Recurrence (%)
1-Year	25	25.4 ± 5.6	77.7 ± 7.33	7.23 ± 7.1	0.36 ± 0.09	92.0 ± 3.13	39.5 ± 10.1	92	12	16	92	12
2-Year	27	25.4 ± 5.3	78.5 ± 7.69	6.86 ± 7.20	0.36 ± 0.09	91.9 ± 3.15	39.7 ± 9.9	88.9	14.8	18.5	88.9	14.8
3-Year	32	25.8 ± 5.1	78.0 ± 7.52	6.51 ± 7.3	0.36 ± 0.08	91.7 ± 3.17	39.6 ± 9.3	87.5	15.6	21.9	87.5	15.6
3-Year LACC	19	25.4 ± 5.8	80.4 ± 6.9	5.21 ± 7.8	0.38 ± 0.1	91.1 ± 3.33	41.6 ± 11.1	84.2	21.1	21.1	84.2	21.1

Table A3. 11. Large HRCTV logistic regression statistics and parameter estimation for the 3-year all patient and 3-year LACC patient data.

Large HRCTV 3-Year Data									
Variable	LF Logistic Regression			LR Logistic Regression			RR Logistic Regression		
	50% Response	γ	P	50% Response	γ	P	50% Response	γ	P
HRCTV (cc)	182	-0.318	0.076	null	null	0.059	null	null	0.159
DV (%)	null	null	0.077	null	null	0.057	-61.0	-0.149	0.074
COIN	0.87	-0.465	0.052	1.76	-0.452	0.054	0.87	-0.310	0.07
CI (%)	null	null	0.078	null	null	0.058	null	null	0.087
C2 (%)	74.0	-0.634	0.036	1.41	-0.506	0.052	73.0	-0.437	0.057
Large HRCTV 3-Year LACC Data									
Variable	LF Logistic Regression			LR Logistic Regression			RR Logistic Regression		
	50% Response	γ	P	50% Response	γ	P	50% Response	γ	P
HRCTV (cc)	182	-0.318	0.076	2.81	-0.016	0.028	48.5	-0.124	0.363
DV (%)	null	null	0.077	null	null	0.064	-34.0	-0.125	0.067
COIN	0.87	-0.465	0.052	null	null	0.064	1.29	-0.164	0.088
CI (%)	null	null	0.078	null	null	0.065	null	null	0.089
C2 (%)	74.0	-0.634	0.036	null	null	0.065	83.0	-0.256	0.082

Table A3. 12. Small HRCTV logistic regression statistics and parameter estimation for the 3-year all patient and 3-year LACC patient data.

Small HRCTV 3-Year Data									
Variable	LF Logistic Regression			LR Logistic Regression			RR Logistic Regression		
	50% Response	γ	P	50% Response	γ	P	50% Response	γ	P
HRCTV (cc)	84.5	-0.73	0.123	null	null	0.036	null	null	0.036
DV (%)	null	null	0.052	null	null	0.035	null	null	0.035
COIN	null	null	0.049	null	null	0.035	null	null	0.035
CI (%)	null	null	0.052	null	null	0.035	null	null	0.035
C2 (%)	null	null	0.049	null	null	0.035	null	null	0.035
Small HRCTV 3-Year LACC Data									
Variable	LF Logistic Regression			LR Logistic Regression			RR Logistic Regression		
	50% Response	γ	P	50% Response	γ	P	50% Response	γ	P
HRCTV (cc)	102	-0.721	0.064	102	-0.721	0.064	102	-0.721	0.064
DV (%)	null	null	0.043	Null	null	0.043	null	null	0.043
COIN	null	null	0.043	null	null	0.043	null	null	0.043
CI (%)	null	null	0.044	null	null	0.044	null	null	0.044
C2 (%)	null	null	0.044	null	null	0.044	null	null	0.044

REFERENCES

1. Siegel RL, Miller KD, Wagle NS, Jemal A. Cancer statistics, 2023. *CA A Cancer J Clinicians*. 2023;73(1):17-48. doi:10.3322/caac.21763
2. Albuquerque K, Hrycushko BA, Harkenrider MM, et al. Compendium of fractionation choices for gynecologic HDR brachytherapy—An American Brachytherapy Society Task Group Report. *Brachytherapy*. 2019;18(4):429-436. doi:10.1016/j.brachy.2019.02.008
3. International Commission on Radiation Units and Measurements. ICRU report 38: Dose and volume specification for reporting intracavity therapy in gynecology. Bethesda: ICRU; 1985.
4. Viswanathan AN, Creutzberg CL, Craighead P, et al. International Brachytherapy Practice Patterns: A Survey of the Gynecologic Cancer Intergroup (GCIG). *International Journal of Radiation Oncology*Biophysics*Physics*. 2012;82(1):250-255. doi:10.1016/j.ijrobp.2010.10.030
5. Marchant KJ, Sadikov E. The evolving practice of intrauterine cervix brachytherapy in Canada: A medical physics perspective. *Brachytherapy*. 2013;12(4):324-330. doi:10.1016/j.brachy.2012.08.005
6. Tanderup K, Nielsen SK, Nyvang GB, et al. From point A to the sculpted pear: MR image guidance significantly improves tumour dose and sparing of organs at risk in brachytherapy of cervical cancer. *Radiotherapy and Oncology*. 2010;94(2):173-180. doi:10.1016/j.radonc.2010.01.001
7. Mourya A, Choudhary S, Shahi UP, et al. A comparison between revised Manchester Point A and ICRU-89–recommended Point A definition absorbed-dose reporting using CT images in intracavitary brachytherapy for patients with cervical carcinoma. *Brachytherapy*. 2021;20(1):118-127. doi:10.1016/j.brachy.2020.07.009
8. International Commission on Radiation Units and Measurements. *Journal of the ICRU*. 2013;13(1-2):NP.2-NP. doi:10.1093/jicru/ndw028
9. Rivard MJ, Coursey BM, DeWerd LA, et al. Update of AAPM Task Group No. 43 Report: A revised AAPM protocol for brachytherapy dose calculations. *Med Phys*. 2004;31(3):633-674. doi:10.1118/1.1646040
10. DeWerd LA, Venselaar JLM, Ibbott GS, et al. Overview on the dosimetric uncertainty analysis for photon-emitting brachytherapy sources, in the light of the AAPM Task Group No 138 and GEC-ESTRO report. *Metrologia*. 2012;49(5):S253-S258. doi:10.1088/0026-1394/49/5/S253
11. DeWerd LA, Ibbott GS, Meigooni AS, et al. A dosimetric uncertainty analysis for photon-emitting brachytherapy sources: Report of AAPM Task Group No. 138 and

- GEC-ESTRO: AAPM TG-138 and GEC-ESTRO brachytherapy dosimetry uncertainty recommendations. *Med Phys*. 2011;38(2):782-801. doi:10.1118/1.3533720
12. Taylor, Barry N., and Chris E. Kuyatt. *Guidelines for evaluating and expressing the uncertainty of NIST measurement results*. Vol. 1297. Gaithersburg, MD: US Department of Commerce, Technology Administration, National Institute of Standards and Technology, 1994.
 13. Liu H, Kinard J, Maurer J, et al. Evaluation of offline adaptive planning techniques in image-guided brachytherapy of cervical cancer. *J Appl Clin Med Phys*. 2018;19(6):316-322. doi:10.1002/acm2.12462
 14. Duane FK, Langan B, Gillham C, et al. Impact of delineation uncertainties on dose to organs at risk in CT-guided intracavitary brachytherapy. *Brachytherapy*. 2014;13(2):210-218. doi:10.1016/j.brachy.2013.08.010
 15. Hellebust TP, Tanderup K, Lervåg C, et al. Dosimetric impact of interobserver variability in MRI-based delineation for cervical cancer brachytherapy. *Radiotherapy and Oncology*. 2013;107(1):13-19. doi:10.1016/j.radonc.2012.12.017
 16. Bell L, Holloway L, Bruheim K, et al. Dose planning variations related to delineation variations in MRI-guided brachytherapy for locally advanced cervical cancer. *Brachytherapy*. 2020;19(2):146-153. doi:10.1016/j.brachy.2020.01.002
 17. Saarnak AE, Boersma M, van Bunningen BNF, Wolterink R, Steggerda MJ. Inter-observer variation in delineation of bladder and rectum contours for brachytherapy of cervical cancer. *Radiotherapy and Oncology*. 2000;56(1):37-42. doi:10.1016/S0167-8140(00)00185-7
 18. Arnesen MR, Bruheim K, Malinen E, Hellebust TP. Spatial dosimetric sensitivity of contouring uncertainties in gynecological 3D-based brachytherapy. *Radiotherapy and Oncology*. 2014;113(3):414-419. doi:10.1016/j.radonc.2014.11.016
 19. Petrič P, Hudej R, Rogelj P, et al. Uncertainties of target volume delineation in MRI guided adaptive brachytherapy of cervix cancer: A multi-institutional study. *Radiotherapy and Oncology*. 2013;107(1):6-12. doi:10.1016/j.radonc.2013.01.014
 20. Patel S, Mehta KJ, Kuo HCG, et al. Do changes in interfraction organ at risk volume and cylinder insertion geometry impact delivered dose in high-dose-rate vaginal cuff brachytherapy? *Brachytherapy*. 2016;15(2):185-190. doi:10.1016/j.brachy.2015.11.004
 21. Kobayashi K, Murakami N, Wakita A, et al. Dosimetric variations due to interfraction organ deformation in cervical cancer brachytherapy. *Radiotherapy and Oncology*. 2015;117(3):555-558. doi:10.1016/j.radonc.2015.08.017
 22. Mazon R, Champoudry J, Gilmore J, et al. Intrafractional organs movement in three-dimensional image-guided adaptive pulsed-dose-rate cervical cancer brachytherapy:

- Assessment and dosimetric impact. *Brachytherapy*. 2015;14(2):260-266. doi:10.1016/j.brachy.2014.11.014
23. Andersen ES, Noe KØ, Sørensen TS, et al. Simple DVH parameter addition as compared to deformable registration for bladder dose accumulation in cervix cancer brachytherapy. *Radiotherapy and Oncology*. 2013;107(1):52-57. doi:10.1016/j.radonc.2013.01.013
 24. Kirisits C, Rivard MJ, Baltas D, et al. Review of clinical brachytherapy uncertainties: Analysis guidelines of GEC-ESTRO and the AAPM. *Radiotherapy and Oncology*. 2014;110(1):199-212. doi:10.1016/j.radonc.2013.11.002
 25. Tanderup K, Nesvacil N, Pötter R, Kirisits C. Uncertainties in image guided adaptive cervix cancer brachytherapy: Impact on planning and prescription. *Radiotherapy and Oncology*. 2013;107(1):1-5. doi:10.1016/j.radonc.2013.02.014
 26. Nesvacil N, Tanderup K, Lindegaard JC, Pötter R, Kirisits C. Can reduction of uncertainties in cervix cancer brachytherapy potentially improve clinical outcome? *Radiotherapy and Oncology*. 2016;120(3):390-396. doi:10.1016/j.radonc.2016.06.008
 27. Nag S, Demanes JD. THE AMERICAN BRACHYTHERAPY SOCIETY RECOMMENDATIONS FOR HIGH-DOSE-RATE BRACHYTHERAPY FOR CARCINOMA OF THE CERVIX. 2000;48(1).
 28. Sharma BA, Singh T, Singh J. Clinical Investigations Evaluation of variation in dose of organs at risk in intracavitary brachytherapy of cervical cancer – a prospective study. *jcb*. 2011;1:23-25. doi:10.5114/jcb.2011.21039
 29. Washington B, Randall M, Fabian D, Cheek D, Wang C, Luo W. Statistical Analysis of Interfraction Dose Variations of High-Risk Clinical Target Volume and Organs at Risk for Cervical Cancer High-Dose-Rate Brachytherapy. *Advances in Radiation Oncology*. 2022;7(6):101019. doi:10.1016/j.adro.2022.101019
 30. van Heerden LE, van Wieringen N, Koedooder K, Rasch CRN, Pieters BR, Bel A. Dose warping uncertainties for the accumulated rectal wall dose in cervical cancer brachytherapy. *Brachytherapy*. 2018;17(2):449-455. doi:10.1016/j.brachy.2017.10.002
 31. Chakraborty S, Patel FD, Patil VM, Oinam AS, Sharma SC. Magnitude and Implications of Interfraction Variations in Organ Doses during High Dose Rate Brachytherapy of Cervix Cancer: A CT Based Planning Study. *ISRN Oncology*. 2014;2014:1-7. doi:10.1155/2014/687365
 32. Jamema SV, Mahantshetty U, Tanderup K, et al. Inter-application variation of dose and spatial location of D 2 cm 3 volumes of OARs during MR image based cervix brachytherapy. *Radiotherapy and Oncology*. 2013;107(1):58-62. doi:10.1016/j.radonc.2013.01.011

33. Brown LD, Hwang JTG. How to Approximate a Histogram by a Normal Density. *The American Statistician*. 1993;47(4):251-255. doi:10.1080/00031305.1993.10475992
34. Engmann, Sonja, and Denis Cousineau. "Comparing distributions: the two-sample Anderson-Darling test as an alternative to the Kolmogorov-Smirnoff test." *Journal of applied quantitative methods* 6, no. 3 (2011).
35. Tanderup K, Hellebust TP, Lang S, et al. Consequences of random and systematic reconstruction uncertainties in 3D image based brachytherapy in cervical cancer. *Radiotherapy and Oncology*. 2008;89(2):156-163. doi:10.1016/j.radonc.2008.06.010
36. Kashihara T, Murakami N, Tselis N, et al. Hyaluronate gel injection for rectum dose reduction in gynecologic high-dose-rate brachytherapy: initial Japanese experience. *Journal of Radiation Research*. 2019;60(4):501-508. doi:10.1093/jrr/rrz016
37. Murakami N, Nakamura S, Kashihara T, et al. Hyaluronic acid gel injection in rectovaginal septum reduced incidence of rectal bleeding in brachytherapy for gynecological malignancies. *Brachytherapy*. 2020;19(2):154-161. doi:10.1016/j.brachy.2019.11.004
38. Viswanathan AN, Thomadsen B. American Brachytherapy Society consensus guidelines for locally advanced carcinoma of the cervix. Part I: General principles. *Brachytherapy*. 2012;11(1):33-46. doi:10.1016/j.brachy.2011.07.003
39. Viswanathan AN, Beriwal S, De Los Santos JF, et al. American Brachytherapy Society consensus guidelines for locally advanced carcinoma of the cervix. Part II: High-dose-rate brachytherapy. *Brachytherapy*. 2012;11(1):47-52. doi:10.1016/j.brachy.2011.07.002
40. Gill BS, Kim H, Houser CJ, et al. MRI-Guided High-Dose-Rate Intracavitary Brachytherapy for Treatment of Cervical Cancer: The University of Pittsburgh Experience. *International Journal of Radiation Oncology*Biophysics*Physic*s. 2015;91(3):540-547. doi:10.1016/j.ijrobp.2014.10.053
41. Dimopoulos JCA, Pötter R, Lang S, et al. Dose-effect relationship for local control of cervical cancer by magnetic resonance image-guided brachytherapy. *Radiotherapy and Oncology*. 2009;93(2):311-315. doi:10.1016/j.radonc.2009.07.001
42. Tanderup K, Fokdal LU, Sturdza A, et al. Effect of tumor dose, volume and overall treatment time on local control after radiochemotherapy including MRI guided brachytherapy of locally advanced cervical cancer. *Radiotherapy and Oncology*. 2016;120(3):441-446. doi:10.1016/j.radonc.2016.05.014
43. Pötter R, Georg P, Dimopoulos JCA, et al. Clinical outcome of protocol based image (MRI) guided adaptive brachytherapy combined with 3D conformal radiotherapy with or without chemotherapy in patients with locally advanced cervical cancer. *Radiotherapy and Oncology*. 2011;100(1):116-123. doi:10.1016/j.radonc.2011.07.012

44. Charra-Brunaud C, Harter V, Delannes M, et al. Impact of 3D image-based PDR brachytherapy on outcome of patients treated for cervix carcinoma in France: Results of the French STIC prospective study. *Radiotherapy and Oncology*. 2012;103(3):305-313. doi:10.1016/j.radonc.2012.04.007
45. Kang HC, Shin KH, Park SY, Kim JY. 3D CT-based high-dose-rate brachytherapy for cervical cancer: Clinical impact on late rectal bleeding and local control. *Radiotherapy and Oncology*. 2010;97(3):507-513. doi:10.1016/j.radonc.2010.10.002
46. Nomden CN, de Leeuw AAC, Roesink JM, et al. Clinical outcome and dosimetric parameters of chemo-radiation including MRI guided adaptive brachytherapy with tandem-ovoid applicators for cervical cancer patients: A single institution experience. *Radiotherapy and Oncology*. 2013;107(1):69-74. doi:10.1016/j.radonc.2013.04.006
47. Chargari C, Magné N, Dumas I, et al. Physics Contributions and Clinical Outcome With 3D-MRI-Based Pulsed-Dose-Rate Intracavitary Brachytherapy in Cervical Cancer Patients. *International Journal of Radiation Oncology*Biography*Physics*. 2009;74(1):133-139. doi:10.1016/j.ijrobp.2008.06.1912
48. Tan LT, Coles CE, Hart C, Tait E. Clinical Impact of Computed Tomography-based Image-guided Brachytherapy for Cervix Cancer using the Tandem-ring Applicator — the Addenbrooke’s Experience. *Clinical Oncology*. 2009;21(3):175-182. doi:10.1016/j.clon.2008.12.001
49. Kharofa J, Morrow N, Kelly T, et al. 3-T MRI-based adaptive brachytherapy for cervix cancer: Treatment technique and initial clinical outcomes. *Brachytherapy*. 2014;13(4):319-325. doi:10.1016/j.brachy.2014.03.001
50. Okunieff P, Morgan D, Niemierko A, Suit HD. Radiation dose-response of human tumors. *International Journal of Radiation Oncology*Biography*Physics*. 1995;32(4):1227-1237. doi:10.1016/0360-3016(94)00475-Z
51. Georg P, Pötter R, Georg D, et al. Dose Effect Relationship for Late Side Effects of the Rectum and Urinary Bladder in Magnetic Resonance Image-Guided Adaptive Cervix Cancer Brachytherapy. *International Journal of Radiation Oncology*Biography*Physics*. 2012;82(2):653-657. doi:10.1016/j.ijrobp.2010.12.029
52. Nesvacil N, Tanderup K, Hellebust TP, et al. A multicentre comparison of the dosimetric impact of inter- and intra-fractional anatomical variations in fractionated cervix cancer brachytherapy. *Radiotherapy and Oncology*. 2013;107(1):20-25. doi:10.1016/j.radonc.2013.01.012
53. Boyer, Arthur L., and Timothy Schultheiss. “Effects of dosimetric and clinical uncertainty on complication-free local tumor control.” *Radiotherapy and Oncology* 11, no. 1 (1988): 65-71.
54. Keall PJ. The management of respiratory motion in radiation oncology report of AAPM Task Group 76a.... *Medical Physics*. 2006;33(10):27.

55. Moiseenko V, Song WY, Mell LK, Bhandare N. A comparison of dose-response characteristics of four NTCP models using outcomes of radiation-induced optic neuropathy and retinopathy. *Radiat Oncol.* 2011;6(1):61. doi:10.1186/1748-717X-6-61
56. Stavreva, N., P. Stavrev, B. Warkentin, and B. G. Fallone. "Derivation of the expressions for γ_{50} and D50 for different individual TCP and NTCP models." *Physics in Medicine & Biology* 47, no. 20 (2002): 3591.
57. Schultheiss, Timothy E., and Colin G. Orton. "Models in radiotherapy: definition of decision criteria." *Medical physics* 12, no. 2 (1985): 183-187.
58. Nesvacil N, Tanderup K, Lindegaard JC, Pötter R, Kirisits C. Can reduction of uncertainties in cervix cancer brachytherapy potentially improve clinical outcome? *Radiotherapy and Oncology.* 2016;120(3):390-396. doi:10.1016/j.radonc.2016.06.008
59. Gonzalez Y, Giap F, Klages P, Owrangi A, Jia X, Albuquerque K. Predicting which patients may benefit from the hybrid intracavitary+interstitial needle (IC/IS) applicator for advanced cervical cancer: A dosimetric comparison and toxicity benefit analysis. *Brachytherapy.* 2021;20(1):136-145. doi:10.1016/j.brachy.2020.09.004
60. Fokdal L, Sturdza A, Mazon R, et al. Image guided adaptive brachytherapy with combined intracavitary and interstitial technique improves the therapeutic ratio in locally advanced cervical cancer: Analysis from the retroEMBRACE study. *Radiotherapy and Oncology.* 2016;120(3):434-440. doi:10.1016/j.radonc.2016.03.020
61. Fokdal L, Tanderup K, Hokland SB, et al. Clinical feasibility of combined intracavitary/interstitial brachytherapy in locally advanced cervical cancer employing MRI with a tandem/ring applicator in situ and virtual preplanning of the interstitial component. *Radiotherapy and Oncology.* 2013;107(1):63-68. doi:10.1016/j.radonc.2013.01.010
62. Zhen X, Chen J, Zhong Z, et al. Deep convolutional neural network with transfer learning for rectum toxicity prediction in cervical cancer radiotherapy: a feasibility study. *Phys Med Biol.* 2017;62(21):8246-8263. doi:10.1088/1361-6560/aa8d09
63. Mazon R, Castelnau-Marchand P, Dumas I, et al. Impact of treatment time and dose escalation on local control in locally advanced cervical cancer treated by chemoradiation and image-guided pulsed-dose rate adaptive brachytherapy. *Radiotherapy and Oncology.* 2015;114(2):257-263. doi:10.1016/j.radonc.2014.11.045
64. Baltas D, Kolotas C, Geramani K, et al. A conformal index (COIN) to evaluate implant quality and dose specification in brachytherapy. *International Journal of Radiation Oncology*Biophysics*Physics.* 1998;40(2):515-524. doi:10.1016/S0360-3016(97)00732-3
65. Hoskin PJ, Bownes PJ, Ostler P, Walker K, Bryant L. High dose rate afterloading brachytherapy for prostate cancer: catheter and gland movement between fractions.

- Radiotherapy and Oncology*. 2003;68(3):285-288. doi:10.1016/S0167-8140(03)00203-2
66. Shin KH, Kim TH, Cho JK, et al. CT-guided intracavitary radiotherapy for cervical cancer: Comparison of conventional point A plan with clinical target volume-based three-dimensional plan using dose–volume parameters. *International Journal of Radiation Oncology*Biology*Physics*. 2006;64(1):197-204. doi:10.1016/j.ijrobp.2005.06.015
 67. Trnková P, Baltas D, Karabis A, et al. A detailed dosimetric comparison between manual and inverse plans in HDR intracavitary/interstitial cervical cancer brachytherapy. *J Contemp Brachytherapy*. 2010;2(4):163-170. doi:10.5114/jcb.2010.19497
 68. Paddick I. A simple scoring ratio to index the conformity of radiosurgical treatment plans: Technical note. *Journal of Neurosurgery*. 2000;93(supplement_3):219-222. doi:10.3171/jns.2000.93.supplement_3.0219
 69. Serban M, Kirisits C, de Leeuw A, et al. Ring Versus Ovoids and Intracavitary Versus Intracavitary-Interstitial Applicators in Cervical Cancer Brachytherapy: Results From the EMBRACE I Study. *International Journal of Radiation Oncology*Biology*Physics*. 2020;106(5):1052-1062. doi:10.1016/j.ijrobp.2019.12.019
 70. Viswanathan AN, Dimopoulos J, Kirisits C, Berger D, Pötter R. Computed Tomography Versus Magnetic Resonance Imaging-Based Contouring in Cervical Cancer Brachytherapy: Results of a Prospective Trial and Preliminary Guidelines for Standardized Contours. *International Journal of Radiation Oncology*Biology*Physics*. 2007;68(2):491-498. doi:10.1016/j.ijrobp.2006.12.021
 71. Nesvacil N, Pötter R, Sturdza A, Hegazy N, Federico M, Kirisits C. Adaptive image guided brachytherapy for cervical cancer: A combined MRI-/CT-planning technique with MRI only at first fraction. *Radiotherapy and Oncology*. 2013;107(1):75-81. doi:10.1016/j.radonc.2012.09.005
 72. Hricak H, Gatsonis C, Coakley FV, et al. Early Invasive Cervical Cancer: CT and MR Imaging in Preoperative Evaluation—ACRIN/GOG Comparative Study of Diagnostic Performance and Interobserver Variability. *Radiology*. 2007;245(2):491-498. doi:10.1148/radiol.2452061983
 73. Krishnatry R, Patel FD, Singh P, Sharma SC, Oinam AS, Shukla AK. CT or MRI for Image-based Brachytherapy in Cervical Cancer. *Japanese Journal of Clinical Oncology*. 2012;42(4):309-313. doi:10.1093/jjco/hys010
 74. Kim, Seung H., Byung I. Choi, Joon K. Han, Hong D. Kim, Hyo P. Lee, Soon B. Kang, Jin Y. Lee, and Man C. Han. “Preoperative staging of uterine cervical carcinoma: comparison of CT and MRI in 99 patients.” *Journal of computer assisted tomography* 17, no. 4 (1993): 633-640.

75. Niemierko A, Goitein M. Implementation of a model for estimating tumor control probability for an inhomogeneously irradiated tumor. *Radiotherapy and Oncology*. 1993;29(2):140-147. doi:10.1016/0167-8140(93)90239-5
76. Huang Z, Mayr NA, Gao M, et al. Onset Time of Tumor Repopulation for Cervical Cancer: First Evidence From Clinical Data. *International Journal of Radiation Oncology*Biography*Physics*. 2012;84(2):478-484. doi:10.1016/j.ijrobp.2011.12.037
77. Oh JH, Craft J, Al Lozi R, et al. A Bayesian network approach for modeling local failure in lung cancer. *Phys Med Biol*. 2011;56(6):1635-1651. doi:10.1088/0031-9155/56/6/008
78. El Naqa I, Pater P, Seuntjens J. Monte Carlo role in radiobiological modelling of radiotherapy outcomes. *Phys Med Biol*. 2012;57(11):R75-R97. doi:10.1088/0031-9155/57/11/R75

VITA

Brien Washington

Education:

University of Kentucky, Lexington, Kentucky

Doctor of Philosophy, Radiation and Radiological Sciences 2019-Present

University of Kentucky, Lexington, Kentucky

Master of Science, Radiological Medical Physics 2019-2022

Presbyterian College, Clinton, South Carolina

Bachelor of Science, Physics 2014-2018

Minor: Mathematics and Chemistry

Professional Experience:

Assistant Medical Physicist

Department of Radiation Oncology at the University of Kentucky 2021-present

Teaching Assistant

Medical Physics Graduate Program at the University of Kentucky 2021-present

Peer-Reviewed Publications Relevant to this Thesis:

1. **Washington, B.**, Randall, M., Fabian, D., Cheek, D., Wang, C., & Luo, W. (2022). Statistical analysis of interfraction dose variations of HRCTV and OARs for cervical cancer HDR brachytherapy. *Advances in Radiation Oncology*, 101019.

Other Peer-Reviewed Publications:

1. Luo, W., Cheek, D., Clair, W. S., & **Washington, B.** (2022). Patient-specific dose correction for prostate postimplant evaluation with flexible timing of postimplant imaging. *Medical Physics*. (Early View).

2. Wanliss, J., Cornélissen, G., Halberg, F., Brown, D., & **Washington, B.** (2018). Superposed epoch analysis of physiological fluctuations: possible space weather connections. *International journal of biometeorology*, 62(3), 449-457.

Abstracts and Presentations:

1. **Washington, B.**, Kudrimoti, M., Fabian, D., Cheek, D., Wang, C., Pokhrel, D., & Luo, W. (2023). “Prediction of the Effect of Dose Variation Uncertainty in High Dose Rat Brachytherapy on Clinical Outcomes for Cervical Cancer”. AAPM Annual Meeting & Exhibition 2023 ePoster presentation.
2. **Washington, B.**, Randall, M., Fabian, D., Cheek, D., Wang, C., & Luo, W. (2022). “A Statistical Analysis of Correlations Between HRCTV Dose and OAR Doses for Cervix HDR”. AAPM Annual Meeting & Exhibition 2022 (general view ePoster).
3. **Washington, B.**, Randall, M., Fabian, D., Cheek, D., Wang, C., & Luo, W. (2022). “Distribution of Interfraction Dosimetric Variation of HRCTV in Cervix HDR Brachytherapy”. AAPM Annual Meeting & Exhibition 2022 (general view ePoster).
4. **Washington, B.**, Randall, M., Fabian, D., Cheek, D., Wang, C., & Luo, W. “An analysis of interfraction dosimetric variations from the prescribed dose and the corresponding effect on organs at risk in CT based, high dose rate adaptive brachytherapy: a dosimetric study.” AAPM ORVC Oral Presentation, 2022.
5. **Washington, B.**, Randall, M., Fabian, D., Cheek, D., Wang, C., & Luo, W. “An evaluation of high-risk clinical target volume coverage in CT based, high dose rate adaptive brachytherapy.” AAPM ORVC Oral Presentation, 2022.
6. **Washington, B.**, Randall, M., Fabian, & Luo, W. “Interfractional Dosimetric Variations of the Target and Organs at Risk for High Dose-Rate GYN Brachytherapy.” AAPM Annual Meeting & Exhibition 2021 (general view ePoster).

Awards and Recognition:

South-Eastern Conference (SEC) Emerging Scholar

One of ten University of Kentucky graduate students selected for inaugural meeting 2021

University of Kentucky Radiation Medicine Research Spotlight

June-July 2022 newsletter

2022

Administrative Experience:

Chair of University of Kentucky Radiation Medicine Search Committee
Represented the Medical Physics Ph.D. program

2022